NASA Contractor Report 165670

USER'S MANUAL FOR STAGS
VOLUME I: THEORY

B. O. Almroth, F. A. Brogan, and G. M. Stanley

LOCKHEED MISSILES AND SPACE COMPANY, INC.
Lockheed Palo Alto Research Laboratory
Palo Alto, California 94304

Contract NAS1-10843
March 1978

National Aeronautics and
Space Administration

Langley Research Center
Hampton, Virginia 23665

TABLE OF CONTENTS

Section		Page
1	INTRODUCTION.	1-1
2	SUMMARY OF THE THEORY	2-1
	2.1 The Variational Approach	2-2
	2.2 Constitutive Relations	2-5
	2.3 Kinematic Relations.	2-7
	2.4 Approximations and Special Procedures.	2-11
3	CONSTITUTIVE RELATIONS (ELASTIC).	3-1
4	THE THEORY OF PLASTICITY.	4-1
	4.1 Classical Plasticity Theory.	4-2
	4.2 Limitations of the Classical Theory.	4-6
	4.3 Other Theories	4-9
	4.4 The State of the Art	4-12
	4.5 Solution Techniques.	4-14
	4.6 Plasticity Theory in STAGS	4-17
5	GEOMETRIC NONLINEARITIES.	5-1
	5.1 Introduction	5-1
	5.2 The Concept of Stability	5-4
	5.3 The Consequence of Instability	5-10
	5.4 Static Stability Analysis.	5-11
6	DISCRETIZATION PROCEDURES	6-1
	6.1 Introduction	6-1
	6.2 Numerical Differentiation.	6-2
	6.3 Numerical Integration.	6-9
	6.4 Numerical Solution Procedures.	6-12
	6.5 Some Special Problems.	6-28
	6.6 Some Options for Discretization.	6-32
	6.7 Discretization in STAGS.	6-46
7	SOLUTION PROCEDURES	7-1
	7.1 Introduction	7-1
	7.2 Linear Equation Systems	7-5
	7.3 Nonlinear Equation Systems	7-8
	7.4 Eigenvalue Analysis	7-14
	7.5 Transient Analysis	7-21

Section 1
INTRODUCTION

The present document is the first of three volumes of the User's Manual for the STAGS computer code. Together the three volumes describe the code and give instructions for its use. The second volume contains the user instructions and the third volume gives the results of a series of example cases. The present volume presents a detailed description of the basic theory (Sections 2 through 8). Nonlinear effects are discussed in Section 4, "Plasticity," and in Section 5, "Geometric Nonlinearities." Section 6 contains a discussion of special problems in discretized analysis (finite differences or finite elements) of shells. Procedures for solution of the algebraic equations are discussed in Section 7.

Before the high speed computer was available and suitable software developed, it was hardly possible to perform an accurate analysis of anything but the very simplest structural components. Today much better tools are available, but this does not necessarily mean that a good analysis always is performed. Complex structures behave in a complex way and therefore a good nonlinear analysis requires not only a good computer code but also the participation of a well-trained analyst. Use of a sophisticated computer program without a reasonable understanding of its theoretical background and the solution procedures involved may be worse than a "quick and dirty" solution because it leads to an unjustified sense of security.

Structural analysis with large high speed computers is a relatively new discipline, still being developed at a rapid pace. As a consequence, there is a shortage of structural analysts whose ability allows them to take full advantage of the more advanced computer codes. It is often suggested, therefore, that the computer programs must be made easier to use.

Unfortunately, there is sometimes a conflict between the demands for efficiency and for ease of use. In many design applications such as flight vehicles, ship structures, nuclear power plant components, the structural analysis must be based on a mathematical model with a large number of degrees of freedom. Often an adequate guarantee of the integrity of such structures must be based on an analysis of their time dependent, nonlinear response to the loading situation. A straightforward approach to problems of this kind is usually prohibited by excessive cost for computer time. The analyst must make many difficult decisions when forced to sacrifice some accuracy in the final results in order to stay within budgetary limits. In order to make good use of the computer codes now available, the analyst must be quite familiar with the basic theory of structures so that he can select the proper level of approximation in the governing equations. He must have a good feeling for structural behavior so that he can devise an adequate mathematical model. He must have a good background in applied mathematics so that he can choose an acceptable solution procedure when given options and avoid use of codes that do not include such a procedure.

The objective of this volume is twofold. It serves as a documentation of the content of the computer code. In addition, the volume summarizes in the simplest possible terms, the general information about theories and procedures which it is felt that a good structural analyst should possess. The volume includes only material that is believed to be of importance to the user of the code. Although specialized for the STAGS user, the volume is applicable in structural shell analysis in a broader sense. Tedious details of the STAGS formulation primarily serving as documentation of the code are not included.

Anyone who plans to make extensive use of the STAGS code is advised to acquaint himself with the content of the volume. It is particularly important that the use of the code are due to approximations in theory or solution procedures. Approximations involved in computations with the STAGS code are summarized as follows:

(1) A shell or plate theory constitutes an approximation which reduces the structural problem to dependence on two spatial coordinates. The shell theory used in STAGS is a first order theory (transverse shear deformations are neglected). In addition, the theory is based on the assumption that strains are small and rotations are moderately large. That is, if the solution shows rotations larger than, say 0.3 radians, the results may be inaccurate. Larger rotations in a limited area, a boundary layer, does not generally prevent the solution outside of this area from being of acceptable accuracy.

(2) The constitutive relations are accurate for shell wall constructions that are homogeneous. In the special routines for computation of shell wall stiffnesses, a homogeneous approximation is used to represent an inhomogeneous construction (smeared stiffeners, corrugated skin).

(3) The material behavior in the inelastic range is complicated and no available plasticity theory truly represents the material behavior in all situations. The plasticity is restricted to small strains ($\varepsilon < 0.1$ or so), since it is based on engineering stress and strain.

(4) If some part of the structure is defined as a beam or a stiffener, its cross-section is assumed not to deform or warp.

(5) The discretization, local power series approximation of the displacements, involves a truncation error (depending on the grid size). Additional approximations are introduced in nonconforming elements and sometimes in numerical integration with respect to spatial coordinates.

(6) The numerical integration in time involves a truncation error (depending on the time step).

(7) The use of bifurcation buckling theory beyond its range of applicability is discussed in Section 5 of this volume.

Section 2
SUMMARY OF THE THEORY

The response of a structure to its environment is given by the solution of the differential equations of motion. These equations may be derived through consideration of a small cubic element in a Cartesian system x_1, x_2, x_3 as shown in Figure 2.1. The equation governing the motion of the element in the x_1 direction, for example, can be written

$$dV\ [\partial\sigma_{11}/\partial x_1 + \partial\sigma_{21}/\partial x_2 + \partial\sigma_{31}/\partial x_3 - \rho\ddot{u}_1] - F_1 = 0 \qquad (2.1)$$

where σ_{11} represents the normal stress, σ_{12} and σ_{13} the shear stresses as shown in Figure 2.1, and F_1 represents the sum of the components in the x_1-direction of body forces and surface tractions. The body forces may, for example, be caused by gravitational field and surface tractions, wherever they occur, are applied forces or reactions. A dot signifies derivation with respect to time, ρ is the mass density of the material, u_1 is the displacement of the element in the x_1-direction, and dV is the volume of the element.

By use of the constitutive equations (Hooke's law generalized to include anisotropic materials), the stresses can be expressed in terms of strains. The kinematic relations give the strains as functions of the displacement components. By substitution of the kinematic and constitutive relations into the equations of motion, the stresses and the strains can be eliminated so that the displacement components represent the only unknowns in the governing differential equations. A more thorough discussion of this topic, including definitions of stress and strain, is given in Ref. 2.1 (Chapter 33), for example. This discussion includes energy principles and the transformations of strains and stresses from one coordinate system to another. The concepts of true strain and true stress are discussed in Chapter 46 of the same reference. However, in the following, the expressions stress and strain refer to engineering stress and engineering strain

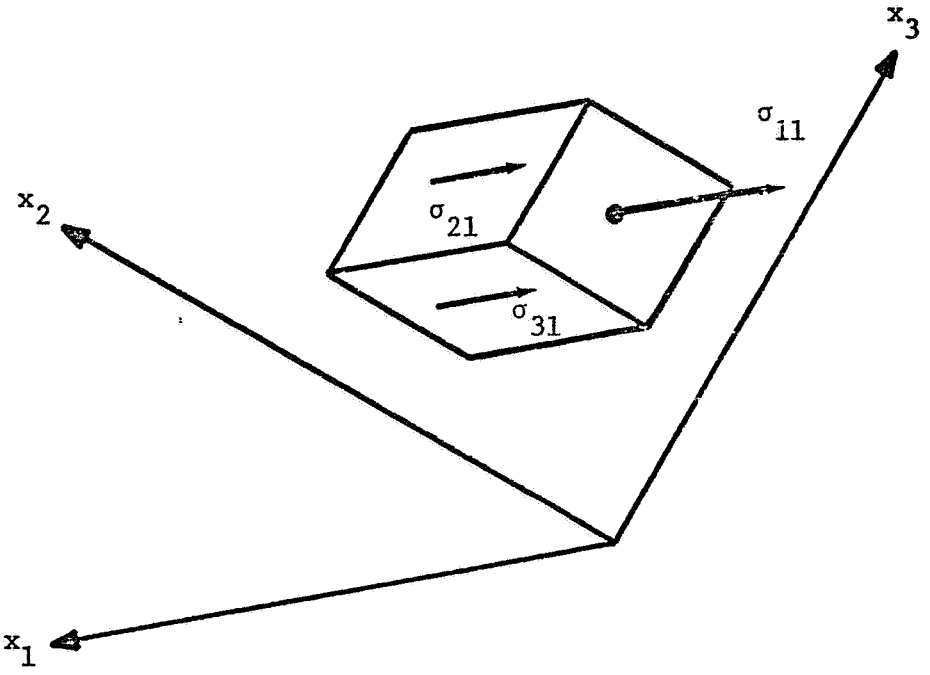

Figure 2.1. Stresses on Small Element

2.1 The Variational Approach

For the moment only elastic deformation is considered and the force vector $\{F_i\}$ is temporarily disregarded. Then it can be shown that the statement represented by Eqs. 2.1 is equivalent to the requirement that the motion of the structure between any two instants of time t_o and t_1 is such that the functional $\int_{t_o}^{t_1} (U-K)\, dt$ is at an extremum with respect to all admissible variations where U is the strain energy and K the kinetic energy. Admissible variations are functions that satisfy given continuity conditions and geometric boundary conditions and are zero at all points of the body at the beginning and the end of the time interval. The equilibrium equations can be derived from the first variation of the energy functional by use of partial integration with respect to time as well as to the space variables.

If the loading is such that it can be represented by the first variation of a single function, then the system is conservative and the equilibrium equations including body and surface forces can be derived from the first variation of the Lagrangian function.

$$\delta \int_{t_o}^{t_1} (U - K + W)\, dt = 0 \qquad (2.2)$$

where W represents the potential of the force system, i.e., the negative of the work done by these forces during the time interval. This is referred to as Hamilton's principle. The question of what constitutes a conservative force system will be discussed in the sequel.

If the motion of the structure is sufficiently slow, the kinetic energy can be omitted. Then, under a conservative force system, the change in total potential energy (U + W) is independent of the path by which the structure moves from one configuration to another. In the static case, Hamilton's principle degenerates into the principle of minimum potential energy, i.e.,

$$\delta\ (U + W) = 0 \qquad (2.3)$$

This principle can be derived from the principle of virtual work (see Ref. 2.1, Chapter 3). The admissible variations (functions of the space variables only) are those that satisfy continuity conditions and geometric boundary conditions.

Other energy theorems can be formulated (see, for example, Ref. 2.2), but have not been used as a basis for the STAGS formulation and are not discussed here. Two major advantages justify the choice of the variational method as a basis for analysis with STAGS. The resulting equation systems are diagonally symmetric and only geometric boundary conditions (corresponding to displacement constraints) need be enforced.

The disadvantage with the variational method is its restriction to conservative systems. Typical of a conservative force system is that the work done by the forces is path-independent, that is, it depends on the initial and final configurations only. An example of conservative forces are those caused by a gravitational field. On the other hand, if the forces are dependent on the deformation of the structure, the system is nonconservative. Thus, aeroelastic problems are nonconservative. Ref. 2.3 contains a discussion of the conservatism of some special force systems.

A hydrostatic pressure load rotates with the structural deformation so that the force on the body always remains normal to the surface. Pressure loading ("live load") therefore is not necessarily conservative. However, it has long been recognized that if a uniform pressure p acts on a closed body, the work done by this pressure is

$$w = p\,\Delta V \tag{2.4}$$

where ΔV is the change in volume of the body. For this case then, the work done by the pressure is path-independent and the force system is conservative. For plates and shells, Ref. 2.4 extends considerably the number of cases in which a live pressure load is conservative. It is sufficient to require that the pressure is continuous and that either of the following quantities is zero at any point on the boundary (of the shell or plate):

1) The pressure p

2) The lateral displacement

3) The scalar product of the displacement vector (u, v) and the normal to the shell boundary in the tangent plane. That is, the boundary points are restricted from displacement in the direction of the in-plane normal $un_1 + vn_2 = 0$ (see Figure 2.2).

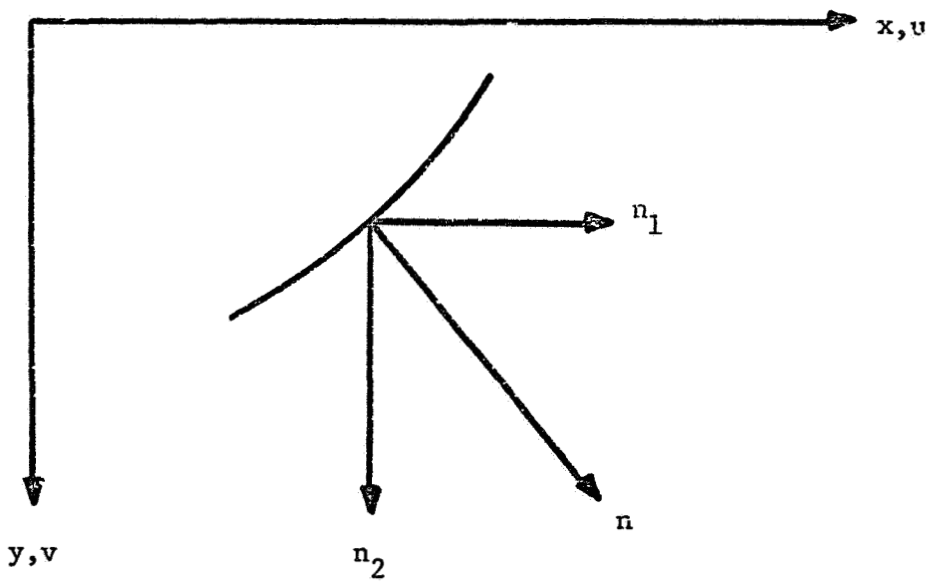

Figure 2.2. Normal to the Shell Edge in the Tangent Plane

2.2 Constitutive Relations

For the three-dimensional continuum, the constitutive relations can be written in the form

$$\left[\sigma_{ij}\right] = \left[c\right] \left[\epsilon_{ij} - \alpha T - \epsilon^{p}_{ij}\right] \tag{2.5}$$

where c is a three by three matrix and α represents the coefficient of thermal expansion, T the temperature above ambient, and ϵ^{p}_{ij} the inelastic part of the strain component. For an isotropic material

$$c = \frac{E}{1-\nu^2} \begin{bmatrix} 1 & \nu & 0 \\ \nu & 1 & 0 \\ 0 & 0 & \frac{1-\nu}{2} \end{bmatrix} \tag{2.6}$$

For shells or plates special "two-dimensional" equations have been derived and use of those offers improved computational efficiency. Because all points of the shell are close to some reference surface, an approximation is possible in which the displacement components at any point of the shell are expressed in terms of displacements (and possibly rotations) at the reference surface. In a shell theory the constitutive equations are written in the form of stress resultants and moments as functions of reference surface strains and changes of curvature.

$$\begin{Bmatrix} N \\ \hline M \end{Bmatrix} = [K] \begin{Bmatrix} \epsilon \\ \hline \kappa \end{Bmatrix} \tag{2.7}$$

where

$$K = \left[\begin{array}{c|c} \int c\, dz & \int cz\, dz \\ \hline \int cz\, dz & \int cz^2\, dz \end{array}\right] \tag{2.8}$$

The derivation of the K matrix is further discussed in Section 3. The STAGS formulation is based on engineering strain. That is, it does not take necking phenomena into account and the results are valid only as long as the strains are relatively small, say below ten percent.

If inelastic deformations are included, the conservatism of the system is lost, even if the applied loads are conservative. However, this problem is readily circumvented. Both thermal expansions and inelastic strains (Eq. 2.5) can be considered as loading terms. Notice that the strain energy can be written

$$U = [\epsilon_{ij}]^T \; [c] \; [\epsilon_{ij} - \alpha T - \epsilon^P_{ij}] \tag{2.9}$$

For the purpose of structural analysis the only difference between αT and ϵ^P_{ij} is that α and T are independent parameters while ϵ^P_{ij} depends on the

deformation pattern. However, estimated values of the plastic strain define "pseudo-loads," and the elastic problem corresponding to this load is conservative. The values of the plastic strains can then be successively improved and if convergence is obtained, the nonconservative problem is solved by consideration of a series of conservative problems. The choice of plasticity theory is discussed in Section 4.

2.3 Kinematic Relations

The kinematic relations for the three-dimensional continuum are simply given by

$$\varepsilon_{ij} = \partial u_i / \partial x_j \qquad (2.10)$$

where the ε_{ij} are the six (note symmetry) components of strain. Nonlinear terms caused by rotations need generally not be included in the range of small strains. In the case of shell structures, a significant reduction in the amount of computations is achieved since the equations can be expressed in terms of two space variables. However, this reduction is not unique and the topic has been subject to much controversy. Here only the kinematic relations for a flat plate are considered (or in flat elements approximating a shell).

The thinness of the shell makes possible the reduction of the problem to one with two space variables. On the other hand, for a thin shell the rotations of structural elements can be quite large even in the range of small strains. Consequently, geometric nonlinearities are often important in thin shell analysis.

In derivation of the nonlinear kinematic relation, a line element of length dx is considered that is initially parallel to the x-axis and later displaced and deformed as shown in Figure 2.3. After the deformation, the length of the element is ds* and its left-end point is given by the coordinate values x*, z*. The displacements are denoted by u and w and the rotation by $\emptyset$. Hence

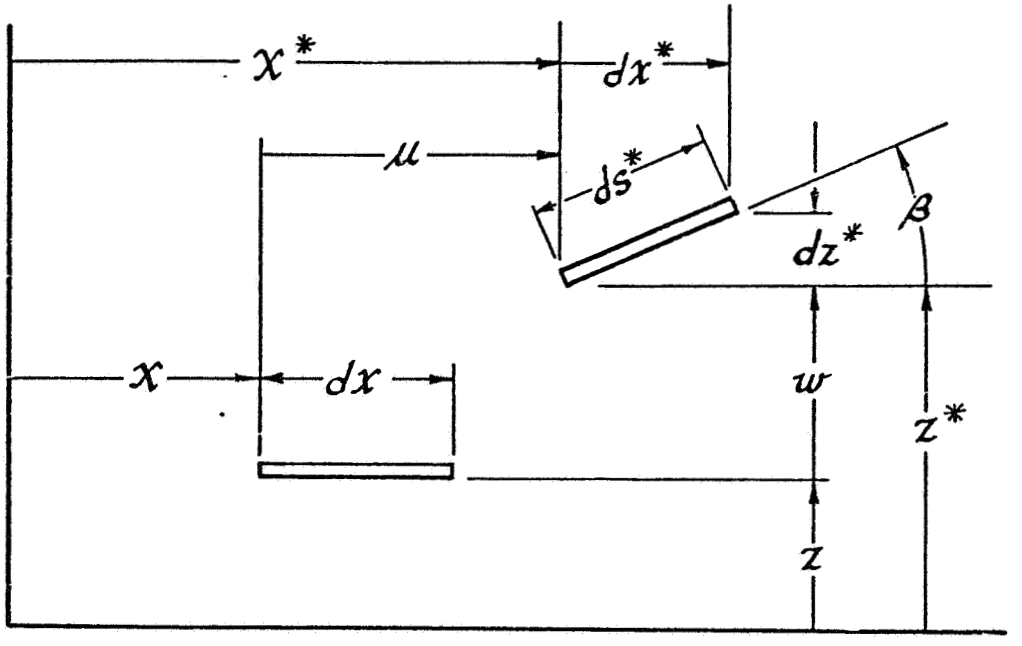

Figure 2.3. Line Element in Deformed State

$$x^* = x + u, \quad x^* = z + w \tag{2.11}$$

and

$$dx^* = dx\,(1 + u_{,x}), \quad dz^* = dx\,w_{,x} \tag{2.12}$$

From Fig. 2.3

$$(ds^*)^2 = (dx^*)^2 + (dz^*)^2 \tag{2.13}$$

It follows from Eqs. (2.12) and (2.13) that

$$\left(\frac{ds^*}{dx}\right)^2 - 1 = 2\,u_{,x} + (u_{,x})^2 + (w_{,x})2 \tag{2.14}$$

The definition of the strain

$$e_x = (ds^* - dx)/dx \tag{2.15}$$

can be rearranged into the form

$$e_x + 1/2\ \epsilon_x^2 = 1/2\ \left[\left(\frac{ds^*}{dx}\right)^2 - 1\right] \tag{2.16}$$

Substitution of Eq. (2.14) into Eq. (2.16) and the assumption that the strain is small so that $1/2\ \epsilon_x^2$ can be dropped in comparison to ϵ_x, leads to

$$e_x = u_{,x} + 1/2\ (u_{,x}^2 + w_{,x}^2) \tag{2.17}$$

It can be shown that this expression yields zero strain for a rigid body displacement. A pure translation will obviously not result in strain so it is sufficient to show that no strain is obtained if the line element rotates about its left end. In that case

$$\left.\begin{aligned} w &= x \sin \phi, \quad u = -x\,(1 - \cos \phi) \\ w_{,x} &= \sin \phi, \quad u_{,x} = -1 + \cos \phi \end{aligned}\right\} \tag{2.18}$$

That is from Eq. (2.17)

$$\varepsilon_x = u_{,x} + 1/2 \left[(u_{,x})^2 + (w_{,x})^2 \right] = -1 + \cos \phi$$
$$+ 1/2 \, (1 + \cos^2 \phi - 2 \cos \phi + \sin^2 \phi) \equiv 0 \tag{2.19}$$

For the case of small strains, Equation (2.17) gives zero strain under pure rotation of an element, independently of the size of the rotation.

For flat plates, the line segment may have one component of rotation in the plane of the plate and one in the normal plane that contains the segment. Consequently.

$$\varepsilon_x = u_{,x} + 1/2 \, (u_{,x}^2 + w_{,x}^2 + \phi^2) \tag{2.20}$$

where ϕ, as in Sander's (Ref. 2.4), shell equations represents a rotation about the normal. However, differently oriented line segments through the same point may rotate through different angles. In an orthogonal system the difference between the rotations of the two coordinate lines represents the shear strain. If ϕ represents an "average" rotation, we have

$$\gamma_{xy} = u_{,y} + v_{,x}$$
and $$\phi = 1/2 \, (u_{,y} - v_{,x}). \tag{2.21}$$

The strain in the x-direction obviously depends on in-plane rotation of a line segment in the x-direction.

Consequently, we have

$$\varepsilon_x = u_x + 1/2 \, (u_{,x}^2 + v_{,x}^2 + w_{,x}^2)$$
and $$\varepsilon_y = v_{,y} + 1/2 \, (v_{,y}^2 + u_{,y}^2 + w_{,y}^2) \tag{2.22}$$

2.4 Approximations and Special Procedures

The nonlinear equations of motion govern the structural behavior. These equations can usually not be solved analytically but numerical methods are applied so that a system with a finite number of degrees of freedom is obtained. Such a reduction to a finite number of degrees of freedom (discretization) is discussed in Section 6. Integration of the equations for the reduced system answers all questions about the behavior of the structure including those of static or dynamic instability. However, it is frequently possible to obtain satisfactory results for special purposes by introduction of certain approximations. Consequently, structural analysis usually consists of the application of one or more of a number of special procedures that are based on some simplification of the governing equations. Traditionally, these procedures (stability, vibrations, etc.) have been considered as separate disciplines having little to do with one another. The high-speed computer has opened more options to the analyst and in order to make the best possible use of available computer programs, he needs a good understanding of the theory and of the relations between the different types of analysis. These relations are illustrated in a block diagram in Figure 2.4.

The basic equations of motion for a discretized system may be written in the form

$$M \ddot{\underset{\sim}{u}} + D\ (\dot{\underset{\sim}{u}}) + B\ (\underset{\sim}{u}) + K\ (\underset{\sim}{u}) = \underset{\sim}{F} \qquad (2.23)$$

where $\underset{\sim}{u}$ is the vector of displacement components, M is the mass matrix, $\underset{\sim}{F}$ is a vector of external forces, and K the generally nonlinear stiffness operator. The operators B and D include forces that are functions of structural deformation and deformation velocity, respectively.

Clearly, if loads vary slowly, all time derivatives of displacement components may be disregarded and a static analysis is sufficient. If that is the case and if the system is conservative, the next question is whether nonlinear terms should be retained. Partly due to economical constraints, the linear static stress analysis has been by far the most commonly used mode of analysis.

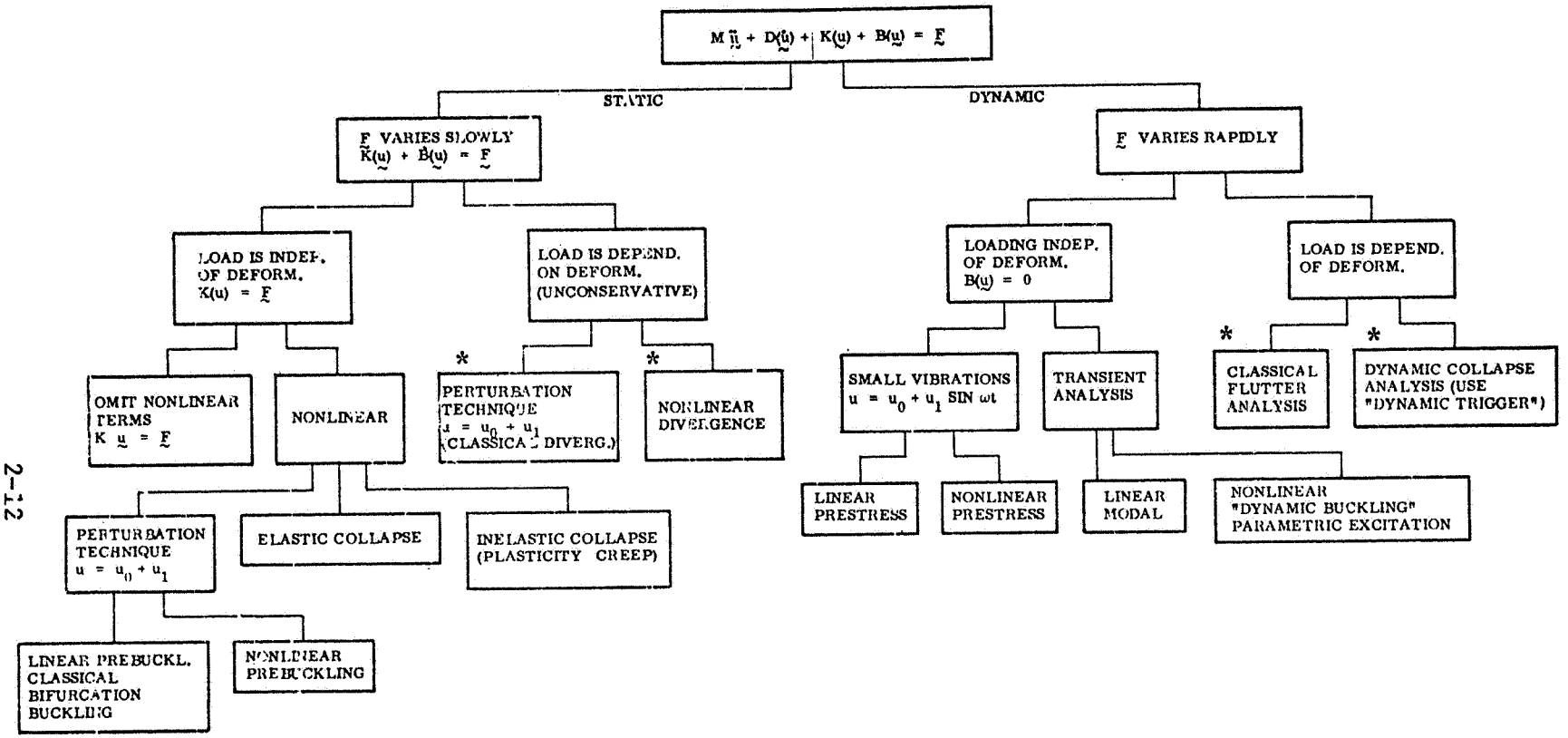

Figure 2.4. Approximations in Structural Analysis

If geometrical nonlinearities must be accounted for, it is possible to obtain limited, but sometimes sufficient, information about their effect without actually solving the nonlinear equations. A perturbation technique then is used, in which

$$\underset{\sim}{u} = \lambda \underset{\sim}{u}_o + \underset{\sim}{u}_1 \tag{2.24}$$

is substituted into the nonlinear equations. Here $\underset{\sim}{u}_o$ represents the solution of the basic equations after omission of nonlinear terms and λ is a load parameter to be determined. The perturbation $\underset{\sim}{u}_1$ is assumed to be small so that higher order terms in $\underset{\sim}{u}_1$ can be discarded. In addition, all terms that do not contain $\underset{\sim}{u}_1$ can be subtracted out by virtue of the fact that $\underset{\sim}{u}_o$ represents an equilibrium configuration. Hence, the equation system is homogeneous in $\underset{\sim}{u}_1$. The so-called bifurcation buckling load is represented by the value of λ that allows nontrivial solutions to this homogeneous equation system. If the precritical behavior is truly linear, the value of λ so computed represents a bifurcation in the load displacement diagram. The bifurcation buckling analysis can often be used as an approximation also for cases with nonlinear precritical behavior. For certain types of structures, such as shells of revolution, it is sometimes practical to consider bifurcation from a nonlinear prebuckling path.

Except for the case of the purely dissipative systems including structural damping or inelastic deformation discussed above, STAGS has not been adopted for solution of nonconservative problems but otherwise it includes all the analysis procedures in general use. This means that any type of analysis represented in the figure is included in STAGS except those marked with a star.

REFERENCES

2.1 Handbook of Engineering Mechanics, edited by W. Flügge, MgGraw-Hill, 1962.

2.2 Gallagher, R. H., Finite Element Analysis, Fundamentals, Prentice Hall, Englewood Cliffs, New Jersey, 1975.

2.3 Bolotin, V. V., Nonconservative Problems of the Theory of Elastic Stability, Pergamon Press, New York, 1963.

2.4 Cohen, G. A., Conservativeness of a Normal Pressure Field Acting on a Shell, AIAA J., Vol. 4, 1966, p. 1886.

Section 3
CONSTITUTIVE RELATIONS (ELASTIC)

The constitutive relations define the stiffness of the material, i.e., they express stresses in terms of strains. They were introduced in Section 2. The discussion here will be restricted to the relations between elastic strain and stress. The elastic strain is obtained after the plastic strain and the thermal expansion have been subtracted from the total strain. Strains due to creep are not included in STAGS. The method by which the plastic strain components are determined is discussed in Section 4.

The special form of the constitutive equations used in shell analysis gives stress resultants and moments in terms of elastic strain components and changes of curvature at a reference surface. The moments are given with respect to the reference surface, not necessarily the neutral surface. Approximations in shell or plate theory are based on the assumption that any point of the shell is close to the reference surface. Therefore, it is practical to define a reference surface close to the neutral surface.

This section is restricted to a discussion of the form of the constitutive equations that is used in the theory of deformation of shells and plates. The shell wall stiffness matrix C relates the stress resultants and moments to the strains and changes of curvature

$$\begin{Bmatrix} N_x \\ N_y \\ N_{xy} \\ M_x \\ M_y \\ M_{xy} \end{Bmatrix} = [C] \begin{Bmatrix} \epsilon_x \\ \epsilon_y \\ \gamma \\ \kappa_1 \\ \kappa_2 \\ 2\kappa_{12} \end{Bmatrix} \tag{3.1}$$

Unless the reference surface coincides with the neutral surface, there will be terms in the C matrix representing the coupling between membrane and bending action.

Even if nonorthogonal surface coordinates are used in STAGS, the stiffness matrix is formed in a set of orthogonal coordinates. The elements of the matrix are (internally to the computer code) transformed into the system of surface coordinates on which the shell equations are based.

Generally, the elements of the C matrix are obtained through integration of the elastic constants for the material through the thickness of the shell wall.

$$C = \left[\begin{array}{c|c} \int C_o \, dz & \int C_o \, z \, dz \\ \hline \int C_o \, z \, dz & \int C_o \, z^2 \, dz \end{array}\right] \tag{3.2}$$

where C_o is a 3x3 symmetric matrix.

$$C_o = \begin{bmatrix} E_{11} & E_{12} & E_{13} \\ E_{12} & E_{22} & E_{23} \\ E_{13} & E_{23} & G \end{bmatrix} \tag{3.3}$$

For an isotropic material $E_{13} = E_{23} = 0$, $E_{11} = E_{22} = E/(1-\nu^2)$, $E_{12} = \nu E_{11}$ and $G = E/[2(1+\nu)]$, For the isotropic monocoque shell, integration according to Eq. (3.2) leads to

$$\begin{aligned} C_{11} &= C_{22} = Et/(1-\nu^2) \\ C_{12} &= \nu C_{11} \\ C_{33} &= [(1-\nu)/2]\, C_{11} \\ C_{44} &= C_{55} = (t^2/12)\, C_{11} \\ C_{45} &= \nu C_{44} \\ C_{66} &= [(1-\nu)/2]\, C_{44} \\ \text{Otherwise } C_{ij} &= 0 \end{aligned} \tag{3.4}$$

The C matrix is readily obtained through the integration indicated in Eq. (3.2) also for shell walls with properties that vary through the thickness in a continuous fashion (thermal degradation) or discontinuously (layered shells).

The shell theory is based on the assumption that the shell wall is homogeneous, i.e., the material and geometric properties are slowly varying. However, it is possible and it has long been customary to approximate the behavior of heterogeneous shell walls, such as a skin with closely spaced ribs, by the use of an equivalent anisotropic (or orthotropic) skin. It is not always possible to find a shell wall that is truly equivalent. For example, in a shell wall composed of one corrugated and one smooth skin riveted or bonded together, the torsional stiffness in the axial direction is relatively large as the torque is carried by closed sections. However, the twist of the shell wall varies with the shell coordinates, and therefore the closed sections are subject to deformation of the cross section. This results in a reduction of the torsional stiffness that is dependent of the deformation pattern and cannot be estimated a priori. For deformation into a short wave pattern, the torsional stiffness is severely reduced, but in a long wave pattern (of buckling, for example) it may be possible to use the closed section stiffness without reduction. The use of an equivalent shell wall approximation is discussed in more detail in Reference 3.1.

In the following, a simple example is given for demonstration of the principles involved in derivation of the properties of an equivalent shell wall. Subsequently, the values of the elements of the C matrix are listed for the types of shell walls that have been included as standards in STAGS.

It is sometimes practical to base the derivation of the C matrix on an expression for the strain energy density of the deformed shell. The strain energy U is expressed in terms of strains and changes of curvature

$$U = U(\eta_i) \qquad i = 1 \text{ through } 6 \tag{3.5}$$

where

$$\{\eta_i\} = < \varepsilon_x, \varepsilon_y, \gamma, \kappa_1, \kappa_2, 2\kappa_{12} >^T$$

If an expression for the density of strain energy in terms of η is available, the coefficients of the C matrix are obtained from

$$C_{ij} = \partial^2 U / \partial \eta_i \partial \eta_j \tag{3.6}$$

As an example the elements of the C matrix are derived for an isotropic skin with a set of closely spaced stiffeners of rectangular cross section. As the skin stringer combination is replaced by a homogeneous shell wall, the contribution of the stringer to the shell wall is uniformly distributed. Stiffeners handled in this way are usually referred to as "smeared stiffeners." For simplicity it is assumed that the torsional stiffness and the resistance to a change in geodesic curvature of the line of attachment to the shell may be omitted. The classification of a structural component as a stiffener implies that all effects of warping and cross section deformation are neglected. Consequently

$$\begin{aligned}
\varepsilon_x &= \eta_1 + \eta_4 z && \text{in skin and stringer} \\
\varepsilon_y &= \begin{cases} \eta_2 + \eta_5 z & \text{in skin} \\ 0 & \text{in stringer} \end{cases} \\
\gamma &= \begin{cases} \eta_3 + \eta_6 z & \text{in skin} \\ \text{irrelevant} & \text{in stringer} \end{cases}
\end{aligned} \tag{3.7}$$

The geometric properties of the skin stringer combination are shown in Figure 3.1. The strain energy per unit area of the shell wall is

$$U = \frac{1}{2d} \int_V (\sigma_x \varepsilon_x + \sigma_y \varepsilon_y + \tau_{xy} \gamma) \, dV \tag{3.8}$$

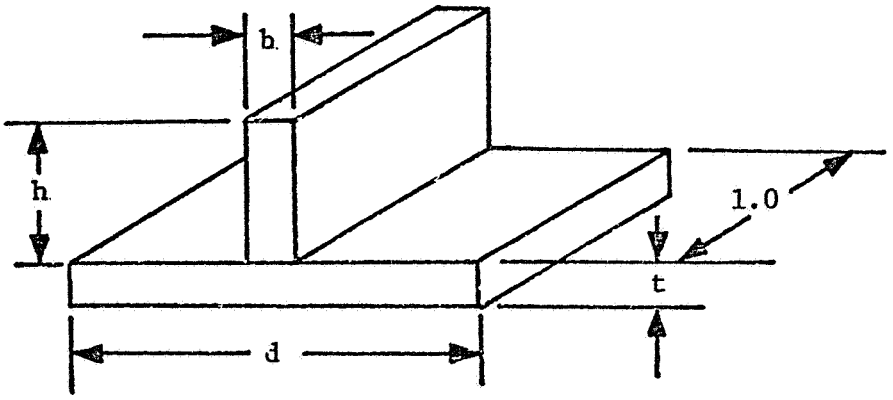

Figure 3.1 Shell Wall with Stiffener

By use of the stiffness matrix C_o for an isotropic material, the stresses are expressed in terms of the strains. After integration through the thickness, the contribution from the skin is

$$U_{SKIN} = \frac{Et_2}{2(1-\nu^2)} \left[\eta_1^2 + \eta_2^2 + 2\nu\,\eta_1\,\eta_2 + (1-\nu)/2\,\eta_3^2\right] + \frac{Et^3}{24(1-\nu^2)} \left[\eta_4^2 + \eta_5^2 + 2\nu\,\eta_4\,\eta_5 + (1-\nu)/2\,\eta_6^2\right] \tag{3.9}$$

Similarly the contribution from the stringer is

$$U_{STR} = \frac{Eb}{2d} \left[h\,\eta_1^2 + (h^2 + ht)\,\eta_1\,\eta_4 + \left(\frac{h^3}{3} + \frac{h^2 t}{2} + \frac{ht^2}{4}\right)\eta_4^2\right] \tag{3.10}$$

or with

$A = bh$ = stringer area

$I = bh^3/12$ = stringer moment of inertia

$e = (h + t)/2$ = stringer eccentricity

$$U_{STR} = \frac{E}{2d}\left[A\,\eta_1^2 + 2Ae\,\eta_1\eta_4 + (I + Ae^2)\,\eta_4^2\right] \qquad (3.11)$$

By use of Eq. (3.5)

$$C_{11} = \frac{Et}{1-\nu^2} + \frac{EA}{d} \qquad C_{22} = \frac{Et}{1-\nu^2}$$

$$C_{12} = \frac{\nu Et}{1-\nu^2} \qquad C_{33} = \frac{Et}{2(1+\nu)}$$

$$C_{14} = \frac{EAe}{d} \qquad (3.12)$$

$$C_{44} = \frac{Et^3}{12(1-\nu^2)} + \frac{E(I + Ae^2)}{d} \qquad C_{55} = \frac{Et^3}{12(1-\nu^2)}$$

$$C_{45} = \frac{\nu Et^3}{12(1-\nu^2)} \qquad C_{66} = \frac{Et^3}{24(1+\nu)}$$

For the standard types of shell walls the position of the reference surface is indicated in the User's Instructions (Volume 2). If the user decides to use another reference surface, he specifies a shell wall eccentricity. The properties are then adjusted in the computer program. For example, corresponding to an eccentricity of Z on the data card, the adjustments of C_{14} and C_{44} are

$$C_{14} = C_{14} + Z\,C_{11}$$
$$C_{44} = C_{44} - C_{14}^2/C_{11} + Z^2\,C_{11} \qquad (3.13)$$

REFERENCE

3.1 Bushnell, D., "Evaluation of Various Analytical Models for Buckling and Vibration of Stiffened Shells," AIAA J., Vol. II, Sept. 1973, pp. 1283-1291.

Section 4
THE THEORY OF PLASTICITY

The physical aspects of the strength of materials, in particular for polycrystalline materials, have been studied by the physicists for the last sixty years or so. The knowledge of the atomic structure and atomic bonds makes it possible to compute with relative accuracy the elastic modulii of metallic materials. In elastic deformation the bonds are strained. Plastic deformation is a much more complicated phenomenon because it includes the breaking of atomic bonds and the forming of new ones. The forces necessary to break the bonds depend on the existing defects in the atomic lattice. Due to extremely complicated interactions between dislocations, grain boundaries, impurities, etc., it does not seem likely that a purely physical theory of plasticity can be developed for use in engineering analysis.

Instead, phenomenological theories based on measurements on the macroscopic scale constitute the backbone of the practical plasticity analysis. Derivation of such a theory is still difficult because some variables defining the state of the material, such as distribution of atomic dislocations and configuration of microstresses, are not measured and not included in the analysis. The plasticity theory expressed in terms of the remaining parameters of state therefore becomes history dependent.

A phenomenological theory of plasticity is a procedure by which a set of constitutive equations in the multiaxial space can be derived from experimental results, usually on uniaxial test specimens. The classical theory of plasticity was developed during the first seventy years or so of research in the area.

This section contains a brief discussion of this development, including a review of its shortcomings. A few more recent theories that have been developed with the purpose of overcoming these difficulties are also presented. The state of the art in plasticity analysis is summarized, and the reason for the choice of plasticity theories for STAGS is explained. A more comprehensive summary of the state of the art is available in Ref. 4.1.

4.1 Classical Plasticity Theory

Efforts to define the relations between stress and strain in the plastic range begin with treatments by Tresca (1868), Sant-Venant (1870), and Levy (1871). The ideas first proposed by these pioneers were further developed by von Karman and Haar (1909), von Mises (1913), and others, resulting in analysis procedures which we refer to as the classical plasticity theories.

The basic elements deployed in the definition of the classical plasticity theory are:

- An initial yield surface, bounding the part of the stress space within which deformation is purely elastic.

- A flow law, indicating the "direction of plastic deformation," i.e., the ratios between the plastic strain components.

- A hardening rule, specifying the modification of the yield surface in the course of plastic deformation.

- A plastic modulus or hardening modulus, i.e., the ratio between increments in "effective stress" and "effective plastic strain." In the classical approach, this ratio is assumed to be independent of loading direction.

The classical theory was developed step by step as experimental data became available. Early efforts were devoted to establishment of the conditions for initial yield. Tresca's experiments led him to conclude that yield begins when the maximum shear stress reaches a critical level. It was also noticed that the plastic flow under pure hydrostatic pressure is negligible. This led to the definition of the deviatoric stress components and the suggestion by von Mises and others that the initial yield limit would be defined by the second invariant of these components.

Many experiments were performed with the purpose of deciding which of these two yield criteria would most accurately reflect the behavior of real materials. For most materials yielding begins gradually, and it is difficult to determine the point of yield even with the sophisticated equipment that is available today. Therefore, very carefully executed experiments failed to give a clear indication in any direction, although it appears that the von Mises theory would be the more accurate. The discussions in the following will be based on the assumption that initial yield is determined by von Mises' criterion.

Following Saint-Venant, von Mises assumed that increments in the components of plastic strain are proportional to the components of the deviatoric stress. This flow rule is identical to the criterion that a small increment in plastic strain is normal to the yield surface and is usually referred to as the normality condition. Also, it implies that plastic deformation takes place without change in volume, which is in agreement with experimental observation. Later Drucker (1954) justified the normality condition on the basis of energy consideration. Experimental support for the flow rule was provided by Lode in Reference 4.2. The work by von Mises was continued by Prandtl (1927) and Reuss (1930) through inclusion of the elastic components of strain. For materials without strain hardening the Prandtl-Reuss equations represent an acceptable set of constitutive equations. For strain hardening materials the definitions of the hardening laws and the hardening modulus present problems.

A uniaxial tension test with unloading followed by reloading exhibits the type of behavior indicated by the solid curve in Figure 4.1. It appears reasonable to assume that unloading as well as reloading up to the point of previous maximum stress takes place according to the elastic law and that unloading has no effect on the stress-strain relations on continued loading beyond the previous maximum.

With this idealized behavior on unloading and reloading, the yield surface must always pass through the point of previous maximum effective

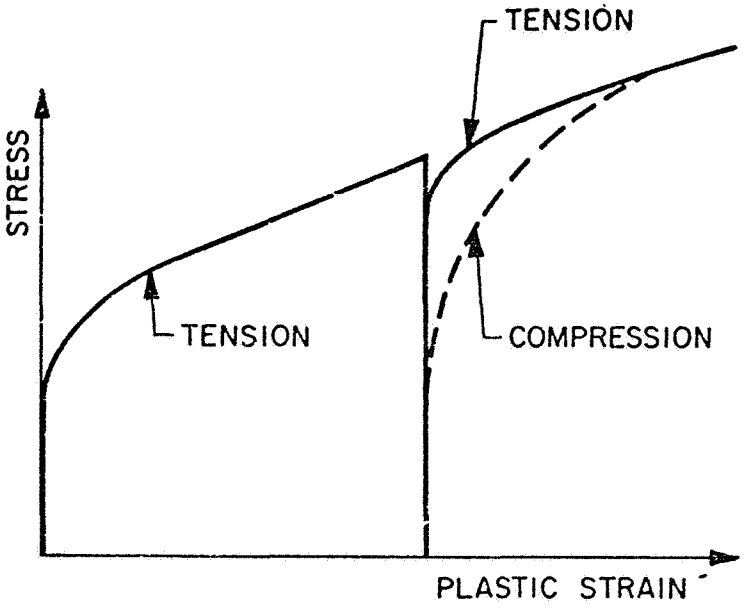

Figure 4.1. Typical Stress-Strain Relations

stress. Consequently, the yield surface is continually changing during the plastic deformation. The effective stress is implicitly defined by the yield condition since it must take on a constant value on the initial yield surface. The choice of the second invariant of the deviatoric stress components as a measure of the effective stress is consistent with the von Mises condition for initial yield. Loading takes place whenever the value of the effective stress is increasing and unloading corresponds to a decrease in its value. A path in the stress space corresponding to a constant value of the second invariant is called neutral loading.

The broken curve in Figure 4.1 shows a typical relation between stress and strain on stress reversal after loading in the plastic range. It is noticed that after a sufficiently deep reversed penetration into the plastic range the solid and broken curves coincide, i.e., the stress as a function of the total plastic strain is independent of the direction of the plastic flow. This leads to the conclusion that the effective plastic strain must be expressed as an integral of some function of the plastic strain increments. In view of the fact that plastic deformation takes place without change in volume, it appears logical to define the effective plastic strain as the

integral of the second invariant of the incremental components of plastic strain. This choice appears to be supported by available experimental results in Reference 4.3, for example.

If it is assumed that unloading and reloading to the same stress follows the elastic law and that the relation between effective strain and total plastic strain is independent of the loading direction, then the yield surface expands uniformly during plastic flow so that it always passes through the point of loading. According to this hardening law, the material remains "isotropic" during coldwork. Such isotropy is generally not exhibited by real materials, as indicated by the broken curve in Figure 4.1. However, in other respects this model of material behavior agrees with observation, and it is easy to apply. It is still by far the most commonly used theory of plasticity. It is referred to as the classical flow theory with isotropic strain hardening.

A major flaw in this theory is related to the difference between the tension and compression curves immediately upon the plastic strain reversal. This phenomenon was observed by Bauschinger (1886) who noticed that after coldwork in tension the compressive yield stress appears to be reduced approximately by an amount equal to the increase in the yield strength under the initial loading in tension. This observation led to the definition of the so-called kinematic strain hardening theory (Reuss, 1935; Prager, 1937; Shield and Ziegler, 1958). According to this criterion, the yield surface translates with loading in the plastic range without change in the shape or size. This theory is still based on the classical approach, i.e., the hardening modulus is independent on loading direction.

A theory of plasticity expressed in terms of total stresses and strains rather than in the increments was first presented by Hencky (1924). This approach was further pursued by many other investigators, notably by Nadai (1931). Such theories are referred to as deformation theories of plasticity. They are definitely repudiated by some experimental observations and they do not have a sound theoretical basis. The first serious

objection to the deformation theories (with elastic unloading) was raised on the grounds that they violate the continuity criterion. That is, a path in the stress space on the outside of but infinitesimally close to the path correspond to neutral loading will lead to a finite change in the plastic strain components while a similar path on the inside will result in no additional plastic strain. However, deformation theories are very easy to use and it has been shown in Reference 4.4 that whenever the curvature of the loading path in the stress space does not exceed a critical value the results obtained are practically identical to those from the classical flow theory.

4.2 Limitations of the Classical Theory

Early experiments were designed to shed some light on the question of whether a deformation theory or a flow theory would be more adequate for practical plasticity analysis (Refs. 4.5 and 4.6). Although more acceptable from a theoretical point of view, the flow theory did not appear to predict experimental results more closely than the deformation theory. The experimental results were obtained by use of tubular test specimens subjected to tension/compression or internal pressure in combination with torsion. The initial application of torsion to a specimen that is loaded beyond yield in tension would correspond to neutral loading according to the classical flow theory. Consequently, the instantaneous shear modulus would take on its elastic value. Generally this was not found to be the case, but the shear modulus was considerably reduced.

Experiments on the buckling of plates and shells in the plastic range did consistently show better agreement with the predictions of deformation theory, Reference 4.7. Such results are consistent with the observation that the instantaneous shear modulus is less than its elastic value for a material subjected to normal strains in the plastic range. The results from application of flow theories to bifurcation buckling problems are generally unconservative because the inplane shear stiffness is overestimated. The problem of plastic buckling has been discussed extensively by Hutchinson in Reference 4.8.

One of the problems that was encountered at an early stage in the development of the theory was the Bauschinger effect. The kinematic hardening model was specifically developed in order that this effect would be accounted for. In Figure 4.2, a comparison is made of the results from the isotropic and kinematic hardening rules to the typical behavior of a metal under uniaxial loading with reversal. Also shown are results from an analysis procedure in which kinematic hardening is used in connection with bi-linear representation of the stress-strain curve. This procedure is presently recommended by AEC in Reference 4.9 for use in the case of cyclic uniaxial loading.

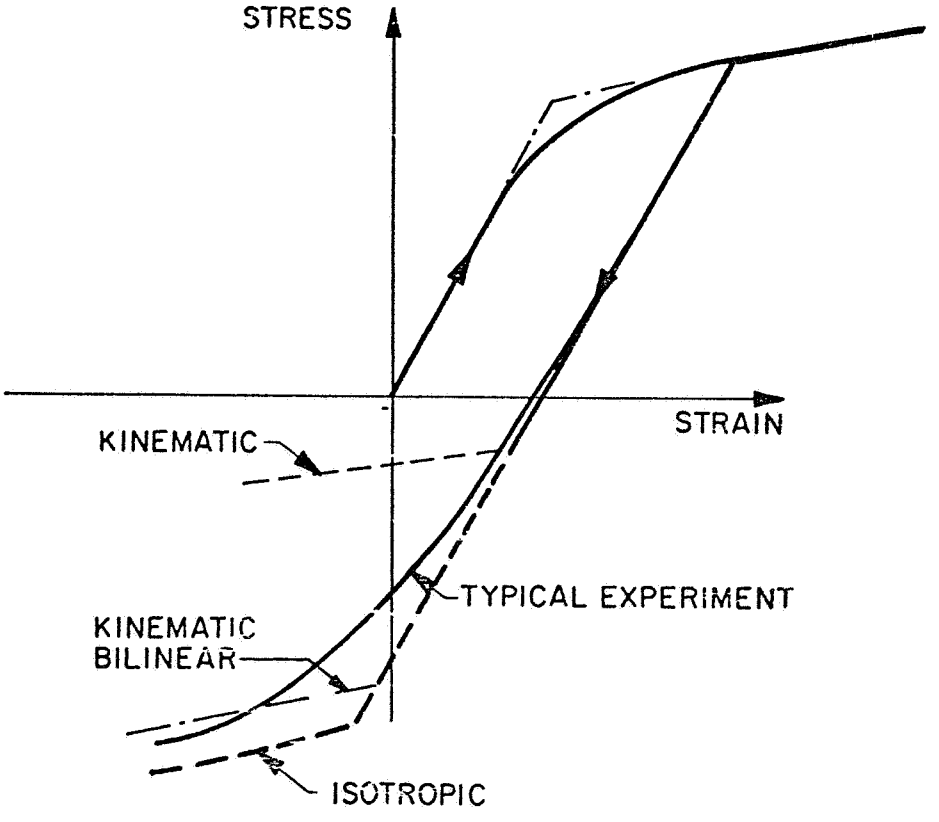

Figure 4.2. Stress-Strain Curves with Stress Reversal

Experiments seem to indicate that after loading, in tension, for example, beyond the elastic limit the yield stress in compression had decreased approximately by the same amount as the increase in the yield stress

in tension. However, the so-called hardening modulus, the rate at which the stress increases with the effective plastic strain, is greater at the onset of plastic deformation in compression, so that after a sufficiently large reversed penetration into the plastic range experimental results again come close to the predictions by the theory with isotropic strain hardening. The kinematic strain hardening rule does not account for this change in hardening modulus. Therefore, it does not appear to represent an improvement on the isotropic strain hardening rule, except possibly for the case in which a bilinear stress strain curve provides a satisfactory representation.

The problem illustrated in Figure 4.2 is a reflection of the inability of the classical theory to cope with plastic anisotropy. Unfortunately, most metals as used in engineering applications show some initial anisotropy. Two types of plastic anisotropy may occur:

- "Crystallographic anisotropy" which is associated with the texture, i.e., nonisotropic distribution of crystal orientations, observable in x-ray investigations.

- Coldwork-generated anisotropy of which the Bauschinger effect is the most generally recognized example. Since coldwork generates microstresses, initially isotropic materials will tend to become anisotropic during plastic deformation. The Bauschinger effect may be defined as inelastic anisotropy caused by coldwork-generated microstresses.

Hill (Ref. 4.10) has presented an extension of the classical theory to include initial anisotropy. The theory consists of the definition of an initial yield surface to be used in connection with an associated flow law. As long as the hardening modulus is a function of the effective plastic strain only, the theory fails to account adequately for the modifications of the anisotropy that may occur as a result of loading into the plastic range (generalized Bauschinger effect).

4.3 Other Theories

The failure of the classical theories to predict the material behavior in certain situations brought about the development of new theories and the introduction of new concepts. Duwez (1935) introduced the idea of a material consisting of a number of separate components, which all undergo the same strain history. If the components behave in a simple manner in the plastic range and have different material properties, the composite will exhibit the complex type of behavior that is characteristic of real materials.

A similar plasticity theory was presented by White (1950) and the concept was further extended and refined by Besseling (Ref. 4.11). This type of plasticity analysis is referred to here as a White-Besseling theory. Since all the difficulties in the definition of a plasticity theory seem to be related to the strain hardening, it appears advantageous to assume that all the separate components exhibit ideal plasticity (plastic flow under constant stress). The different components have different yield strengths. If the components have the same elastic modulus and if they are subjected to the same strain, the yield stress of the composite will be the same as that of the weakest of its components. However, since the other components can take additional load, the composite will exhibit strain hardening with a piecewise linear stress-strain curve.

If the stress is reversed after loading beyond the yield limit for one or more components, yield will occur in the reversed direction when the average stress in the composite reaches the value $\sigma = \sigma_1 - 2\sigma_y$ where σ_1 is the maximum stress during initial loading and σ_y corresponds to the yield limit for the weakest components (the initial yield limit for the composite) (see Fig. 4.3). As in the kinematic strain hardening theory, the yield stress under the reversed load occurs at a level that is reduced by the amount of strain hardening for loading in the initial direction. However, in contrast to the kinematic theory, the White-Besseling theory gives a hardening modulus at the outset of reversed yield which equals the hardening modulus at initial yield. This agrees well with the experimentally

observed material behavior. Due to the formation of a system of self-balancing stresses in the separate components, plastic anisotropy develops automatically in the model during loading in the plastic range.

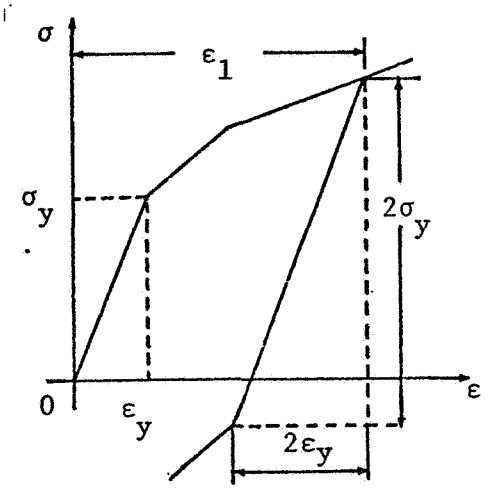

Figure 4.3. Stress-Strain Relations According to White-Besseling Theory

In this form of the White-Besseling theory for plastic analysis, the material behavior is defined through specification of

- The number of material components
- The relative volume of each component
- The yield strength of each component

Use of only one component results in the application of ideal plasticity. With two components of which one has an infinite yield limit (in practical application large but finite), the White-Besseling theory becomes identical to the kinematic strain hardening theory with a bilinear stress-strain curve.

The difficulties with the classical theory, in particular the failure of the flow theory in buckling analysis, inspired Batdorf and Budiansky (1949) to re-examine the problem of plastic deformation. These investigators attempted to utilize the insight into the physics of metallic materials in a mathematical plasticity theory. The approach is based on the

concept of slip and is therefore referred to as a slip theory. The slip theory as presented by Batdorf and Budiansky (Ref. 4.12) does indicate a reduction in the shear modulus in the presence of normal strain in the plastic range. The agreement is only of a qualitative nature as the slip theory overestimates the reduction in shear stiffness. The Batdorf-Budiansky slip theory leads to excessive numerical manipulations and it fails to predict the creation of plastic anisotropy with coldwork. While it is doubtful that the concept can be modified so that it becomes useful in engineering analysis, it has served its purpose by demonstrating the possibility of defining models that give better results than the classical theories for the tension-torsion case.

Mroz (Ref. 4.13) introduced the concept of "a field of work-hardening modulii." That is, he introduced a number of different yield surfaces. On loading, all of these surfaces are being shifted in stress space according to the rules of kinematic hardening. The hardening modulus depends on how many of the moduli are currently active. The results obtained by use of the Mroz model are almost identical to those obtained by use of the White-Besseling theory. Other models of material behavior have recently been presented that employ non-intersecting yield and loading surfaces.

Dafalias and Popov (Ref. 4.14) and Krieg (Ref. 4.15) presented independently and almost simultaneously very similar models of this type which improve the representation of material behavior for reversed plastic loading. The yield surface is always contained inside a limit surface. Both yield and limit surfaces can change with plastic loading. The isotropic or the kinematic hardening rules or combinations of the two can be applied. The hardening modulus is expressed as a function of the distance in the stress space from the point of loading to the limit surface along the normal to the yield surface. If the hardening modulus is proportional to this distance, the material behavior on reversed yield is equally well represented as in the White-Besseling theory. The advantage with the "Two-Surface" model is that a piecewise linear representation of the stress-strain relation is not needed.

4.4 The State of the Art

Although some efforts have been devoted to evaluation of the proposed procedures for inelastic analysis, many questions remain unanswered. The early efforts to determine the relative merits of the Tresca and von Mises criteria for initial yield and the comparisons between the flow and deformation theories led to inconclusive results. Later experiments (Ref. 4.16) indicate that the flow theory gives a relatively good prediction for the loading sequence torsion-tension-torsion but fails for the sequence tension-torsion-tension.

The yield surface corresponding to the Batdorf-Budiansky slip theory exhibits a corner at the end of the loading. This tends to explain why the classical flow theories led to unconservative results in buckling analysis. After publication of the slip theory, many experiments were carried out with the purpose of determining whether or not such corners did exist. Again, the results were inconclusive.

Clearly, there are several mathematical models of material behavior with merits that warrant their inclusion in computer programs for inelastic structural analysis. The isotropic strain hardening theory in many cases leads to results that are as good as those obtained by use of more complex material models. Since such factors as computer run time and storage capacity must be considered, the isotropic strain hardening theory probably should be retained as an option in an efficient computer program.

At the ONR workshop on strain hardening at Texas A&M 1975, two types of situations were identified in which many of the commonly used theories appear to be inadequate. Results presented by Hunsaker, et al. (Ref. 4.17) indicate that the isotropic strain hardening and the kinematic strain hardening rules yield poor results in the case of cyclic loading. On the other hand, the "mechanical sublayer" (White-Besseling) and the Mroz models represent actual material behavior reasonably well. The models presented by Krieg and by Dafalias and Popov improve considerably on the classical theories in the case of cyclic loading.

For bifurcation buckling analysis the classical flow theory or one of the more sophisticated theories, if appropriate, can be used for the prebuckling analysis. However, for determination of the incremental stiffness corresponding to buckling, the analyst is advised to rely on the deformation theory.

Special problems occur when the loading is cyclic, i.e., the loading in the plastic range is reversed a number of times. Accurate representation of cyclic hardening or softening phenomena may require that a hardening modulus is defined that varies with the number of cycles experienced by the material.

The other situation in which difficulties are apparent is the case in which sharp turns, other than full-reversal, occur in the loading path in the stress space. Such turns may occur for example, during buckling or collapse. Experiments indicate that even the more sophisticated theories fail to represent adequately the incremental stiffnesses at or immediately after such turns. There is in fact little evidence to indicate that any of the theories so far proposed give acceptable results except for near-proportional loading, including reversal on a proprotional path. Other loading histories are referred to as complex loading. Cases with complex loading have been presented (e.g., Refs. 4.16 and 4.18) in which the flow theory with isotropic strain hardening gives exceptionally poor results. With the possible exception of a slip theory, it seems unlikely that any material model so far proposed will lead to reasonably accurate results for the cases considered.

Three separate cases can be distinguished:

- Near-proportional monotonic loading; for this case all commonly used theories result in practically identical results for analysis of initially isotropic materials.

- Uniaxial loading with reversal; for this case the classical theories fail to represent the actual material behavior but more sophisticated models have been developed and appear to be adequate.

- Complex loading; for this case little is known about the applicability of available theories.

4.5 Solution Techniques

Independently of which plasticity theory has been chosen, two basically different techniques are appropriate for solution of inelastic structural problems based on the displacement method. These may be termed (Ref. 4.19, for example) the pseudo force method (also referred to as the initial strain method) and the tangent stiffness method.

The pseudo force method is named so becasue the inelastic strains (creep or plasticity) are treated in the same way as if they were applied forces. That is, their contributions appear only on the right-hand side of the equation system. The validity of this approach is discussed above in relation to Eq. (2.9). The following outline of the procedure in the pseudo force method applies with the use of any incremental (flow) theory.

At any time during the computations, an estimate of the values of the degrees of freedom of the system, displacement and rotation components, is available. Generally, the solution vector in previous iterations is used. For the first iteration at a load or time step, the estimate is obtained through extrapolation from the previous solutions. Values of the plastic strain in previous steps are saved, or equivalently, stresses and total strains are saved so the elastic and plastic parts of the strain can be determined. Based on current total strain, computed from the displacement configuration, and total plastic strain in previous load or time step, the plasticity theory allows the computation of current plastic strains. These strains correspond to pseudo forces which are used when the total displacements are computed in the next iteration. The iterative procedure has

converged when the computed and estimated solution vectors agree within predetermined bounds. At that point the requirement of minimum elastic energy as well as that of the plasticity theory are satisfied.

The psuedo force method has the advantage that reformulation and factoring of the second variation is avoided except when required due to geometric nonlinearities. Whenever the stress strain curve has a relatively small slope, the convergence with the pseudo force method may be very slow because the second variation derived from the left-hand side of the equation system corresponds to elastic deformation. If nonlinear terms are allowed to affect only the right-hand side of the equation system, the convergence cannot be improved by refactoring.

In the tangential stiffness method the effects of inelastic deformation are introduced on the left-hand side of the equation system, i.e., the stiffness matrix is modified so that it includes inelastic effects. If {n} represents the components (in the stress space) of the unit normal to the yield surface, the increments in plastic strain can be written in the form

$$\{\Delta\varepsilon^P\} = \{n\}\,\Delta\bar{\varepsilon}^P \tag{4.1}$$

where $\Delta\bar{\varepsilon}^P$ is the increment in total plastic strain, a scalar.

A matrix $[C^P]$ is defined so that

$$\{\Delta\varepsilon^P\} = [C^P]\,\{\Delta\varepsilon - \Delta\varepsilon^T\} \tag{4.2}$$

where the components of ε^T represent the thermal expansion. If [C] represents the elastic stiffness matrix

$$\begin{aligned}\{\Delta\sigma\} &= [C]\,(\Delta\varepsilon - \Delta\varepsilon^T - \{n\}\,\Delta\bar{\varepsilon}^P) \\ &= [C]\,([I] - [C^P])\,\{\Delta\varepsilon - \Delta\varepsilon^T\}\end{aligned} \tag{4.3}$$

The tangential stiffness matrix then is given by the relation

$$[C^T] = [C]\,([I] - [C^p]) \tag{4.4}$$

where [I] is the identity matrix. The components of the normal {n} are determined by the stress field at the beginning of the load step. Therefore, $[C^T]$ can be determined from an estimate for $\Delta\bar{\varepsilon}^p$. At each load or time step the plasticity theory and the equations of motion (or equilibrium) are enforced to give a corrected value of the total plastic strain $\Delta\bar{\varepsilon}^p$. Convergence is obtained when the corrected value agrees with the estimate. The tangent stiffness method has the advantage that it allows improvement of the convergence rate through updating of the second variation (the first variation can be computed without reference to a tangential stiffness). The matrix $[C^T]$, therefore, needs to be computed only when slow convergence requires refactoring of the coefficient matrix. Possibly, the use of the tangent stiffness method may lead to convergence difficulties, if unloading begins at a significant part of the structure of the same load or time step.

A subincremental technique is sometimes used in plasticity analysis. This system allows the use of larger step size. It is described in detail in Reference 4.20. Whenever material rather than geometric nonlinearities are critical, the choice of step size is governed by two factors. The first is related to the assumption that the plastic strain increment vector is normal to the yield surface at a point determined by the stresses at the beginning of the step. Consequently, the step must be small enough so that changes in the direction of the normal to the yield surface from one step to another are insignificant. Secondly, at any iteration the application of the plasticity theory involves the solution of a nonlinear equation system (of rank three for a first order shell theory). If the step size is too large, this nonlinear system may not have a real solution.

In the subincrement method the total strain increment, as obtained from extrapolation or previous iteration, is subdivided into a

number of subintervals. For each of these the plastic strain increment can be made small enough so that the equations based on the plasticity theory always have a solution and so that the effects of the difference in direction of the normal to the yield surface between two adjacent subintervals can be neglected.

4.6 Plasticity Theory in STAGS

STAGSC-1 includes the classical theories with isotropic or kinematic strain hardening and the deformation theory. In addition, the White-Besseling theory is included for use in cases with more complex loading history. This theory is easily applied to simulate ideal plasticity and for representation of the kinematic strain-hardening model with a bilinear stress strain relation

The solution technique in STAGS is based on a mixture of the pseudo force and the tangential stiffness method. The first variation is generally computed based on the pseudo force method. However, if convergence difficulties are recurring, the tangential stiffness based on $[C_T]$ will be periodically updated unless such action is disallowed by user input.

The White-Besseling plasticity theory is implemented in the computer program in the following manner:

(1) The inelastic behavior of the material is defined through specification of:

- The number of components
- The relative volume of each component
- The yield strength for each component

(2) The strains are estimated for all points in the shell over the shell coordinates and through the thickness. This generally is done through extrapolation from previous solutions.

(3) A subroutine is called within which, for each of the material components, the stresses corresponding to the assumed strains are determined. The total stresses for the composite are computed.

(4) Once total strains and stresses are known, the plastic part of the strain increment can be determined and added as a pseudo-load in an elastic analysis.

(5) New strains are computed and used as estimates. The procedure is continued until the computed strains agree to within a given margin with the estimated strains.

REFERENCES

4.1 Knets, I. V., Fundamental Modern Direction in the Mathematical Theory of Plasticity (in Russian), Zinatne Press, Riga USSR, 1971. Translated to English by Morris Friedman, Lockheed MSC, Palo Alto, Ca. (available through National Translation Center, Chicago, Ill.).

4.2 Lode, W., Versuche über den Einfluss der Mittleren Hauptspannung auf das Fliessen der Metalle, Eisen, Kupfer und Nickel, Z. Für Physik, Vol. 36, March-May 1926, pp. 913-939.

4.3 Lubahn, J.D., "Bauschinger Effect in Creep and Tensile Tests on Copper," J. of Metals, Vol. 7, No. 9, September 1955, pp. 1031-1033.

4.4 Budiansky, B., "A Reassessment of Deformation Theories of Plasticity," J. Appl. Mech., Vol. 26, No. 2, June 1959, pp. 259-264.

4.5 Hohenemser, K., and Prager, W., Z. Für Ang. Math. und Mech., Vol. 12, No. 1, February 1932, pp. 1, 14.

4.6 Batdorf, S. B., "Theories of Plastic Buckling," J. A. S., Vol. 10, No. 7, July 1949, pp. 405-408.

4.7 Bijlaard, P. P., "Theory and Tests on the Plastic Stability of Plates and Shells," J. A. S., Vol. 16, No. 9, September 1949, pp. 529-541.

4.8 Hutchinson, J. W., "Plastic Buckling," Advances in Appl. Mech. (Ed. by C. S. Yih), Vol. 14, Academic Press, 1974, pp. 67-143.

4.9 Anon, "Requirements for Design of Nuclear System Components at Elevated Temperatures (Supplement to ASME Code Case 1331) - Vol. II, Div. of Reactor Research and Development, U. S. Atomic Energy Commission, 1973.

4.10 Hill, R., "Theory of Yielding and Plastic Flow of Anisotropic Metals," Proc. Roy. Soc., A 193, 1948, pp. 281-297.

4.11 Besseling, J. F., "A Theory of Elastic, Plastic, and Creep Deformation of an Initially Isotropic Material Showing Strain Hardening, Creep Recovery and Secondary Creep," J. Appl. Mech., Vol. 25, No. 4, Dec. 1958, pp. 529-536.

4.12 Batdorf, S.B., and Budiansky, B., "A Mathematical Theory of Plasticity Based on the Concept of Slip," NACA TN 1971, April 1949.

4.13 Mroz, Z., "An Attempt to Describe the Behavior of Metals Under Cyclic Loads Using a More General Work Hardening Model," ACTA Mech., Vol. 21, March 1975, pp. 173-192.

4.14 Dafalias, Y. F., and Popov, E. P., "A Model of Nonlinearly Hardening Materials for Complex Loading," ACTA Mech., Vol. 21, March 1975. pp. 173-192.

4.15 Krieg, R. D., "A Practical Two-Surface Plasticity Theory," J. Appl. Mech., Vol. 42, No. 3, September 1975, pp. 641-646.

4.16 Hunsaker, B., Vaughan, D. K., and Sticklin, J. A., "A Comparison of the Capability of Four Hardening Rules to Predict a Material's Plastic Behavior," Texas Engineering Experiment Station, Proc. of the Office of Naval Research Plasticity Workshop, June 1975, pp. 27-65.

4.17 Gill, S. S., "Three Neutral Loading Tests," J. Appl. Mech., Vol. 23, No. 4, December 1956, pp. 497-502.

4.18 Smith, S., and Almroth, B. O., "An Experimental Investigation of Plastic Flow Under Biaxial Stress," Exp. Mech., Vol. 10, No. 6., June 1970, pp. 217-224.

4.19 Marcal, P. V., "Finite-Element Analysis with Material Nonlinearities - Theory and Practice," in Recent Advances in Matrix Methods of Structural Analysis and Design, University of Alabama Press, 1971, pp. 257-282.

4.20 Bushnell, D., "A Strategy for the Solution of Problems Involving Large Deflections, Plasticity and Creep," Int. J. Num. Meth. in Eng., Vol. 11, 1977, pp. 683-708.

Section 5
GEOMETRIC NONLINEARITIES

5.1 Introduction

The shallow link system in Figure 5.1 illustrates the effect of geometric nonlinearity on the structural behavior. Figure 5.1a shows the case in which the load is directed so that tension develops in the links. As the links are extended, the angle θ increases and the ratio between the reaction force N and the applied load becomes smaller. The result is that the structure stiffens with increasing load as is indicated by the diagram showing the load P versus the deformation δ.

In Figure 5.1b the load is applied in the opposite direction. The angle between the links becomes less favorable as they shorten under compressive forces. The structure is continuously softening until at the limit point, $P = P_{MAX}$, the slope of the load displacement curve vanishes.

A perfectly straight, centrally loaded column is shown in Figure 5.2a. If the column is given a slight displacement, the internal elastic forces will tend to restore the column to its original straight form. The external force P gives rise to a bending moment that tends to increase the deformation. For sufficiently small loads, the elastic forces dominate and the straight form is the only possible equilibrium configuration. However, if P exceeds some value, say $P > P_{CRIT}$, the column can be maintained in a bent equilibrium form. This is a result of geometric nonlinearity. For sufficiently small loads, the straight column is the only possible equilibrium form; the deformation pattern exhibits no rotations and the column behavior is linear. However, due to the nonlinear character of the governing equations, secondary solutions corresponding to bent equilibrium forms, do also exist, although not in the immediate neighborhood of the origin of the load displacement diagram.

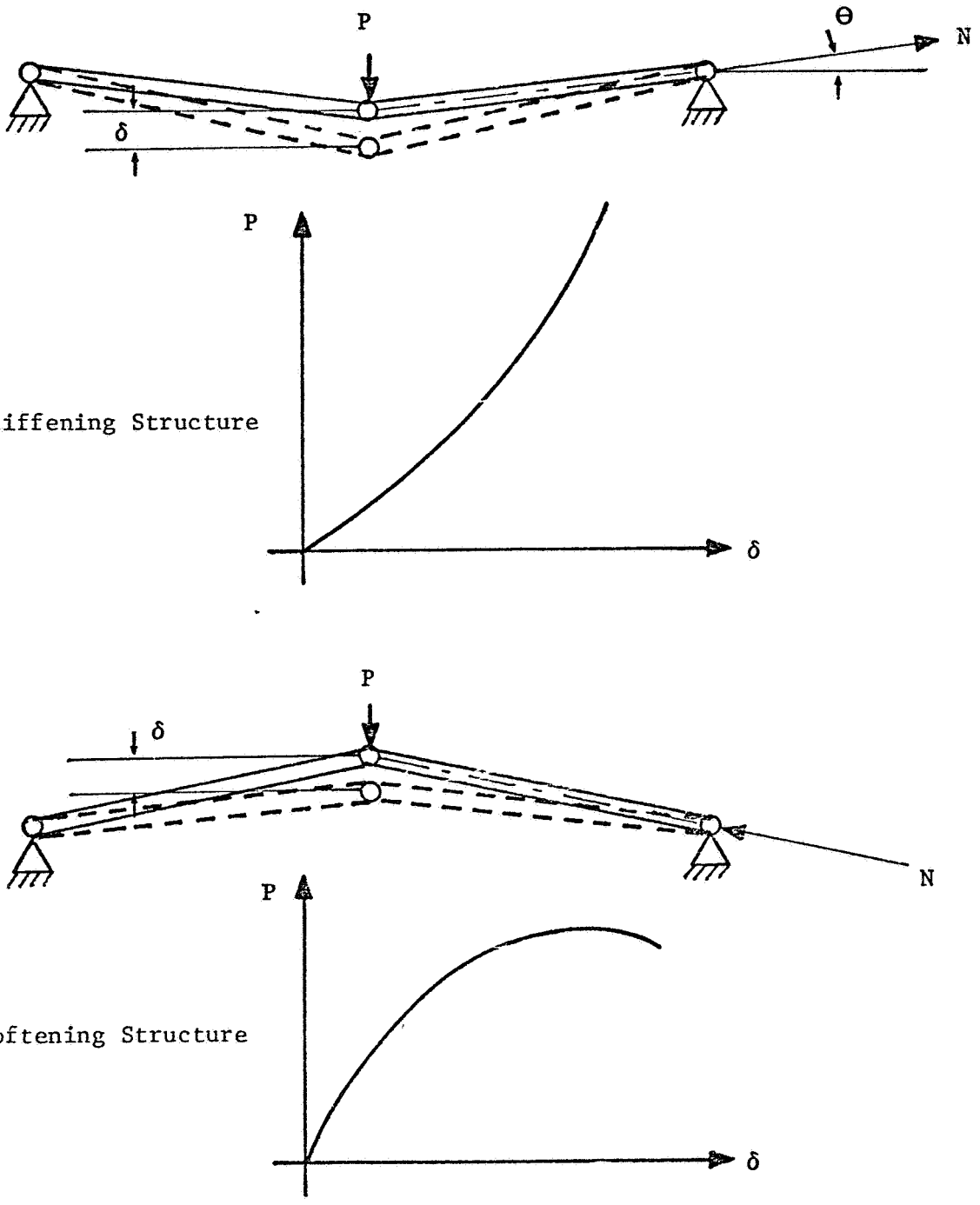

Figure 5.1. The Effects of Geometric Nonlinearity

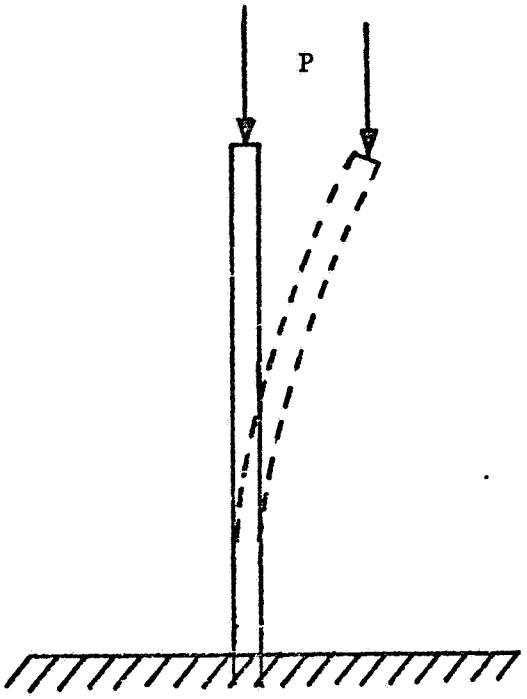

a) A Conservative System

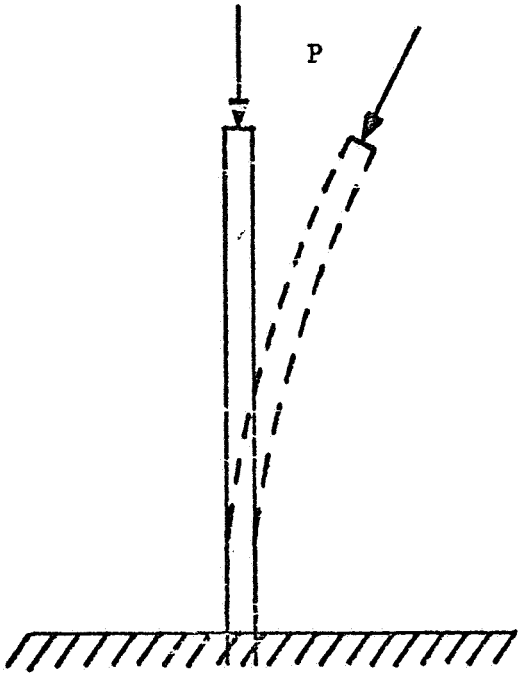

b) A Nonconservative System

Figure 5.2. Columns Under Axial Load

The column in Figure 5.2b illustrates the possible behavior of a nonconservative system (see Section 2). The load, a following force, is now directed along the tangent to the deformed column. In this case, the external force as well as the elastic forces tend to restore the column to its initial straight shape. If we release the column after giving it a small displacement, it will start to vibrate around its equilibrium configuration. The amplitude of the vibration will increase with time if the following force is sufficiently large. In that case, the smallest disturbance will eventually result in a violent motion. The critical load in this case is the load level at which self-induced vibrations develop.

In summary, geometric nonlinearities are the source of the follow-types of behavior:

- The structure stiffens with deformation;
- The structure weakens with deformations so that its load carrying capability is limited;
- Secondary solutions of the governing equations may affect the structural behavior; and
- Self-induced vibrations develop at some critical load level.

5.2 The Concept of Stability

The last three of the types of behavior listed above are related to the concepts of buckling and structural stability. The word buckling conveys a visual conception of the structural deformation and does not have a universally accepted scientific definition. Therefore, it is better to avoid use of the word in a discussion of the effects of geometric nonlinearities. Our interest is in the load limit below which deformations and stresses are of acceptable magnitude. Structural stability is a useful concept in a discussion of means to determine this load level. For simplicity, the discussion is at first limited to static systems.

The definition of stable equilibrium of a deformable body follows as an obvious extension of the concept of stable equilibrium of a rigid body. A given displacement field u corresponds to stable equilibrium if any additional permissible (by continuity and boundary conditions) displacement field Δu of sufficiently small amplitude produces elastic forces that tend to restore the basic displacement field u. This is equivalent to the requirement that the displacment field u corresponds to a true minimum of the total potential energy. The body is in unstable equilibrium if the potential energy has a maximum or an inflexion with zero slope with respect to at least one of its degrees of freedom. For the shallow link system shown in Figure 5.1b the load displacement relation representing static equilibrium is indicated in Figure 5.3. The equilibrium is stable on the parts of the curve at which the load increases with the deformation, and it is unstable (as indicated by a dotted line) in the range where the curve has a negative slope. If the load is increased beyond the limit point at A, there is no equilibrium configuration available in the immediate neighborhood. Therefore, the structure must be set in motion. In this particular case, the link system "snaps through" into a configuration at point B with tension forces in the links.

For sufficiently small loads, a centrally loaded column exhibits no rotation in its deformation pattern. In the range of small strain, its behavior is linear. The path in the load displacement diagram that passes through the origin is referred to as the primary path. If the path depicts the maximum lateral displacement versus axial load it will coincide with the vertical axis (Figure 5.4). Due to the nonlinear character of the governing equations, secondary solutions corresponding to bent equilibrium forms do also exist, although not in the immediate neighborhood of the origin. Whether or not the primary path is linear, there is a possibility that it is intersected by a path corresponding to a secondary solution as indicated in Figure 5.4. The point of intersection between the two load paths is referred to as a bifurcation point and the corresponding load is called the bifurcation buckling load.

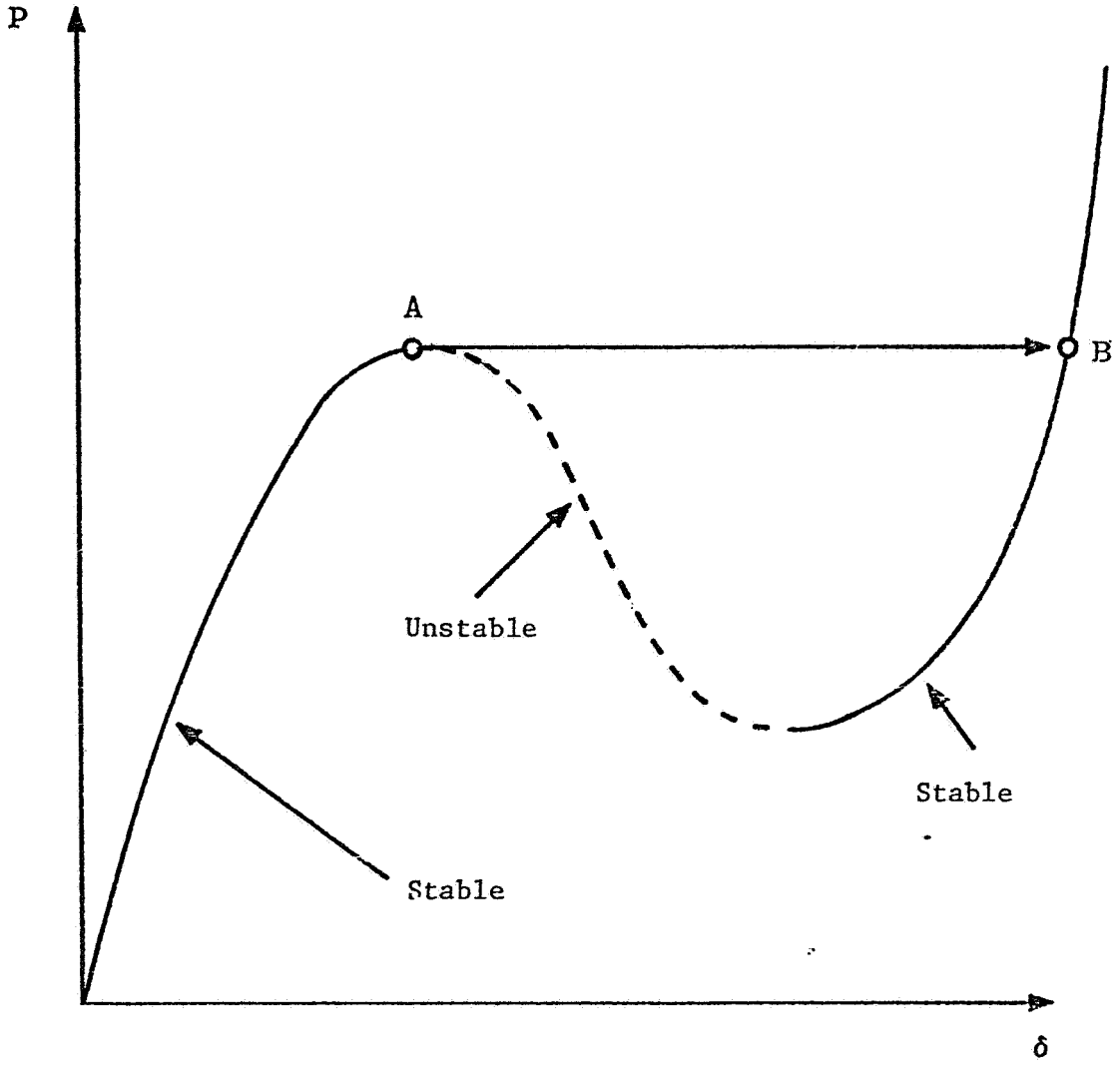

Figure 5.3. Load Displacement Curve for a Shallow Link System

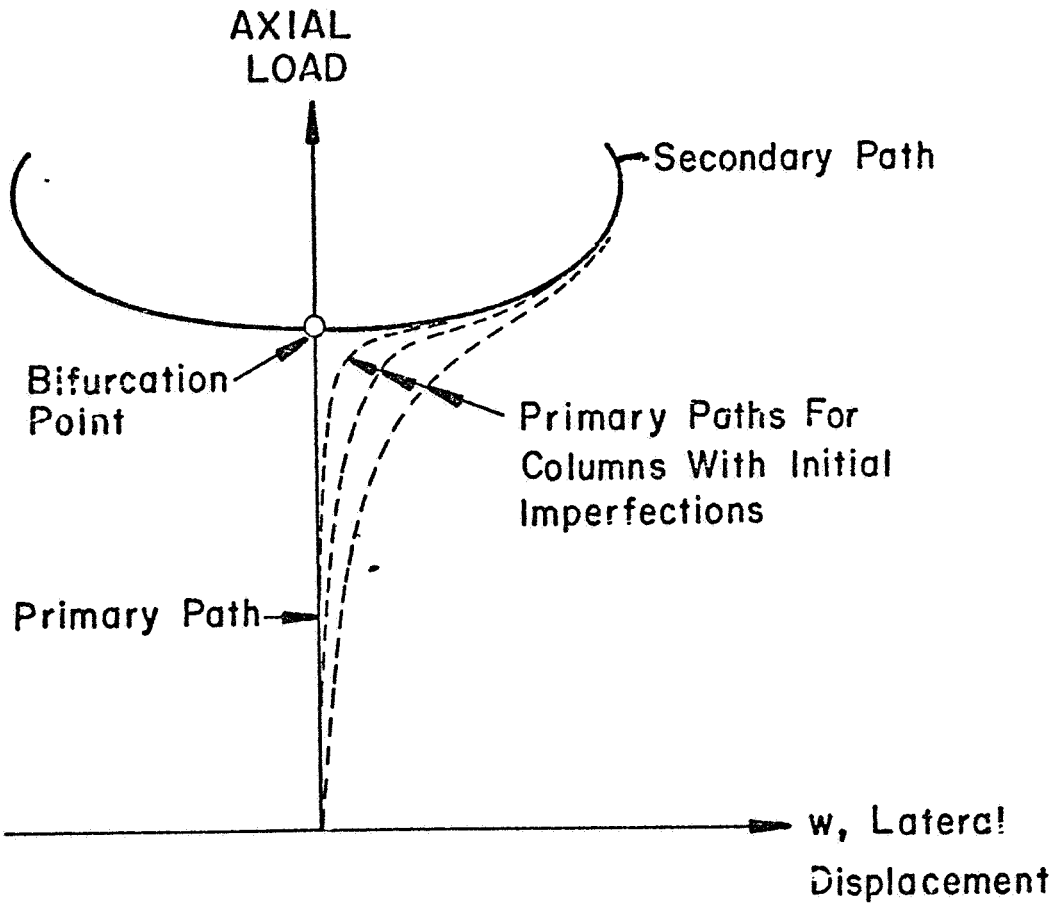

Figure 5.4. Equilibrium Paths for Column

Bifurcation points can be found by use of a linearized analysis. This is discussed in more detail in Section 7. The equations that govern the structural behavior are of the form

$$L(u) = 0 \tag{5.1}$$

where L is a nonlinear differential operator. If u_o represents an equilibrium configuration on the primary path, then $L(u_o) = 0$. At any point of intersection with a secondary path Eq. (5.1) must have multiple solutions. The existence of multiple solutions can be determined from

$$L(u_o + \Delta u) - L(u_o) = 0 \tag{5.2}$$

All terms in this equation that do not contain the incremental displacement Δu cancel one another since $L(u_o) = 0$. If, in addition, Δu is infinitesimal so that higher order terms may be omitted, Eq. (5.2) becomes homogeneous. The trivial solution $\Delta u = 0$ corresponds to equilibrium on the primary path. The existence of a nontrivial solution at some load level indicates the presence of a bifurcation point. This value of the load parameter is the eigenvalue and the nontrivial solution for Δu is the eigenfunction or, for a discrete system, the eigenvector. The eigenfunction defines the deformation mode on the secondary path in the immediate neighborhood of the bifurcation point. This deformation pattern, the buckling mode, is distinct from the deformation pattern on the primary path. Bifurcation can occur only into some deformation pattern that is orthogonal to the deformation pattern on the primary path.

The meaning of this orthogonality requirement may be clarified by observation of the behavior of a structure with some degree of imperfection. If, for example, a column has some small initial curvature or some eccentricity in loading, the straight form is not an equilibrium configuration at any load level. There is no bifurcation point, but the primary path for the imperfect column gradually approaches the secondary path for the perfect column as indicated in Figure 5.4.

It can be shown that the equilibrium on the primary path loses its stability at the first bifurcation point. Consequently, the limit of stability can be determined either through consideration of adjacent equilibrium as discussed above or through a consideration of the total potential energy of the system. The structure will cease to be in stable equilibrium when the load is raised to such a level that the total potential energy is no longer a true minimum. That is, the level at which the second variation of the potential energy ceases to be positive definite. The behavior of the initially crooked column illustrates a third somewhat less precise way to determine the limit of stability: With a very small imperfection included, a nonlinear analysis will indicate rapid growth of the secondary deformation mode as the bifurcation point is approached.

To these three stability criteria, Ziegler (Ref. 5.1) adds a kinetic criterion. Stability analysis according to this criterion requires a dynamic analysis. The structure under load is released after it is given a small deformation. It is in stable equilibrium only if this procedure results in a vibration with constant or decreasing amplitude. If the equilibrium is unstable according to any of the three static criteria, the structure will not return to the initial state but will move toward some other equilibrium position. Ziegler's kinetic stability criterion will in addition reveal the type of instability that manifests itself as a self-induced vibration. In summary then, there are four stability criteria:

- The Adjacent Equilibrium Criterion;
- The Energy Criterion;
- The Imperfection Criterion; and
- The Kinetic Criterion.

The first three are equivalent, but the fourth adds a capability to predict self-induced vibrations. A vibration with increasing amplitude means that energy is added to the system. The work done by a conservative load system along a closed loop equals zero. Consequently, for a system initially at rest, this form of instability can only occur if the load system is nonconservative. For systems in motion, such as rotating shaft,

self-induced vibrations are possible (critical rpm) even with conservative systems. For such cases, instability can still be predicted by use of the energy criterion. The kinetic criterion is only needed for analysis of systems with nonconservative forces.

5.3 The Consequences of Instability

The primary interest of a structural designer is not whether one form of equilibrium or another is stable, but rather how the structure responds to a given loading environment in terms of stresses and deformations. The stability criteria will be meaningful only if it can be predicted also how instability in a given case affects the general structural behavior.

The case in which stability is lost at a limit point will be considered first. If the load is controlled, rather than the displacement, the structure will be set in motion when the critical load is exceeded. Exactly how violent the snap-through is and how badly deformed the structure is after it has come to rest in another stable equilibrium configuration can only be determined by use of a postbuckling analysis. A true representation of the structural behavior will be gained if after static loading to a level just below the limit point, the analysis is restarted in a dynamic mode (including damping) at a load level just above the limit point. However, it is usually assumed that a limit point represents the ultimate load carrying capability of the structure, although it is possible in a complex, redundant structure that the snap-through only occurs in a small and rather insignificant part of the structure.

The effect of bifurcation on the general structural behavior is not immediately clear. As the equilibrium on the primary path loses its stability at the bifurcation point, the structural behavior beyond bifurcation is governed by the conditions on the secondary path. Thus a bifurcation point signifies a load level at which a new deformation pattern begins to develop. The primary path defines the prebuckling behavior and the secondary path the postbuckling behavior. If the equilibrium on the secondary path is stable at the bifurcation point, the structure may have considerable

postbuckling strength. The loss of stability of the equilibrium on the primary path need not mean that the structure collapses. On the other hand, if equilibrium on the secondary path is unstable at the bifurcation point, buckling is sudden and the buckling load of the structure may be sensitive to imperfections. The behavior of the structure is much the same as it is at a limit point. Acutally, if a small imperfection in the form of the buckling mode is included, a limit point will occur just below the bifurcation point for the perfect structure. Three different types of behavior at a bifurcation point are illustrated in Figure 5.5.

The type of behavior indicated by case (a) corresponds to stable equilibrium on the postbuckling branch. In such a case, the occurrence of bifurcation may be rather inconsequential. One such example is the spherical shell subjected to a point load, in which case bifurcation means that the dimple around the point load slowly begins to ovalize. The reduction in stiffness, i.e., in the slope of the load displacement curve, is barely noticeable. On the other hand, a column under an axial load shows a considerable lateral displacement at load levels only slightly above the bifurcation buckling load. The cases (b) and (c) indicate the structural behavior in case the equilibrium is unstable on the secondary path. The limit point for the imperfect structure may be well below the bifurcation point for the perfect structure.

Detailed information about the structural behavior beyond bifurcation can be obtained if the secondary path is traced through solution of the nonlinear equilibrium equations. However, limited, but sometimes useful, information may be obtained by use of the Koiter Theory (Ref. 5.2). This theory is based on determination of the stability of equilibrium on the intersecting secondary path at the bifurcation point. It does determine which of the three cases in Figure 5.4 represents the structural behavior.

5.4 Static Stability Analysis

Before the high speed computer became available, solutions were obtained to some buckling problems with linear precritical behavior. For example, Euler solved the problem of column buckling more than 200 years

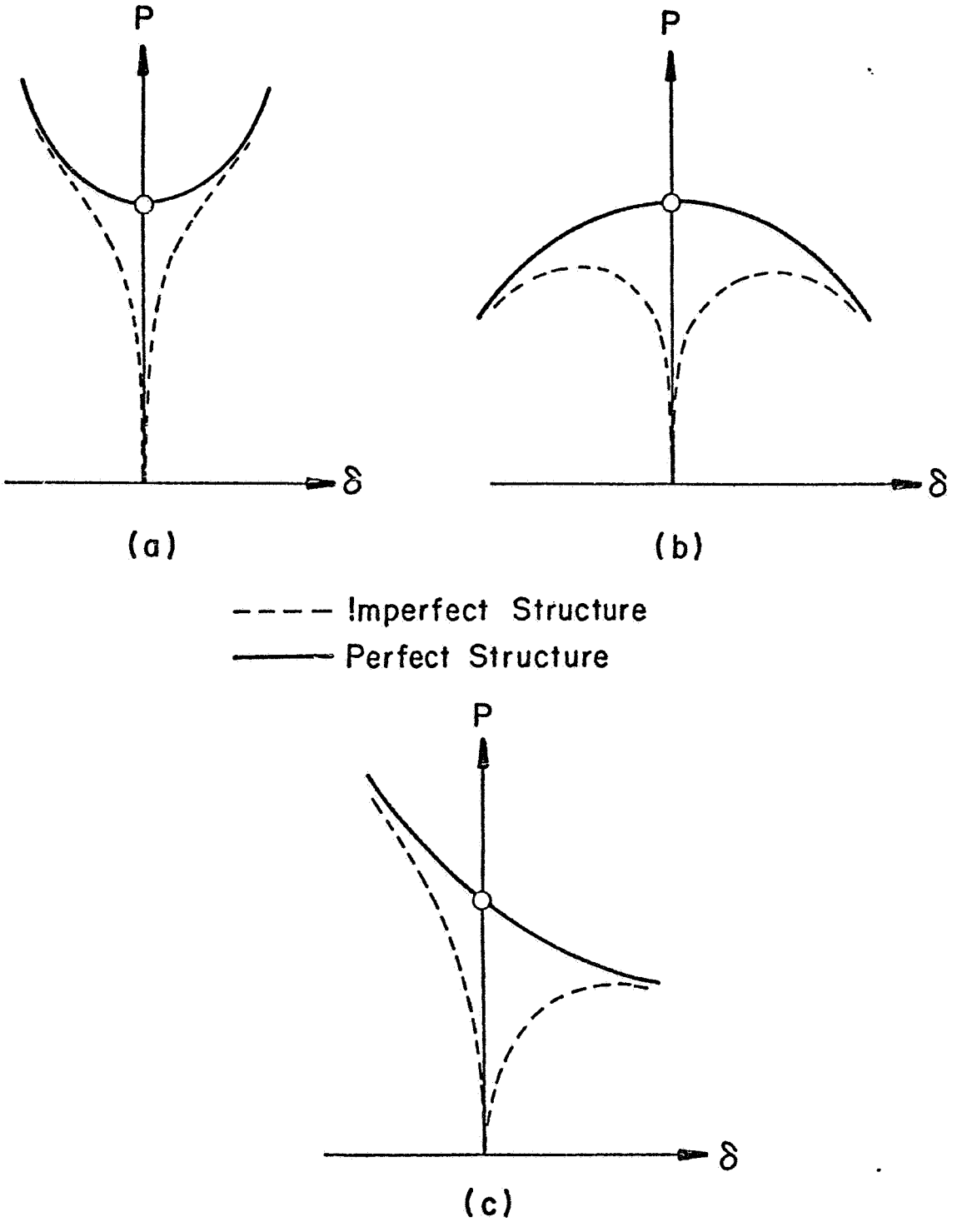

Figure 5.5. Typical Load-Displacement Relations

ago and Lorenz published a solution of the bifurcation buckling problem for an axially loaded cylinder in 1911. Approximate solutions were obtained for some simple cases in which loss of stability occurs at a limit point. Notable is the analysis by Brazier in 1926 of the collapse of long cylinders in bending. Somewhat more difficult problems could be handled when digital computers first were engaged in stability analysis. An example of how the computer was used to improve previously existing solutions is provided by the analysis of buckling of cylinders in bending by Seide and Weingarten (Ref. 5.3). Buckling of cylindrical shells under axial compression was considered by Stein in Ref. 5.4, where it first is recognized that bifurcation is possible even if the primary path is nonlinear. The production of design charts for the handbooks remained the main purpose of stability analysis for a few years after introduction of the high speed computer. Eventually, more complex problems were solved and the number of independent parameters became too large to allow simple graphical representation. At that point the research and development department would hand a special purpose program to the stress analyst, who performed the still relatively simple duty of punching input cards and reading a critical load from the output.

The introduction of multipurpose codes including effects of stability and geometric nonlinearities has greatly enhanced the capability of making accurate analysis of complex structures, but it has also enormously increased the burden on the stress analyst. The stress analyst must now make major decisions regarding modeling of the structure and analysis procedure so that failure is avoided without unnecessary penalties in weight or cost. Consequently, he must have a relatively good understanding of the basic principle underlying the theory of structural stability. Some of these ideas were discussed above and additional detail is given in modern textbooks such as Ref. 5.5. The practical approach to some specific structures is discussed in the following.

Flat plates with only inplane loading exhibit linear behavior on the primary path. If compressive stresses are present, there will be a

bifurcation point. If the plate is perfectly flat, lateral displacements begin to develop at the bifurcation buckling load. For the imperfect plate, the buckling load represents a load level at which lateral displacements grow more rapidly. It has long been known that thin plates with supported edges can carry loads well above the bifurcation buckling load. This is due to the fact that a stress redistribution takes place so that more load is carried by the material that is close to the supported edges. Handbooks contain design charts and simple formulas for buckling loads and ultimate loads of rectangular and circular plates with uniform loading. For more complex cases, multipurpose programs can be used. For bifurcation buckling analysis of flat plates, the number of degrees of freedom can be reduced. All rotations and lateral displacements vanish on the primary path and all inplane displacements vanish on the secondary path (in the buckling mode). In analysis with STAGS, it is possible to suppress such freedoms with data cards and thus reduce computer runtime. However, in a postbuckling analysis, it is necessary to include all freedoms.

If a postbuckling analysis is used for computation of the ultimate load, it is necessary to include a small imperfection or load eccentricity. Otherwise the computer results obtained will represent those on the unstable primary path. The behavior of flat plates under compression or shear is generally of the type represented by case (a) in Figure 5.5. The equations for the perfect plate have multiple solutions at loads above the bifurcation buckling load. If equilibrium configurations are determined under increasing load through solution of the nonlinear equations, extrapolated values are usually used as initial estimates. Since the procedure tends to converge toward the solution closest to the estimates, the solution cannot be expected to automatically leave the trivial primary path at the bifurcation point and turn onto the secondary path. However, when the solution procedure requires refactoring of the coefficient matrix after a bifurcation point is passed (see Section 7), it will be found that the matrix is not positive definite. This means that the structural configuration defined by the analysis is not in stable equilibrium.

In order to find solutions on the secondary branch, it is necessary to rerun the case including a small imperfection, so that the solution

follows a path like the dashed curve in Figure 5.5, case (a). An important observation may be made here. If the solution representing unstable equilibrium for the perfect structure is substituted into the equilibrium equations for the imperfect shell, the individual equations will not be in balance but the residuals will be very small. Smaller imperfections lead to smaller residuals and unless the convergence criterion used is sufficiently severe, a false solution may be accepted by the computer. As in the case of a true but unstable equilibrium configuration, refactoring would show that the matrix is not positive definite (the computer output indicates the presence of negative roots). Since the existence of roundoff errors and the demands on computer economy set an upper limit for the convergence criterion, the possibility must be recognized that the computer will accept a solution that leads to small residuals in the equation system but still does not at all represent structural behavior. The existence of false convergence is not restricted to flat plates, but it represents a problem that often appears in nonlinear structural analysis. Whenever negative roots indicate a problem of this nature it is necessary to rerun the case with a larger imperfection amplitude to trigger the secondary deformation mode or possibly with a more severe convergence criterion.

A shell of revolution with axisymmetric loading exhibits, in general, nonlinear prebuckling behavior. A shallow spherical cap under external pressure softens with load and a torospherical pressure vessel head under internal pressure stiffens. One possible failure mode is axisymmetric collapse at a limit point. Another possibility is that stability is lost as bifurcation occurs into a nonsymmetric deformation mode.

If advantage is taken of symmetry, stability analysis of axisymmetric shells becomes relatively inexpensive. The eigenfunctions are of the form $\Delta u(x,\phi) = \Delta u(x) \sin(n\phi)$ or $\Delta u(x)\cos(n\phi)$ where ϕ is the circumferential coordinate and n the number of circumferential waves in the buckling mode. These buckling modes are mutually orthogonal and also orthogonal to the axisymmetric prebuckling state. Corresponding to each buckling mode there exists an equilibrium path in the load displacement space. None of

these paths passes through the origin but a number of them may intersect the primary path and each of these intersections corresponds to a bifurcation point.

According to the discussion above, bifurcation need not be a critical condition. For example, if a spherical cap is loaded by an inward radial point force at the apex, the lowest bifurcation point corresponds to buckling into two waves. Beyond bifurcation, the two-wave deformation pattern grows slowly under increasing load. In other cases, structural failure occurs approximately at or even below the bifurcation point because the amplitude of the mode grows very rapidly beyond bifurcation, or because the equilibrium on the secondary path is unstable.

If it is sufficient to consider axixymmetric collapse and bifurcation only, the stability analysis for the axisymmetrically loaded shell of revolution is reduced to a one-dimensional problem (i.e., the problem can be solved by use of ordinary differential equations). The critical load for the shell can be found in the following way: The nonlinear prebuckling equations are solved under stepwise increasing load. For each load step, the value of the determinant of the coefficients in the homogeneous system for incremental displacements (Cf. Eq. 5.2) is computed for a range of values of n. The computations are continued until for some value of n this stability determinant changes sign, or until axisymmetric collapse occurs. The latter case is indicated by a horizontal slope in a graph depicting the load versus some typical displacement. If the load is controlled rather then some displacement the collapse load may be more easily recognized as the load at which the stability determinant becomes zero.

A one-dimensional analysis is possible as long as there is no need to trace the secondary branch or to include nonsymmetric imperfections. For such cases, special programs exist and should be more efficient than the more general codes such as STAGS. In BOSOR (Ref. 5.6), for example, a capability to compute bifurcation from a nonlinear basic stress state is included. This bifurcation buckling analysis is based on the tangential stiff-

ness at some point on the nonlinear primary path. Since the tangential stiffness varies with the load level, the bifurcation point is exactly located only if the eigenvalue equals zero. One of the procedures used in BOSOR to close in on a true bifurcation point is illustrated in Figure 5.6 for a stiffening structure. The first estimate of the critical load can be determined by use of a linear basic stress state. The nonlinear equations are solved at this load level and subsequently a new bifurcation buckling load is computed. This iterative procedure is continued as indicated in the figure until the eigenvalue is sufficiently close to zero. For softening system the initial estimate is likely to overestimate the critical load. Such an overestimate may result in the presence of negative roots or in failure of convergence in the following attempt to solve the nonlinear prebuckling equations. For such cases, a somewhat more complicated strategy is provided in the program.

The effect of prebuckling nonlinearity on the bifurcation buckling load for axisymmetrically loaded shells of revolution is often insignificant. For axially loaded cylinders, with clamped edges, the effect is to reduce the critical load by about 10%. On the other hand, for a spherical cap prebuckling nonlinearity may reduce the critical load by about 40% or more. For a stiffening system, a bifurcation buckling analysis based on a linearized primary path may locate a bifurcation point although in reality buckling will not occur. Such an example is given in Ref. 5.7 in which a torospherical pressure vessel head under internal pressure is considered.

The limit point corresponding to axisymmetric collapse usually represents an upper bound of loading. This limit is generally not sensitive to imperfections. On the other hand, if bufurcation is critical, information is often needed about possible postbuckling strength or imperfection sensitivity. It is quite feasible, for example, that axisymmetric collapse is critical for the perfect structure, but a slightly imperfect structure buckles into a nonsymmetric mode. Such is the case for a cylinder under an axial load combined with a small internal pressure. This case may serve to illustrate one of the many pitfalls in nonlinear structural analysis.

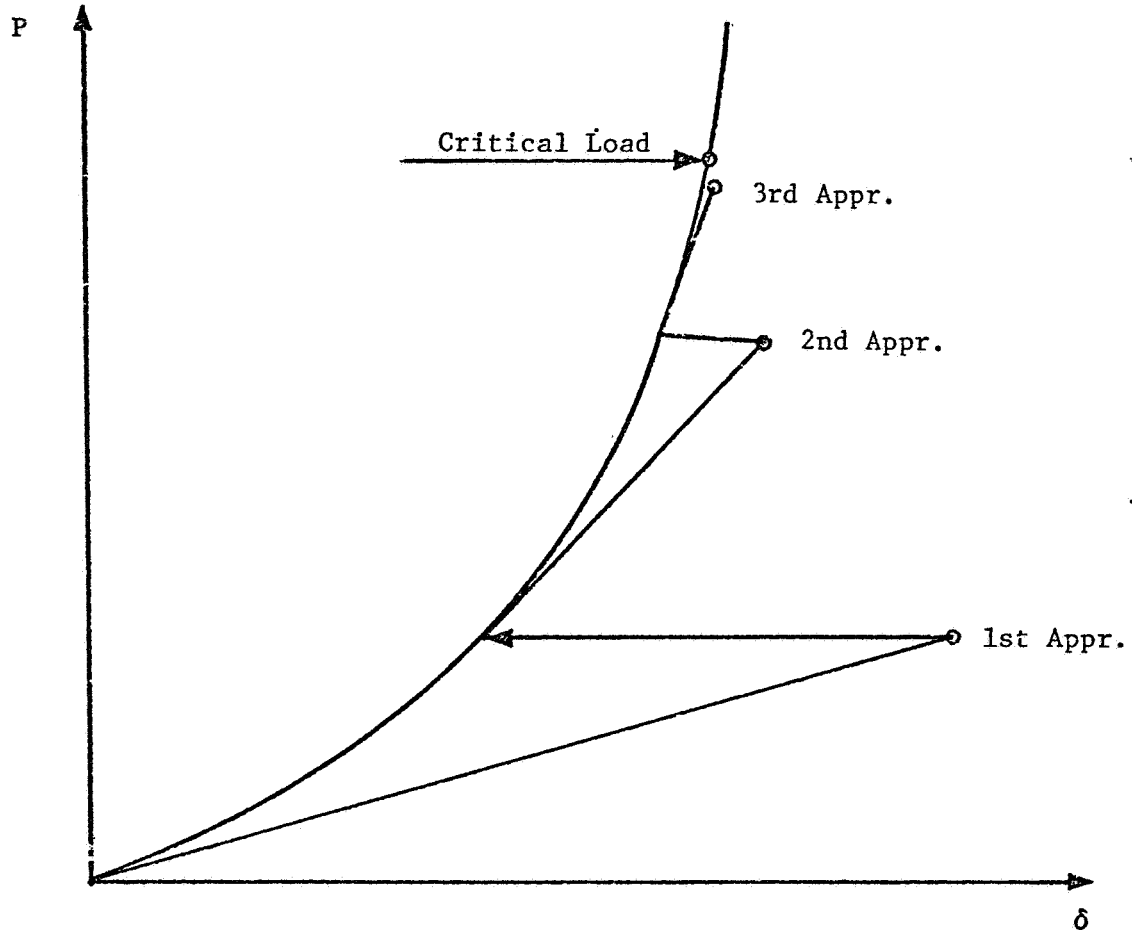

Figure 5.6. Bifurcation Buckling with Nonlinear Basic Stress State

Knowledge about post-critical behavior can be gained if the secondary path of equilibrium is traced. The eigenfunction or buckling mode represents the deformation pattern on the secondary path within an infinitesimal neighborhood of the bifurcation point but the sinusoidal buckling pattern becomes distorted away from the bifurcation point. Therefore, a one-dimensional analysis is not sufficient for the analysis of postbuckling behavior or of imperfect shells. With stable postbuckling behavior the secondary path can readily be found by consideration of a shell with a small imperfection. This imperfection can have any form as long as it is not orthogonal to the buckling mode corresponding to the lowest eigenvalue. If for the imperfect structure the load is gradually increased to a level above the bifurcation point, solutions are obtained which are close to the displacements on the secondary path for the perfect structure. These can be used as starting values if the secondary path for the perfect structure is desired.

If the equilibrium on the secondary path is unstable, a straightforward nonlinear analysis of a shell with an imperfection leads to the limit point. To determine the entire secondary path is more difficult in this case. However, it is generally sufficient to determine the value of the load at the limit point. The entire path can often be computed if a displacement is controlled rather than the load (controlled end shortening, for example). Recent research papers have propsoed procedures that would make it easier to find solutions beyond the limit point in the case of controlled load. One possible method is to solve the nonlinear equations by use of dynamic relaxation (see Sections 5.3 and 7.3).

A shell of revolution subjected to nonsymmetric loading will generally lose stability at a limit point. Bifurcation is possible whenever the loading contains one or more planes of symmetry. In that case all deformation modes that are antisymmetric with respect to such a plane are orthogonal to the deformation pattern on the primary path and these are possible bifurcation buckling modes.

· Whenever symmetry planes in the loading coincide with symmetry planes in the structure, the size of the problem can be reduced. In a nonlinear analysis of the equilibrium configuration on the primary path, it is assumed that the displacements are symmetric with respect to such planes. At selected load steps, the determinant of the coefficients in the equations for the incremental displacements can be computed. These are antisymmetric with respect to the symmetry plane. A change of sign in this determinant would indicate a bifurcation into an antisymmetric pattern. It is possible also to use repeatedly the eigenvalue analysis based on a nonlinear basic stress state and tangential stiffness (see Figure 5.6). In that case, the load on which the basic stress state is based is a bifurcation buckling load or a limit point if the computed eigenvalue equals zero. An automatic procedure to close in on a bifurcation point as discussed above is probably not suitable for shells with nonsymmetric loading or for general shells because convergence can only be obtained if very good initial estimates are available for the nonlinear prebuckling analysis.

As an alternate procedure, no advantage is taken of the symmetry. The entire structure is included in the analysis and a small antisymmetric imperfection is added. This method may be somewhat more expensive, but it yields some information about possible postbuckling strength. When the critical load is approached the antisymmetric component will begin to grow more rapidly. However, the convergence criterion does not distinguish deformation in the buckling mode from the total deformation. Therefore, if the imperfection is too small, its relative growth may be rapid but still remain small in comparison to the growth of the total displacements. This represents the type of behavior referred to as false convergence in the discussion of flat plates above. The symmetric displacement pattern does not satisfy the equations but the residuals in all the equations are small. The false solution is accepted because it corresponds to small residuals (errors) in the equation system. The problem will be revealed on factoring of the matrix.

The risk that the computer will accept a false solution is not limited to the case in which a fictitious imperfection has been used to

trigger a specific deformation pattern. The deformation on the primary path may contain only a small component of the collapse mode that is triggered by nonaxisymmetric loading, i.e., the deformation pattern that grows rapidly in the neighborhood of the limit point. In that case, the load displacement curve will have a very sharp maximum as shown in Figure 5.7. As this maximum is approached, the convergence criterion may not function properly because the rapidly growing collapse mode is dominated by the basic deformation pattern. The dashed line in Figure 5.7 represents a path in the load displacement space along which false convergence is likely because the equilibrium equations are almost satisfied. Substitution of the false solution into the equation system leads to small residuals although the solution is far removed from any true solution. This situation can be remedied by introduction of a fictitious imperfection in the analysis. As an example, consider a very short cylindrical shell subjected to a lateral pressure of the form

$$p = p_o \cos 2\phi \tag{5.3}$$

where ϕ is the circumferential coordinate. Due to the nonlinear coupling between different harmonics, the displacement pattern on the primary path does not vary sinusoidally with the circumferential coordinate. All Fourier components, symmetric about the plane through $\theta = 0$ and π are included in the prebuckling deformation mode. However, the higher the wave number, the smaller is the amplitude of the corresponding component. If the critical wave number is relatively high, as is the case for a very short cylinder, it is necessary to use an imperfection to trigger the critical deformation pattern.

A shell of a general shape behaves similarly to the shell of revolution with nonsymmetric loading. In general, loss of stability occurs at a limit point. Bifurcation points may exist if geometry and loading are symmetric about some plane. Again, if such planes are present, the options are available to take advantage of this symmetry by considering antisymmetric bifurcation buckling modes with a nonlinear basic stress state or to

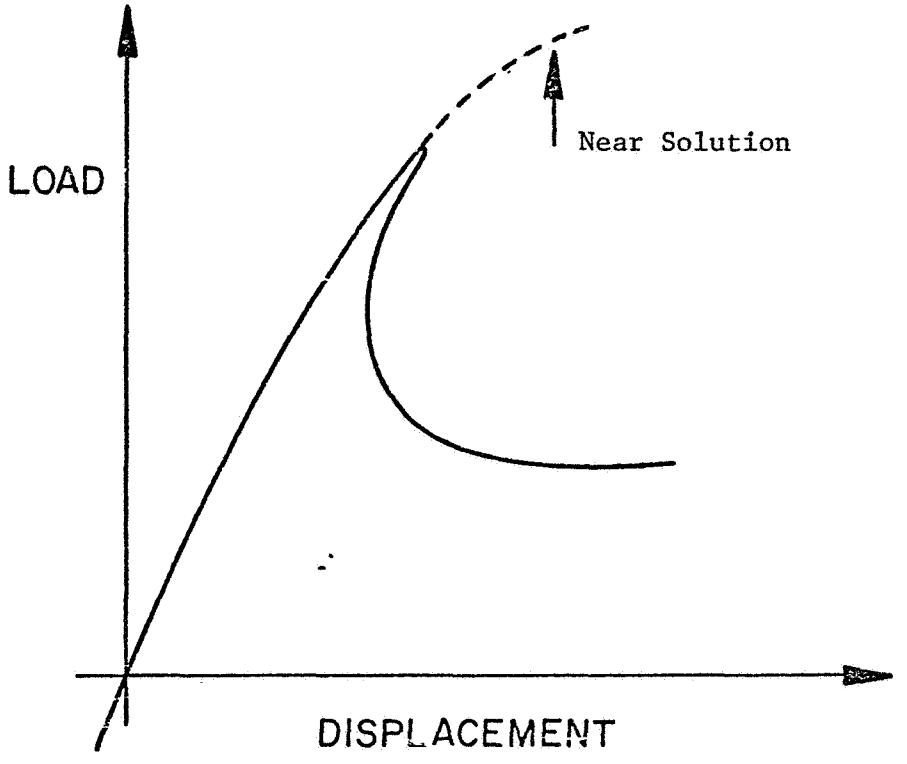

Figure 5.7. Load Displacement Curve with a Sharp Maximum

introduce antisymmetric imperfections. The latter approach was used in an analysis in Ref. 5.8 of the nonlinear behavior of elliptic cylinders under axial compression.

The behavior of the elliptic cylinder under axial compression provides another illustration of the problem with a path in the load displacement space that is far removed from any true solution but still results in an insignificant unbalance in the equilibrium equation. As the ellipse ratio approaches one (a circular cylinder), the symmetric component of the collapse mode contained in the prebuckling deformation pattern vanishes. For an ellipse ratio of about 1.4, it was possible (see Ref. 5.8) to establish the collapse load either after the convergence criterion had been tightened or after symmetric imperfection had been introduced. For cylinders with even smaller ellipse ratios solutions can only be obtained after introduction of a symmetric imperfection.

Although in reality, all structures have some degree of imperfection and a situation of pure bifurcation never exists, the bifurcation approach is often very useful. If it can be assumed that the prebuckling behavior is linear, the bifurcation buckling approach leads to considerable savings in comparison to a nonlinear analysis. Often previous experiments give some idea about the degree of imperfection sensitivity. In such cases the bifurcation buckling load can be used in connection with a more or less intuitively chosen knockdown factor as a design limit. The true imperfections are usually not known in detail. Therefore, this semiempirical method represents the only practical approach. If the equilibrium on the secondary branch is stable, the bifurcation buckling load is useful as a conservative estimate of the critical load.

If the bifurcation buckling load is not used directly as a design limit, it may still be worthwhile to perform a bifurcation analysis based on a linear prebuckling state as a preliminary to a nonlinear analysis. The bifurcation buckling load may be used as a guide in the choice of step size and starting loads for the nonlinear analysis. The buckling mode can

be used as a guide in the selection of an initial imperfection. A bifurcation analysis can be used in a preliminary study of the effect of grid size.

Sometimes it is possible to use the bifurcation approach with a linear prebuckling analysis as an approximation beyond its range of applicability. This can be done only if experience from similar cases indicates that the solution is adequate. The bifurcation buckling analysis may be a too conservative estimate of the collapse load if the structure allows considerable redistribution of stress. On the other hand, if the stiffness of the structure deteriorates due to geometrical changes caused by the load, the bifurcation buckling load may be several times higher than the actual collapse load. These problems are illustrated by some examples in Ref. 5.9.

In the absence of planes of symmetry in geometry and loading, bifurcation is extremely unlikely. It may in that case at first appear meaningless to perform a bifurcation buckling analysis based on a nonlinear basic stress state. However, if a nonlinear analysis is carried to the design load, it may be useful to perform a bifurcation buckling analysis based on the final stress state. This would give some idea about possible margin against collapse. Also, if negative roots appear on refactoring of the matrix at some load step, a bifurcation buckling analysis may reveal the reason for the problem, and the buckling mode may indicate what type of imperfection should be included.

REFERENCES

5.1 Ziegler, H., Principles of Structural Stability, Blaisdell, Waltham, Mass. 1968.

5.2 Koiter, W. T., "On the Stability of Elastic Equilibrium" (in Dutch), thesis, Delft, H. J. Paris Amsterdam, 1945, English Translation by E. Riks, Report AFFDL-TR-70-25, Wright-Patterson Air Force Base, Dayton, Ohio, 1970.

5.3 Seide, P., and V. I. Weingarten, "On the Buckling of Circular Cylindrical Shells under Pure Bending," J. App. Mech., Vol. 28, 1961, pp. 112-116.

5.4 Stein, M., "The Influence of Prebuckling Deformations and Stresses on the Buckling of Perfect Cylinders," NASA TR-R-190, 1964.

5.5 Brush, D. O., and B. O. Almroth, Buckling of Bars, Plates and Shells, McGraw-Hill, New York, 1975.

5.6 Bushnell, D., "BOSOR5 - Program for Buckling of Elastic-Plastic Complex Shells of Revolution Including Large Deflections and Creep," Computers Structures, Vol. 6, 1976, pp. 221-239.

5.7 Bushnell, D.,"Nonsymmetric Buckling of Internally Pressurized Ellipsoidal and Torisphrical Elastic-Plastic Pressure Vessel Heads," J. Pressure Vessel Technology, Vol. 99, 1977, pp. 54-63.

5.8 Almroth, B. O., F. A. Brogan, and M. B. Marlowe, "Collapse Analysis for Elliptic Cones," AIAA J., Vol. 9, 1971, pp. 32-37.

5.9 Almroth, B. O., and F. A. Brogan, "Bifurcation Buckling as an Approximation of the Collapse Load for General Shells," AIAA J., Vol. 10, 1972, pp. 463-467.

Section 6
DISCRETIZATION PROCEDURES

6.1 Introduction

The structural response to a given environment is determined by the equations of motion of deformable bodies. If solutions are to be obtained to these equations for a reasonably large class of structural configurations, analytic solutions are clearly inadequate. Consequently, the mathematical problem is recast into a numerical problem for solution on the computer.

The output from the computer consists of a sequence of numbers, somehow representing the functions satisfying equilibrium equations and boundary conditions. The solution may be represented by a linear combination of a set of "basis functions." Then the output vector consists of the coefficients in this linear combination. This is the case if the Galerkin or Rayleigh-Ritz procedures are used. In finite difference or finite element procedures, the solution function is represented by its discrete values at a number of points within the domain of the structure. The discretized methods, especially the finite element method, are more readily applied in computer programs for structures of a general type. Therefore, they have been gaining in popularity to the extent that presently all major computer programs of significant scope are based on such methods. The discretized methods make use of numerical differentiation and numerical integration. A review of these operations here is intended to serve as a background to a discussion of the different options that are available for numerical analysis of shell structures. A review of some numerical procedures is presented in Section 6.4. Special problems in discretization are discussed in Section 6.5 and a brief discussion of some special discretization configurations (finite difference and finite element procedures) is given in Section 6.6. Finally, in Section 6.7, the special procedures

selected for the STAGS program are presented together with a justification for this choice.

6.2 Numerical Differentiation

Numerical differentiation consists of the replacement of the derivatives of a function by difference quotients (or finite difference expressions). Such expressions are generally based on local polynomial approximations. In the following a truncated Taylor series will be used for this purpose. In the one-dimensional case (one space variable), the series can be written in the form

$$f(x) = f(0) + xf'(0) + \frac{x^2}{2} f''(0) + ... \frac{x^n}{n!} f^{(n)}(0) + R \qquad (6.1)$$

where the primes denote differentiation with respect to x. The remainder R representes the sum of the terms that were excluded when the series was truncated after the (n+1)th term. It can be shown that (see Ref. 6.1, for example) .

$$R \leq \frac{x^{n+1}}{(n+1)!} F \qquad (6.2)$$

$$F = \max (f^{(n+1)}(\zeta)); \quad 0 \leq \zeta \leq x$$

This bound on the truncation error may be useful for estimates of the accuracy of the output vector.

By use of a suitably truncated Taylor series, the function values at a number of discrete node points can be expressed in terms of the derivatives at each of a number of control points. In Equation (6.1) it is assumed that x = 0 at the control point. A set of linear equations is obtained and through solution of this, expressions are obtained for the derivatives at the control point in terms of the function values at the selected node points. The number of node point values included must be equal to the number of derivatives in the Taylor series. In the general case the

highest order derivative so determined will be of first order accuracy, i.e., the error $E = O(h)$. If the highest order derivative included in the expansion is of nth order, the kth derivative ($k \leq n$) will be of order $(n - k + 1)$, $E = O(h^{n-k+1})$.

Figure 6.1 illustrates how finite difference expressions can be derived in the two-dimensional space. A Taylor series approach gives

$$f_{(\text{at } N_i)} = (f + \alpha_{ij} f' + \beta_{ij} f^{\cdot} + \frac{1}{2}\alpha_{ij}^2 f'' + \alpha_{ij}\beta_{ij} f'^{\cdot} + \frac{1}{2}\beta_{ij}^2 f^{\cdot\cdot} + \ldots)_{(\text{at } P_j)} \tag{6.3}$$

where a prime indicates differentiation with respect to the x_1 coordinate and a dot differentiation with respect to the x_2 coordinate.

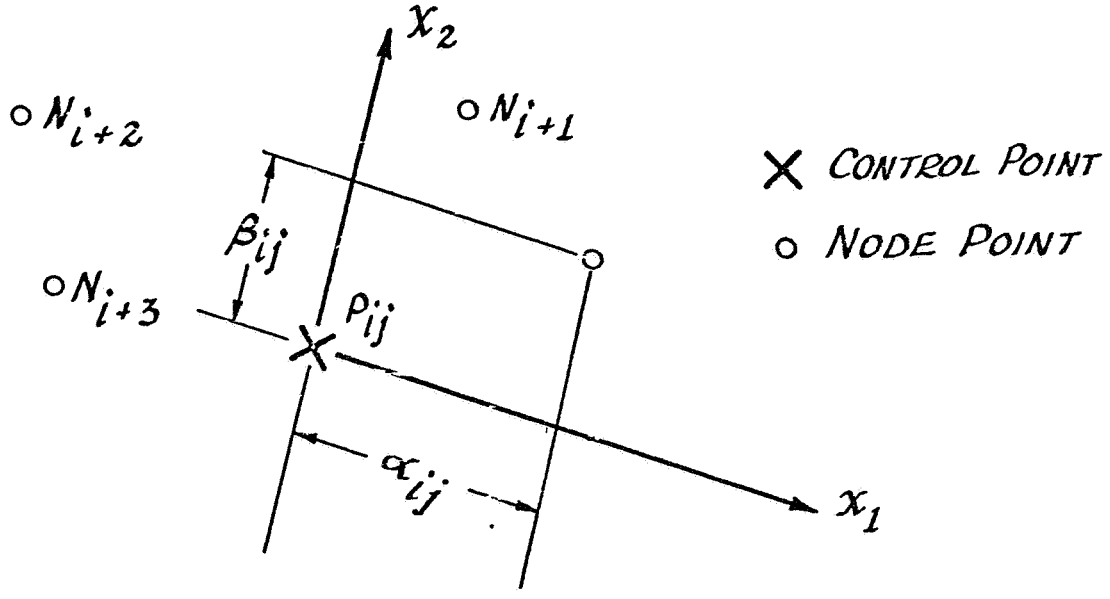

Figure 6.1 Two-Dimensional Finite Difference Grid

If derivatives up to the second order are to be determined, it is sufficient to specify for each control point a set of six neighboring node points (N_i to N_{i+5}). By applying Eq. (6.3) at each of the six node points, the following equation system is obtained

$$\begin{Bmatrix} f_1 \\ f_2 \\ f_3 \\ f_4 \\ f_5 \\ f_6 \end{Bmatrix} = \begin{bmatrix} 1 & \alpha_{1j} & \beta_{1j} & \frac{1}{2}\alpha_{1j}^2 & \alpha_{1j}\beta_{1j} & \frac{1}{2}\beta_{1j}^2 \\ 1 & \alpha_{2j} & \beta_{2j} & \frac{1}{2}\alpha_{2j}^2 & \alpha_{2j}\beta_{2j} & \frac{1}{2}\beta_{2j}^2 \\ 1 & \alpha_{3j} & \beta_{3j} & \frac{1}{2}\alpha_{3j}^2 & \alpha_{3j}\beta_{3j} & \frac{1}{2}\beta_{3j}^2 \\ 1 & \alpha_{4j} & \beta_{4j} & \frac{1}{2}\alpha_{4j}^2 & \alpha_{4j}\beta_{4j} & \frac{1}{2}\beta_{4j}^2 \\ 1 & \alpha_{5j} & \beta_{5j} & \frac{1}{2}\alpha_{5j}^2 & \alpha_{5j}\beta_{5j} & \frac{1}{2}\beta_{5j}^2 \\ 1 & \alpha_{6j} & \beta_{6j} & \frac{1}{2}\alpha_{6j}^2 & \alpha_{6j}\beta_{6j} & \frac{1}{2}\beta_{6j}^2 \end{bmatrix} \begin{Bmatrix} f_j \\ f_j' \\ f_j^{\cdot} \\ f_j'' \\ f_j^{\prime\cdot} \\ f_j^{\cdot\cdot} \end{Bmatrix} \tag{6.4}$$

The solution of the equation system (6.4) for f_j and its derivatives yields a set of finite difference expressions for the derivatives at control point j. The error bound for the second order derivatives is of order $E = O(h)$. The first order derivatives are of second order accuracy. Notice that if one of the second order derivatives were left out, the remaining derivatives would be expressed in terms of five nodal values. Then the first order derivatives are only of first order accuracy and the expressions for the second order derivatives may be meaningless ($E = O(h^0)$). Since there are four different third order derivatives, we must include ten nodal function values in order to raise the accuracy by one order to $E = O(h^3)$ for first order and to $E = O(h^2)$ for second order derivatives. In

finite difference analysis, it has been a rather common practice to determine lower order derivatives from a smaller set of degrees of freedom so that derivatives of different order still are of the same order of accuracy (see Ref. 6.2, for example).

The nodal freedoms need not be restricted to function values. A higher order derivative at a control point can be expressed in terms of lower order derivatives at the nodal points. The second order derivatives in the one-dimensional case can be obtained from the difference between two adjacent first-order derivatives. The lower order derivatives are then included among the degrees of freedom of the system. Such procedures are discussed in Ref. 6.3, for example.

A different but equivalent procedure is usually applied in finite element analysis. The coefficients in a linear superposition of a set of polynomial shape functions are chosen so that the function values at the nodes agree with the degrees of freedom. Since derivatives of all orders are determined from these polynomials, lower order derivatives are usually of higher order accuracy than derivatives of higher order.

The location of points at which derivatives are approximated by finite difference expressions can be chosen so that the order of accuracy is improved. As an example, the one-dimensional finite difference configuration shown in Figure 6.2 is considered.

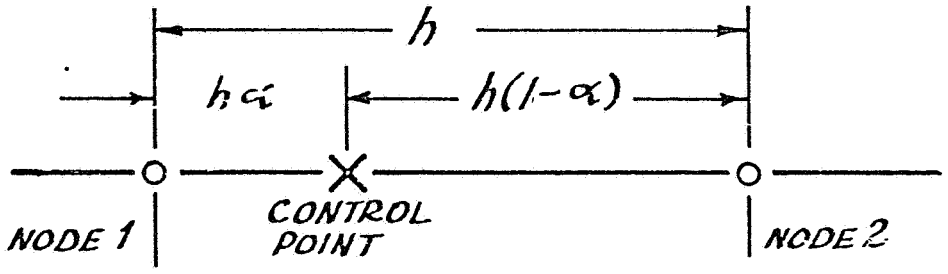

Figure 6.2. One-Dimensional Finite Difference Grid

The degrees of freedom of the system are the function values f_1 and f_2 and the first order derivatives (rotations) f_1' and f_2' at the node points. The second order derivative at some point in the interval is determined.

A one-dimensional Taylor series expansion gives

$$f = f_o + xf_o' + \frac{x^2}{2} f_o'' + \frac{x^3}{6} f''' + \frac{x^4}{24} f_o^{lv} + \ldots$$

and (6.5)

$$f' = f_o' + xf'' + \frac{1}{2} x^2 f''' + \frac{x^3}{6} f_o^{lv} + \ldots$$

In the following, for simplicity, the subscript zero referring to the control point is dropped. The finite difference expression, the second derivative f'', is obtained from the equation system

$$\begin{aligned}
&f + h(1-\alpha) f' + \frac{h^2}{2} (1-\alpha)^2 f'' + \frac{h^3}{6} (1-\alpha)^3 f''' + \frac{h^4}{24} (1-\alpha)^4 f^{lv} = f_2 \\
&f - h\alpha f' + \frac{h^2\alpha^2}{2} f'' - \frac{h^3\alpha^3}{6} f''' + \frac{h^4\alpha^4}{24} f^{lv} = f_1 \\
&f' + h(1-\alpha) f'' + \frac{h^2}{2} (1-\alpha)^2 f''' + \frac{h^3}{6} (1-\alpha)^3 f^{lv} = \beta_2 \\
&f' - h\alpha f'' + \frac{h^2\alpha^2}{2} f''' - \frac{h^3\alpha^3}{6} f^{lv} = \beta_1
\end{aligned} \qquad (6.6)$$

The solution of this equation system includes

$$f'' = \frac{1}{h^2} \left[6 (1 - 2\alpha) (f_2 - f_1) - 2h (2 - 3\alpha) \beta_2 + (1 - 3\alpha) \beta_1 \right.$$

$$\left. - \frac{h^2}{12} (6\alpha^2 - 6\alpha + 1) f^{lv} + O(h^3) \right| \qquad (6.7)$$

If α is chosen so that $6\alpha^2 - 6\alpha + 1 = 0$, i.e., $\alpha = (1 \pm 1/\sqrt{3})/2$, then the second derivative in Eq. (6.7) is of third order accuracy. The function $y = 6\alpha^2 - 6\alpha + 1$ is shown in Figure 6.3. Points at which the coeffi-

cient of the first term in the error vanishes are sometimes in the finite element literature referred to as stress windows (Ref. 6.4). The accuracy of the local approximation at such points is one order higher than it is at other points in the interval.

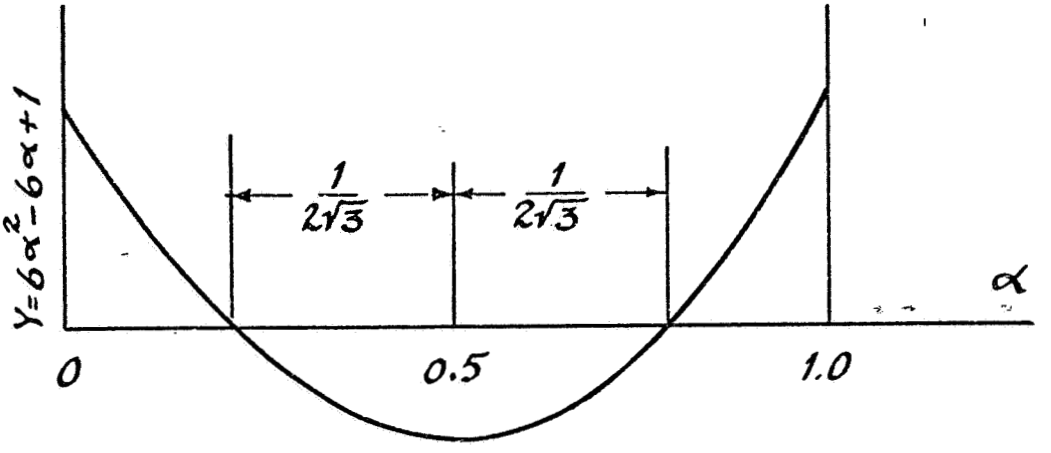

Figure 6.3 Error Function

The analysis becomes more efficient if numerical derivatives need to be determined only at points where they are most accurate. This is further illustrated by the two finite difference schemes shown in Figure 6.4.

With a uniform spacing the stress windows are located at the node points for even order derivatives and halfways between them for odd order derivatives. With scheme A we find

$$f' = \frac{1}{2h}(f_{+1} - f_{-1}) - \frac{1}{6}h^2 f'''$$

$$f'' = \frac{1}{2h^2}(f_{+1} - 2f_o + f_{-1}) - \frac{1}{12}h^2 f^{lv} \qquad (6.8)$$

and with scheme B

$$f' = \frac{1}{h}\left(f_{+1/2} - f_{-1/2}\right) - \frac{1}{24} h^2 f''' \qquad (6.9)$$

$$f'' = \frac{1}{2h^2}\left(f_{+3/2} - f_{+1/2} - f_{-1/2} + f_{-3/2}\right) - \frac{5}{24} h^2 f^{lv}$$

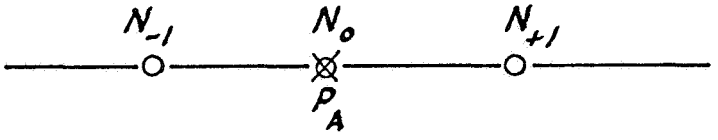

Scheme A

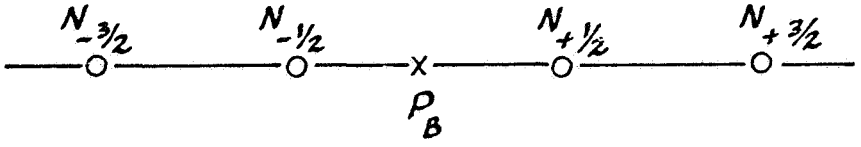

Figure 6.4. Two Finite Difference Schemes

The somewhat paradoxical result here is that if we attempt to determine a first order derivative at P_B with first order accuracy using two points and the first of Eqs. (6.9), the error is of the second order because the coefficient is zero for the leading term in the deleted sequence. Actually, it is only one quarter of the size of the error that is obtained at a node point from a three point scheme, Eq. (6.8). With a three point scheme, second order accuracy for the first derivative is obtained at any

point in the interval, but it is most accurately determined at the midpoint between two nodes where it is identical to the expression from the two-point scheme. On the other hand, the stress window for second order derivatives is located at the node points and the error in f″ in the second of Eqs. (6.8) is less than the error of f″ in the second of Eqs. (6.9). A formula for the first derivative at a node point determined from two function values (forward or backward difference) is of the first order accuracy only, i.e.,

$$f' = \frac{f_2 - f_1}{h} - \frac{h}{2} f'' \tag{6.10}$$

6.3 Numerical Integration

The purpose of numerical integration is to compute an approximate value of

$$\int_a^b f(x)\, dx \tag{6.11}$$

It is an essential procedure in finite element analysis and also in finite difference analysis based on the energy approach, as discussed below in Section 6.4. The value of the integral is determined after the range $a \le x \le b$ is divided into a number of small subintervals. For simplicity, the case in which all intervals are equal is considered here. With the function values determined at the midpoints of N intervals (see Figure 6.5a), the integral can be obtained by use of the so-called rectangle rule, i.e.,

$$\int_a^b f(x)\ dx \approx h \sum_{i=1}^{N} f_i \tag{6.12}$$

If instead the function values are determined at points of division between the intervals (including the end points, a, b), the trapezoidal rule can be used as illustrated in Figure 6.5b.

$$\int_a^b f(x)\, dx = h\,(1/2\, f_0 + f_1 + f_2 \cdots f_{n-1} + 1/2\, f_n) \tag{6.13}$$

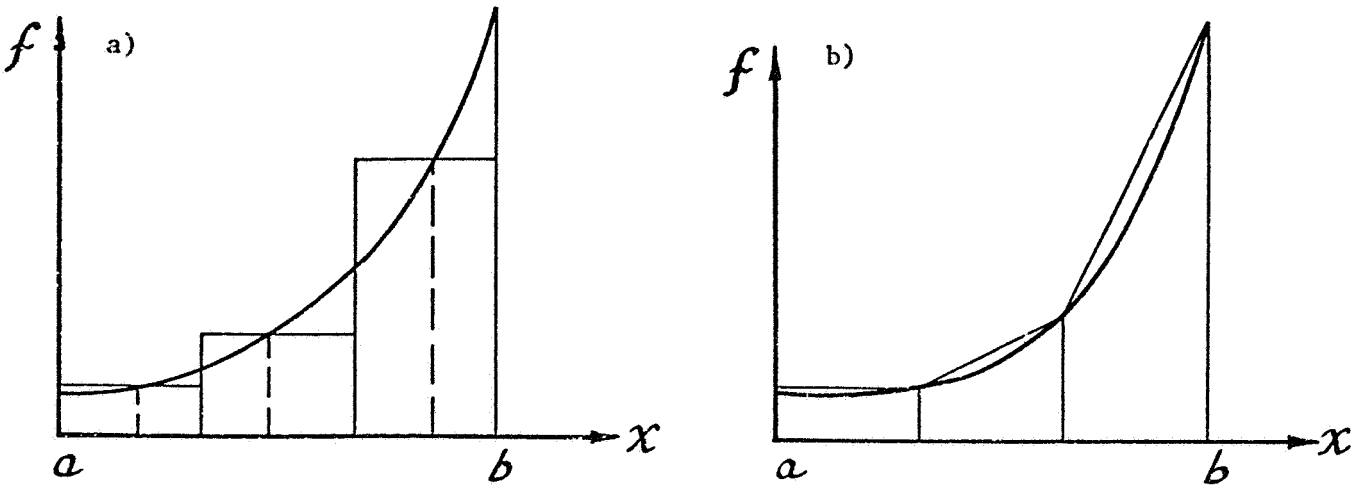

Figure 6.5. Numerical Integration Schemes

It is shown in Ref. 6.1 that both these methods are of second order accuracy. The rectangle rule is somewhat more accurate with the error bound

$$E = \frac{|b-a|h^2}{24} f''(\xi); \quad a \le \xi \le b \tag{6.14}$$

while the error bound for the trapezoidal rule is

$$E = \frac{|b-a|h^2}{12} f''(\xi); \quad a \le \xi \le b \tag{6.15}$$

A number of procedures of higher accuracy have been proposed (Euler-McLaurin, Stirling). The Newton-Cotes series of integration formulas are based upon the passing of a polynomial through a sequence of function values and integration of this polynomial over the subintervals. Since the trapezoidal rule is based on a linear approximation over the subintervals, it may be considered as the lowest order method in the Newton-Cotes series. A Newton-Cotes formula of third order accuracy is obtained if we use second order polynomials for interpolation between node points. This member of the Newton-Cotes family is well known as Simpson's formula

$$\int_a^b f(x)\,dx = \frac{h}{3}\,(f_0 + 4f_1 + 2f_2 + \ldots. 4f_{n-1} + f_n) \qquad (6.16)$$

Use of Simpson's formula requires that the number of subintervals is even. Higher order Newton-Cotes formulas are increasingly restrictive with regard to the permissible number of subintervals.

The integration procedure referred to as Gaussian Quadrature is based on finding strategic positions for the points at which the function value is determined. For demonstration of the principle it is shown here how a two point integration scheme is derived. If the function values at $x = \pm\,\alpha\,\ell$ are f_1 and f_2, where x is measured from the midpoint of the element, the function is approximated by

$$f = \frac{f_1 + f_2}{2} + \frac{f_2 - f_1}{\alpha\,\ell}\,x + F_2(x) + R \qquad (6.17)$$

Here, $F_2(x)$ is a function of second degree in x which vanishes at $x = \pm\,\alpha\,\frac{\ell}{2}$ while R is a power series beginning with the third order term. That is

$$f = \frac{f_1 + f_2}{2} + \frac{f_2 - f_1}{\alpha\,\ell}\,x + c\,(\alpha^2\,\frac{\ell^2}{4} - x^2) + \ldots \qquad (6.18)$$

and

$$\int_{-\ell/2}^{\ell/2} f(x)\,dx = \frac{\ell}{2}\,(f_1 + f_2) + c\,\frac{\ell^3}{4}\,(\alpha^2 - \frac{1}{12}) + \ldots \qquad (6.19)$$

The third order term will vanish if $\alpha = \pm\,1/2\sqrt{3}$ or $x = \pm\,\frac{\ell}{2\sqrt{3}}$. If the function is evaluated at these Gaussian points the integration is more accurate. The position of the Gaussian points coincides with the stress windows as defined in the example on numerical differentiation above. The rectangle rule is identical to the use of a Guassian Quadrature over each of the individual

intervals with only one integration point in each. In finite element analysis numerical integration is usually carried out separately over each element by use of Gaussian Quadrature. For a polynomial of any order the number of Gaussian points can always be chosen so that the integration is exact. The above example with two integration points gives the exact value of the integral for any polynomial up to the second order.

6.4 Numerical Solution Procedures

The Galerkin Method

A widely used procedure for obtaining approximate solutions to differential equations is known as the Galerkin method. The method is applicable to partial as well as ordinary differential equations. For simplicity, the equation is written in the form

$$L(u) = 0 \tag{6.20}$$

where L is a differential operator and u represents the displacement field. A solution is pursued in the space of trial functions of the form

$$u_N = \sum_{n=1}^{N} a_n \phi_n \tag{6.21}$$

where the basis functions, ϕ_n are kinematically admissible functions, i.e., they are continuous and satisfy given boundary conditions. A trial function consists of a linear superposition of a finite number of basis functions. The components of the output vector are the a_n. In the Galerkin method, the a_n are determined through solution of the equation system:

$$\int_V L(u)\, \phi_m \, dV = \int_V L\left(\sum_{n=1}^{N} a_n \phi_n\right) \phi_m \, dV = 0; \quad m = 1, N \tag{6.22}$$

where V represents the volume of the structure.

Convergence to the correct solution is implied if

$$\| u^N - u \| \to 0 \text{ as } N \to \infty \tag{6.23}$$

where u^N is the solution of Eq. 6.22 and u the solution of the mathematical problem L(u) = 0. The notation $\| u \|$ represents a norm of the function u.

The norm of u on the domain V may be defined as

$$\| u \| = \int_V u^2 \, dV \tag{6.24}$$

The question of convergence of the Galerkin method will be considered in connection with the discussion of the Rayleigh-Ritz method.

The Finite Difference Method

In the original form of the finite difference method (in contrast to the energy method discussed below), the derivatives in the equilibrium equations are replaced by finite difference expressions (see Section 6.2). An algebraic equation system is then formed in which each equation expresses equilibrium at one of the control points. The number of equations must be equal to the number of degrees of freedom of the system. Many examples of application of this procedure are given in the literature. In Ref. 6.5, it is applied in an analysis of column buckling.

The practical problems involved in finite difference analysis are much the same if finite differences are used in combination with the energy approach. The discussion of these problems is deferred to the paragraph on finite difference energy methods. Here only the conditions for convergence with the grid size will be considered. Over the years many efforts (Ref. 6.6, for example) have been made to show that the method converges with decreasing node point spacing to the solution of the differential equation, i.e.,

$$\| u^h - u \| \to 0 \text{ as } h \to 0 \tag{6.25}$$

where u^h is the finite difference solution corresponding to a node point spacing h.

Rigorous mathematical proofs have been presented for special cases, but due to the diversity of differential equation forms, boundary conditions and shape of domain, it appears to be difficult to establish a general proof of convergence. However, mathematical rigor has never been the trademark of engineering analysis. Often the assumptions and simplifications in modeling a structure are of such a nature as to make the quest for mathematical rigor rather extravagant. If the application of a reasonable method had been deferred in anticipation of rigorous proof, technical progress might have been considerably delayed. The finite difference approach is acceptable to an engineering analyst without a completely general and mathematically rigorous proof. The difficulty in proving convergence is due to the fact that the error bound in the numerical approximation of a derivative contains a higher order derivative of the solution function itself. If the solution function varies continuously with the input data (the loads), then the derivative in the error bound is itself bounded in terms of independent variables. Unless such continuity can be established, the error bound on the local approximation becomes meaningless.

It is possible to define finite difference formulations that are of order O(h) or better which still lead to spurious results. Consider, for example, the case of a beam or a column. The second order derivative in the column buckling equation is substituted by a three point central finite difference expression except at one internal point where either a backward or a forward difference expression is used. Then a beam is defined that has a link at the exceptional point.

It is proposed in Ref. 6.4 that the finite difference approach to the solution of differential equations converges toward the correct solution if:

1) The local truncation error vanishes with the gridsize; and
2) The solution varies continuously with the input data (loads) for small values of h.

The deformation of a beam with a link does not vary continuously with the load so the second requirement will exclude a spurious solution such as the one for the column discussed above.

The Rayleigh-Ritz Method

The total potential energy of a static system is the sum of the strain energy and the potential energy of the force system. The system is called conservative if the change in the total potential energy in passing from one configuration to another is independent of the path (compare Section 2). A static conservative system is in equilibrium if its potential energy is stationary. As formulated in Reference 6.5, the Theorem of Stationary Potential Energy states: "Of all displacements satisfying the given boundary conditions, those which satisfy the equilibrium equations make the potential energy a minimum." The condition of minimum energy is then equivalent to the requirement of structural equilibrium. The equilibrium equations can be derived from the first variation of the total potential energy through integration by parts. They are then referred to as the Euler equations of the calculus of variations.

The equilibrium problem for deformable bodies can also be solved directly through minimization of the energy, bypassing the explicit equilibrium equations. In the Rayleigh-Ritz method a sequence of trial functions is substituted for the displacement field. Each trial function is expressed as a linear combination of a set of basis functions. The method is thus closely related to the Galerkin procedure, although the trial functions are substituted into the expression for the total potential energy rather than in the equilibrium equations. The sequence of trial functions is given by

$$u^N = \sum_{n=1}^{N} a_n \phi_n , \quad N = 1, 2, 3..... \tag{6.26}$$

and the basis functions ϕ_n are chosen so that they satisfy displacement boundary conditions. The unknown coefficients a_n are determined by the

requirement that the total potential energy is stationary. Natural boundary conditions (stress-free edges) are automatically satisfied because they correspond to an energy minimum. Convergence toward the correct solution is guaranteed if the set of trial functions is complete in the space of continuous functions satisfying essential boundary conditions (displacement constraints). A convergence proof is given in Ref. 6.8.

The Galerkin method discussed above may be considered as an extension of the Rayleigh-Ritz method being applicable also to differential equations that cannot be derived through a variational approach. It is shown in Ref. 6.8 that the Galerkin method when applied to variational problems with quadratic functionals is identical to the Rayleigh-Ritz method.

Before the introduction of the digital computer, the Rayleigh-Ritz and Galerkin procedures were frequently applied with trial functions chosen intuitively. Because of computational difficulties, very few terms were included. With the arrival of the high-speed computer, it became popular to use as trial functions a finite number of terms in complete series of basis functions (generally trigonometric series). With increasing demand for general purpose programs, these methods have been gradually abandoned in favor of finite element and finite difference methods.

Finite Difference Energy Methods

The use of finite differences in a variational approach is discussed in Ref. 6.9 on page 182. Finite difference expressions are introduced directly into the energy expression and the potential energy is minimized with respect to the nodal displacement components. Convergence of the procedure is not discussed in Ref. 6.9. An appeal may be made to equivalence with a finite difference solution of the Euler equations discussed above. A rigorous and general proof of convergence does not appear to be available. However, whenever the procedure has been applied to a case with a known solution, it has been found to converge toward that solution.

The advantages of introducing difference quotients into the potential energy expression rather than into the equilibrium equations are that the coefficient matrix of the resulting equation system is symmetric and the natural boundary conditions are automatically satisfied. For a simple demonstration of the method, the buckling of a column with uniform cross-section (compare Ref. 6.5, page 283) subjected to an axial compressive force P is considered. The first variation of the potential energy vanishes for all equilibrium configurations. The bifurcation buckling load can be defined as the load level at which the second variation of the total potential energy vanishes. Hence, the critical value of P is obtained from

$$\delta^2 V = \int_0^L [EI(w,_{xx})^2 - P(w,_x)^2] \, dx = 0 \tag{6.27}$$

Advantage is taken of the stress windows as discussed above (see Eqs. 6.8 and 6.9), if $w,_x$ is determined at midnodes and $w,_{xx}$ at node points as shown in Figure 6.6.

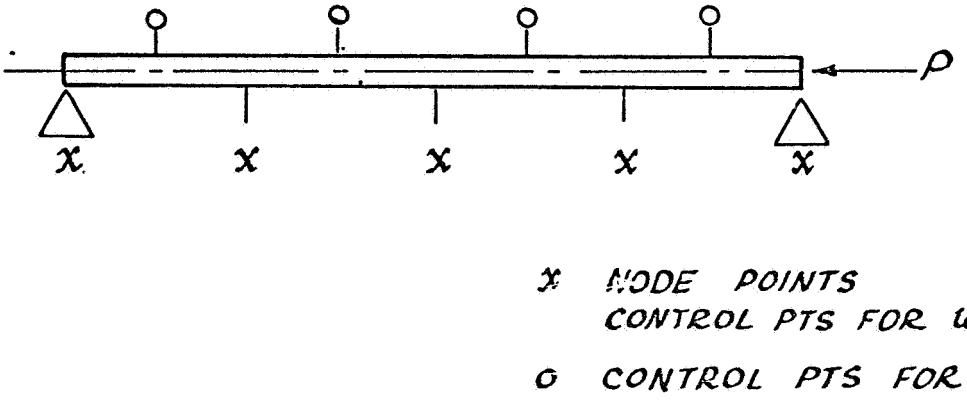

Figure 6.6 Finite Difference Scheme for Column

Then, $w,_x^2$ can be integrated by use of the rectangle rule but since $w,_{xx}^2$ is most accurately determined at node points it will be integrated by use of the trapezoidal rule. It follows that

$$\int (w,_x)^2 \, dx = h \sum_{i=1}^{N-1} \frac{1}{h} (w_{i+1} - w_i) \tag{6.28}$$

and

$$\int (w_{,xx})^2 \, dx = \frac{1}{2h^2} (w_2 - 2w_1 + w_0)^2 + h \sum_{i-2}^{N-1} \left[\frac{1}{h^2} (w_{i+1} - 2w_i + w_{i-1}) \right]^2 \tag{6.29}$$

$$+ \frac{1}{2h^2} (w_{N-1} - 2w_N + w_{N+1})^2$$

Fictitious points corresponding to w_0 and w_{N+1} are introduced so that the second order derivatives can be determined at the end points. Forward and backward derivatives could be introduced instead at these points or the rotations (w_x) at the end points could be used as freedoms of the system.

After the number of uniformly spaced node points has been chosen, a homogeneous linear equation system is formed by differentiation of $\delta^2 V$ with respect to the degree of freedom. The load P appears as the eigenvalue parameter. From Reference 6.5:

Number of Nodes on Half Column i	$P_{CR}/[EI(\pi/L)^2]$
3	0.9495
4	0.9774
5	0.9872
7	0.9943
9	0.9968
11	0.9979
∞	1.0000

Since the finite difference expressions as well as the numerical integrations are of second order accuracy, the error in the solution is expected to be proportional to the square of the spacing between node points. The natural boundary conditions can be shown to be satisfied to the same degree of accuracy. As the spacing equals L/2(i-1), the first two results in the table above indicate that

$$\left.\begin{aligned} c\left[\frac{L}{2(3-1)}\right]^2 &= \bar{P}_{CR} - 0.9495 \\ c\left[\frac{L}{2(4-1)}\right]^2 &= \bar{P}_{CR} - 0.9774 \end{aligned}\right\} \qquad (6.30)$$

If the first of Eqs. (6.30) is divided by the second, an equation is obtained that yields $\bar{P}_{CR} = 0.9997$. In view of the fact that the values of $\bar{P}_{CR}$ for 3 and 4 points were rounded to four figures, this is as close to the exact solution as can be expected. By use of two solutions with very coarse node spacing, and the assumption of second order accuracy, it is possible in this case to predict a very accurate result through extrapolation. The method is generally referred to as Richardson's extrapolation.

In shell or plate analysis the displacements are functions of two space parameters. In that case it is more difficult to utilize stress windows to gain one level in the order of accuracy. Considerable effort has been devoted to the task of defining efficient finite difference schemes for rectangular nets with uniform spacing. Examples of two-dimensional finite difference schemes are the STAGS half-station scheme and the STAGS whole-station scheme and Noor's scheme, shown in Figure 6.7. Noor's scheme and the STAGS half-station scheme define node points for displacements in the plane of the shell that are different from those at which normal displacements are defined. This has considerable disadvantages in a complicated structure with intersecting branches and attachments of beams or springs.

Finite Element Analysis

In contrast to the finite difference method, the finite element method was originally derived through physical and largely heuristic considerations in the field of structural mechanics. As an afterthought, the method

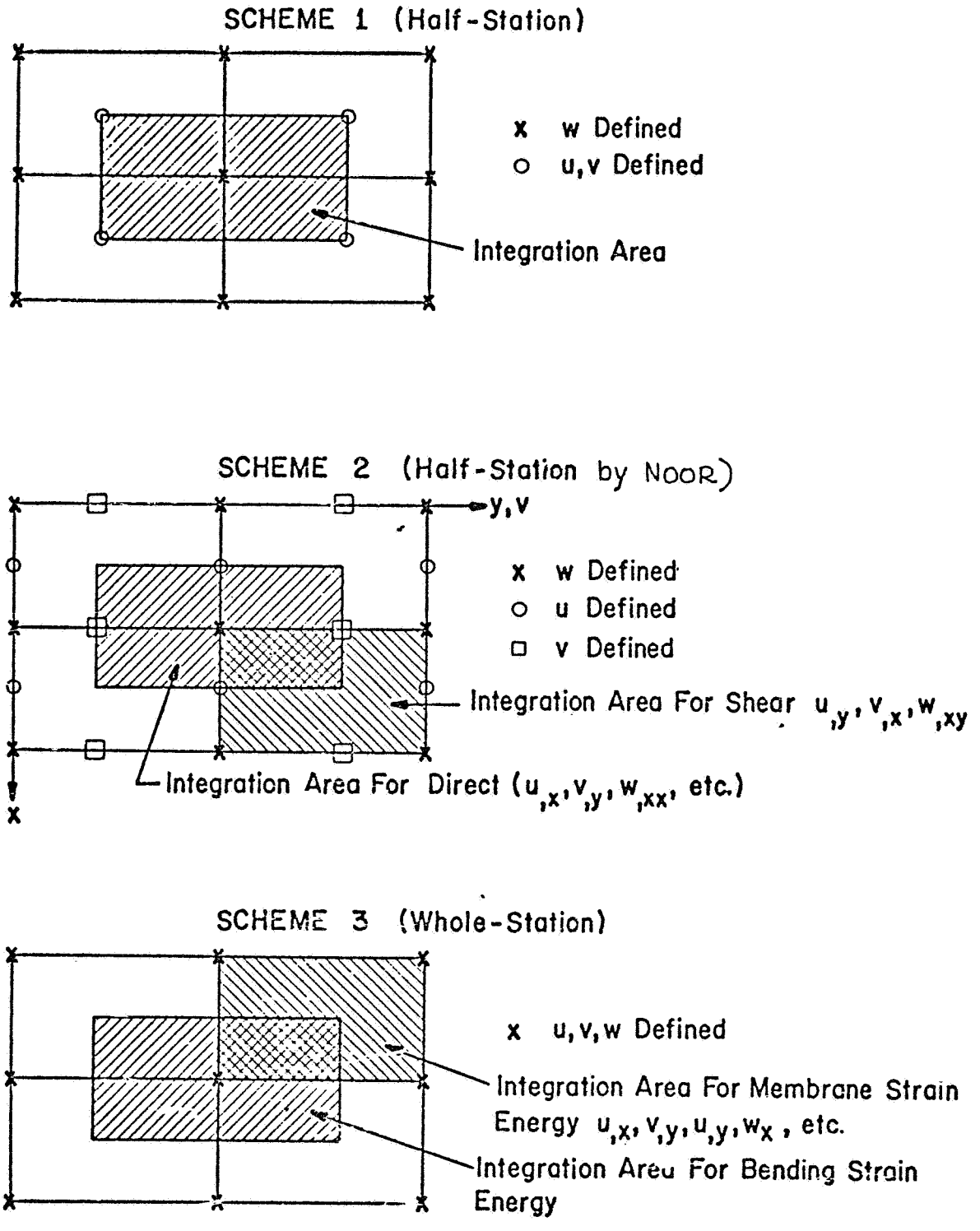

Figure 6.7. Two-D Finite Difference Schemes

was given a mathematical interpretation. This led to considerable refinement of the method and made possible its extension to problems outside of the field of structural mechanics.

The mathematical interpretation of the finite element method is based on the Ritz principle. In a departure from the historical development, the method is discussed here as an extension of the Rayleigh-Ritz method, much in the same way as it is presented by Strang and Fix in Ref. 6.4 where the reader is introduced to the finite element method primarily through a detailed discussion of its application to solution of first order ordinary differential equations. In the one-dimensional (ordinary differential equations) case, the domain of the equation is divided into a number of intervals, finite elements, through the introduction of a sequence of node points.

The conditions under which a Rayleigh-Ritz analysis converges to the right solution will now be discussed. Let C^n be the space of all functions which have continuous derivatives up to the nth order. If the functional under the integral includes derivatives up the kth order, it is required that the trial functions belong to C^{k-1}. Hence, for solution of problems with only first order derivatives in the integrand, it is sufficient that that the trial functions belong to the space C^0, i.e., the function itself must be continuous, but its derivatives are allowed to have a finite number of discontinuities. A sequence of piecewise linear functions satisfies this requirement. Such a space of trial functions is complete, because any function u in the solution space can be arbitrarily closely approximated by the limit of a sequence of piecewise linear functions. The trial functions can be written in the form

$$u^N = \sum_{n=1}^{N} a_n \phi_n \tag{6.31}$$

where the basis functions ϕ_n are piecewise linear, equal to one at node n and zero everywhere else. The function ϕ_n is shown in Figure 6.8.

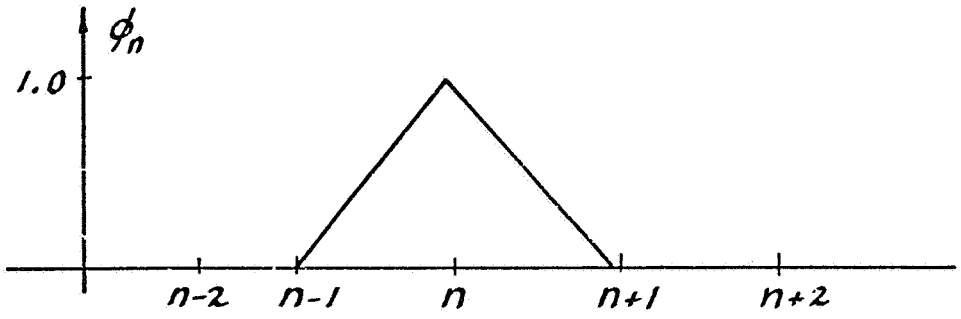

Figure 6.8. Linear Basis Function ϕ_n

For a functional including derivatives of the second order, it is required that the trial functions belong to C^1, i e., that the function itself and its first order derivative are continuous. This is achieved if we introduce rotations (first order derivatives) as well as displacements as nodal freedoms. In this case, the basis functions cannot be piecewise linear. Only a polynomial of third or higher order can match any set of values of the four freedoms, the function and its first order derivative at the two end points of the element.

The trial functions corresponding to a third order polynomial can be written in the form

$$u^N = \sum_{n=1}^{N} (a_n \phi_n + b_n \Psi_n) \tag{6.32}$$

where the basis functions ϕ_n and Ψ_n can be defined as shown in Figure 6.9 and Figure 6.10. With this choice, the ϕ_n correspond to $f = 1.0$, $f' = 0$ at node n and $f = f' = 0$ at all other nodes. The Ψ_n give $f = 0$, $f' = 1.0$ at node n

and $f = f' = 0$ at the other nodes. This formulation is equivalent to the first of Eqs. (6.5) after insertion of the solution of the Eq. System (6.6).

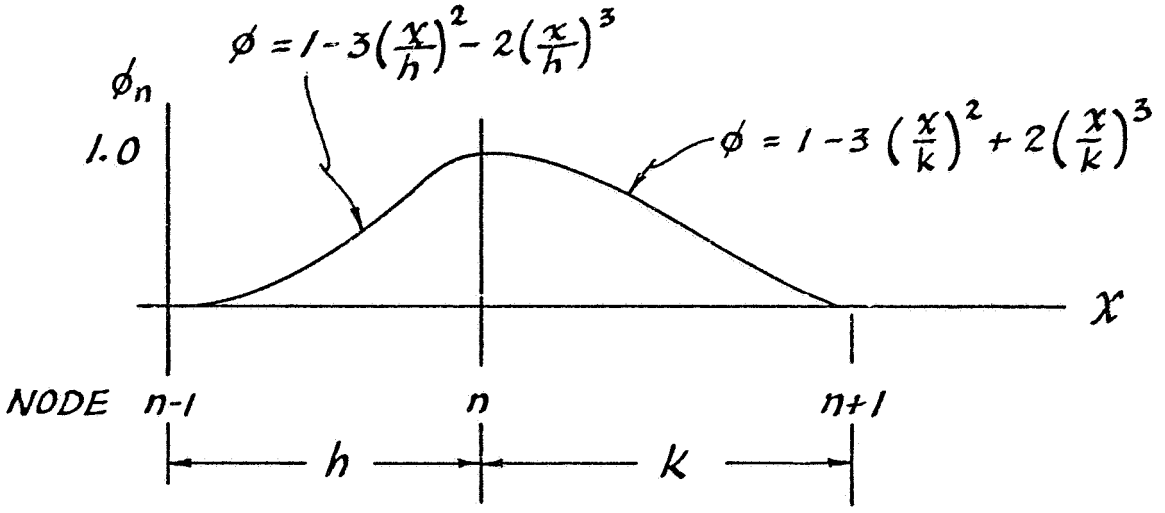

Figure 6.9. Cubic Basis Function ϕ_n

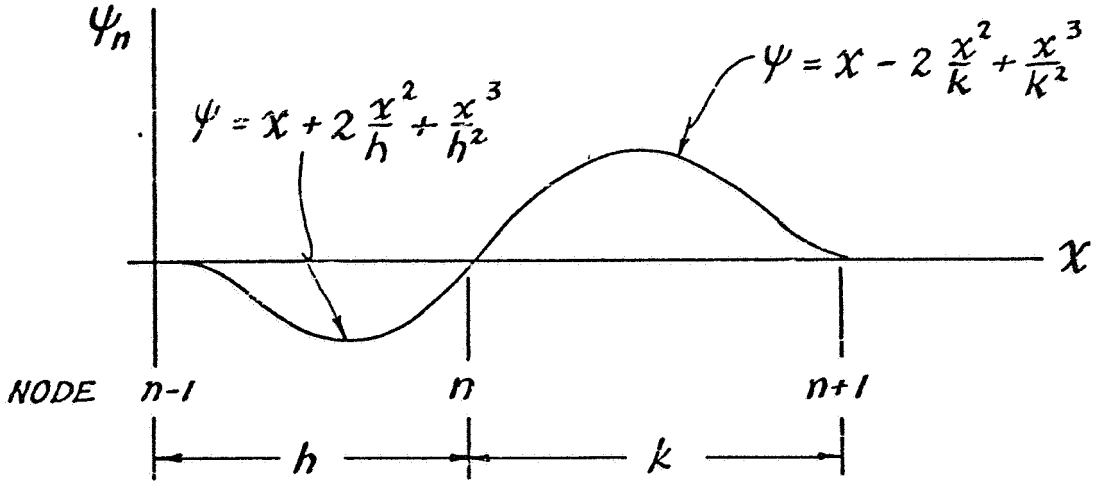

Figure 6.10. Cubic Basis Function Ψ_n

In application of the finite element method to the buckling of a column, the above equation for the critical load (Eqs. 6.27) can be used together with the cubic basis functions of Figures 6.9 and 6.10. First order derivatives are determined with third order accuracy by a complete cubic. Second order derivatives are of third order accuracy at the points defined by $\alpha = (1 \pm 1/\sqrt{3})/2$ (see Fig. 6.2). Since the Gaussian Quadrature (Cf. Section 6.3) also gives third order accuracy, the error bound is expected to be $E = 0(h^3)$. The Euler load for a column with L = 6.0 and EI = 10./12. is

$$P_{CR} = 0.22846307$$

Finite element (or Rayleigh-Ritz) analysis with piecewise cubic basis functions gives

Number of elements on half column (i)	P_{CR}
1	0.23190140
2	0.22869537
3	0.22850905
4	0.22847706
5	0.22846843
6	0.22846645
7	0.22846371

The indication from these numbers is that the error approximately varies with the fourth rather than the third power of the node point spacing. A possible explanation is that errors in first and second order derivatives tend to cancel one another.

For plate and shell buckling or bending problems, the lateral displacements w appear in derivatives up to second order. The inplane displacements u, v are only included in derivatives up to first order. Therefore, admissable displacement functions in the Rayleigh-Ritz sense are such that u and v are in C^0 and w in C^1.

At an element interface, as shown in Figure 6.11, this means that u,v,w and $\partial w/\partial \zeta$ are required to be continuous, where ζ is any coordinate in the plane of the element not parallel to the boundary.

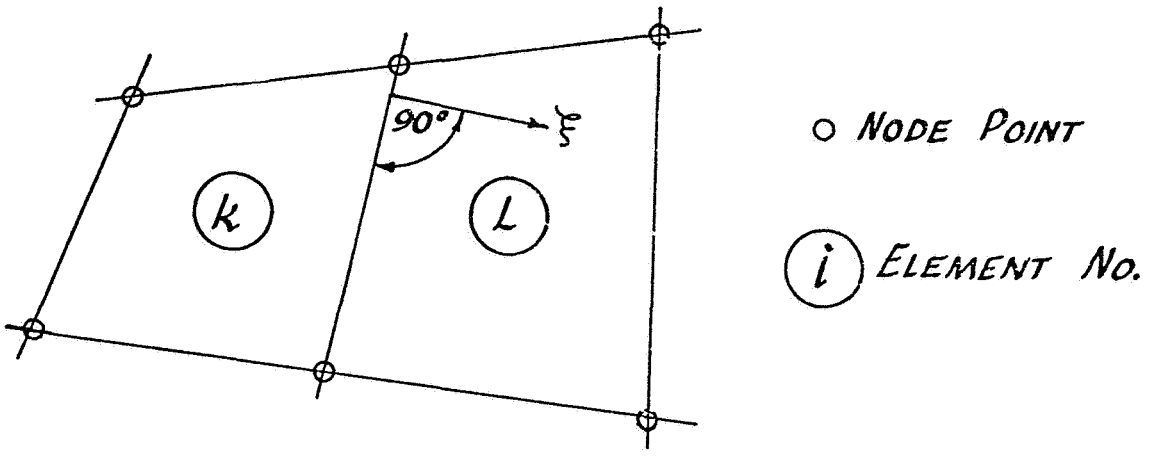

Figure 6.11. Adjacent Plate Elements

Plate or shell elements that satisfy these conditions are referred to as conforming elements. If such elements are used, convergence is assured (Rayleigh-Ritz equivalent), provided that the polynomial approximations are at least of first order accuracy, E = O(h). Convergence is from above, i.e., the coarser the grid is, the higher the strain energy in the system and the higher the buckling load. Finite elements were used successfully for plate and shell analysis before the method was established as a form of the Rayleigh-Ritz procedure. These elements were not conforming.

Experience has shown that an analysis based on nonconforming elements may converge to the correct solution. In fact, it has often been found (see Ref. 6.7, for example) that within the level of accuracy generally required in engineering analysis the nonconforming elements show better convergence properties. The reason for this is that the conforming ele-

ments, with convergence from above, overestimate the stiffness of the structure. Relaxation of interelement displacement constraints results in an error of opposite sign. Moreover, this is an error of lower order than the error introduced through truncation of the local power series representing the displacements.

If two methods with different order of accuracy are applied to models with identical grids, the ratio between the error bounds for the two methods can be written in the form

$$R = ch^{m-n}, \quad m > n \tag{6.36}$$

where c is some constant and m and n the orders of accuracy of the two methods. For a relatively coarse grid, the error may be much smaller than the error bound, and it is possible that a lower order method will give more accurate results. However, for sufficiently small grid spacing, the lowest order term in the error will dominate and the higher order method must result in a smaller error. The analysis with conforming elements converges from above and the corresponding analysis with relaxed compatibilty requirements gives a lower value of the strain energy. Since the analysis with nonconforming elements (being of lower order) results in larger error for small grid spacing, it may be concluded that a nonconforming element cannot converge uniformly from above. Also, if for some grid size, the nonconforming element underestimates the stiffness, the error can only be increased by introduction of freedoms that do not affect interelement compatibility, such as displacements at internal nodes.

In addition to the use of nonconforming elements, Strang (Ref. 6.8) lists among "variational crimes" the use of numerical integration and approximation of domain and boundary conditions. Use of integration with too few Gaussian points tends, like displacement incompatibility, to weaken the system. As a consequence of the tendency of such approximations to weaken a structural model that otherwise is too stiff, the world of finite elements is indeed one in which "crime" pays!

After the finite element method was given a theoretical foundation as a form of the Rayleigh-Ritz procedure, the wisdom of using nonconforming elements was questioned. However, the evidence of success in previous applications is compelling, and eventually the authors of Ref. 6.7 suggested that non-conforming elements can be accepted if they pass "the patch test." For plate and shell ements the patch test requires that constant strain and constant change of curvature are maintained through any patch of elements whenever corresponding conditions are applied at patch boundaries.

It has not been established in a rigorous mathematical way that the patch test is a sufficient condition for convergence to the correct solution. However, Irons (Ref. 6.9) presents a heuristic argument for sufficiency. With decreasing grid size the variation of strain and change of curvature diminishes so that in the limit these quantities are essentially constant in any loading case.

Regarding the necessity of the requirement, it is easy to construct a counter example. Consider, for example, two elements, one of which, ℓ_1, is conforming and the other, ℓ_2, is nonconforming, does not pass the patch test, and actually converges toward an inaccurate solution. If the stiffness matrices of ℓ_1 and ℓ_2 are K_1^e and K_2^e, then a new element, ℓ_3, can be defined so that its stiffness matrix $K_3^e = (1 - \alpha)\, K_1^e + \alpha K_2^e$ where α approaches zero with the grid size h. The element ℓ_3 will not pass the patch test for any finite value of h. However, in the limit, it is conforming so that convergence to the correct solution is certain. For most element configurations the patch test is indifferent to the size of the element. Therefore, it is a practical test, but possibly it should be relaxed so that compliance is required only in the limit $h \to 0$.

There is no clear distinction between the finite element method and the finite difference energy method. It seems reasonable to define as a finite element method a discretization scheme in which the displacement pattern inside the element is determined without the use of nodal freedoms outside the closed domain of the element. With this requirement, each basis function

is nonzero at one node only. This simplicity allows a certain formalism in the derivation of stiffness matrices and the development of comptuer programs. The lucidity of the method and its well established formulation are probably the major reasons for its great popularity. The finite difference energy method is somewhat less restrictive. The finite element method could have been arrived at by specialization of the finite difference energy method. We may notice that in the finite difference energy method we allow incompatible trial functions in the one-dimensional as well as in more general cases. The use of different polynomials for different derivatives of the same function in the finite difference discretization obviates a convergence proof based on equivalence with the Ritz procedure. However, it can be shown that the difference between equations based on this approach and one that is consistent with a Rayleigh-Ritz approach vanishes with decreasing grid size.

6.5 Some Special Problems

In this section some special problems connected with the use of discretized numerical analysis are discussed.

- First, the choice of Gaussian points for the numerical integration is considered. The strain energy is expressed as a polynomial in the spatial coordinates. It is possible to choose sufficiently many integration points to make integration of a given order polynomial exact. If fewer points are selected, the computer run time for formulation of a stiffness matrix is reduced, but at the same time an error is introduced through inaccuracy in the integration. This error usually results in an underestimate of the strain energy in the element for a given displacement configuration. As was pointed out above, this underestimation may in some cases be beneficial. On the other hand, it may lead to spurious results. In particular, some displacement pattern that produces no strain energy at all may be permitted. In the literature (Ref. 6.4) such a displacement pattern is sometimes referred to as a spurious mechanism. In a rectangular constant strain element (Figure 6.12), for example, one Gaussian point may be used (analogous to the rectangle rule in one-dimensional discretization) - see Figure 6.5(a).

For a flat element and with u denoting the displacement in the x-direction, $\epsilon_x = u_{,x}$. The stress window for ϵ_x is located at P with

$$e_x = \frac{u_2 - u_1}{2h} + \frac{u_4 - u_3}{2h} \tag{6.37}$$

This expression is of second order accuracy, but a displacement pattern in which

$$u_3 = u_2 = -u_1 = -u_4 \tag{6.38}$$

produces no strain energy at the integration point.

The option of using four integration points increases the formulation time considerably and at the same time it lowers the order of the error bound. Therefore, it appears to be preferable to use only one integration point and to use other means for suppression of the spurious deformation modes. It is probably sufficient to include four (or possibly two) integration points only in elements along shell edges on which inplane displacement components are not constrained.

- Special problems may be introduced if the strain energy in the element due to a rigid body displacement is not exactly zero, but rather approaches zero with the node point spacing. For illustration of this problem, an element of a circular arc is shown in Figure 6.13.

The case is considered in which the circular arch is rigidly displaced a distance δ in the x-direction. The displacement components are then defined by

$$\begin{aligned} w &= \delta \sin(\theta + \phi) \\ v &= \delta \cos(\theta + \phi) \end{aligned} \tag{6.40}$$

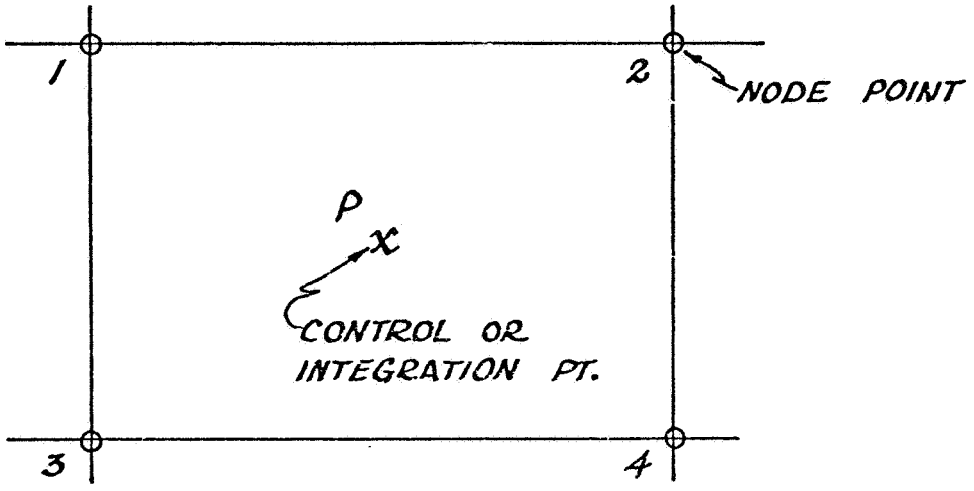

Figure 6.12. Rectangular Membrane Element

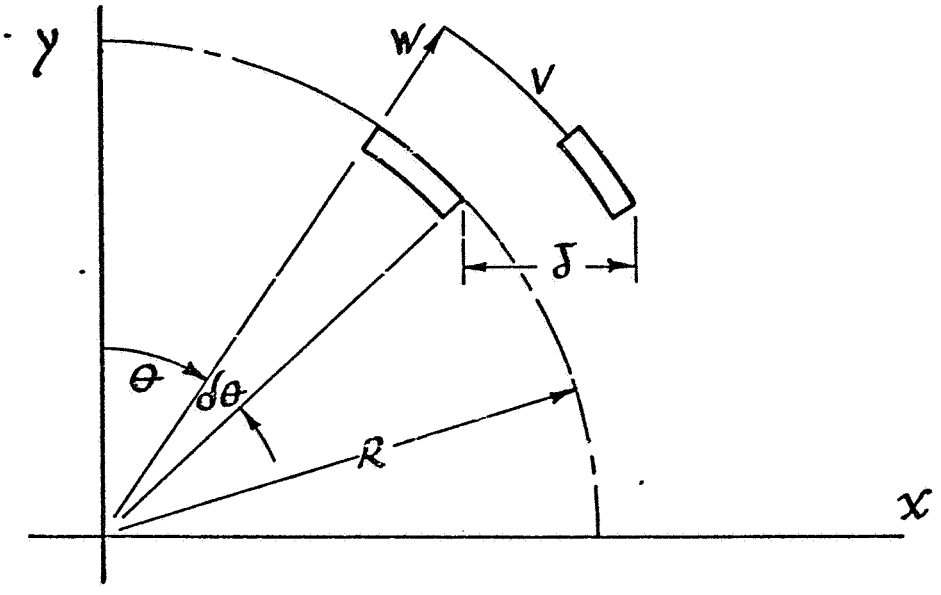

Figure 6.13. Rigid Displacement of Curved Element

It is not possible with a truncated power series in ϕ to represent this displacement pattern exactly. The strain energy in the arc due to this rigid body displacement will approach zero only with vanishing grid size. This problem will recur whenever the geometry of the element is defined by use of polynomials that are of higher order than those that represent the displacement components (super parametric mapping). There are cases in which the rigid body displacement of an element is very large in comparison to the displacements corresponding to element distortion. In such cases convergence may be very slow for elements in which the rigid body energy is not exactly zero but rather proportional to some power of the nodal point spacing.

- In nonlinear analysis or in stability analysis, the direction of convergence may present a special problem. It is often undesirable to use elements resulting in convergence from below for the critical load. Whenever the buckling pattern is local, a rather fine grid must be used in the area where buckling occurs. If the convergence is from above, a coarser grid can be used in the remaining part of the structure. With convergence from below, a relatively fine spacing must be maintained over a larger part of the structure, since otherwise the analysis may indicate spurious buckling in an area with lower stresses but coarser spacing.

6.6 Some Options for Discretization

For plate or shell bending analysis, a fully satisfactory discretization procedure has still to be developed. Finite difference methods generally fail to satisfy the requirement of zero strain energy under rigid body displacements. Further, the direction of convergence with the grid size is unpredictable. Most conforming finite elements have a large number of degrees of freedom and require many integration points. The computer time for formulation of the first and second variations is large. Conforming elements of lower order are very stiff and convergence with grid size is slow. The conforming plate or shell elements may have a place when a very accurate solution is required or if for some reason convergence from above must be assured.

A number of discretization options for STAGS are discussed in this subsection. The shortcomings and possible advantages are briefly discussed here. A more extensive analysis of the merits of the different formulations is given in Appendix D. The results of a few convergence studies are also included in this Appendix.

STAGS Half-Station Scheme

The first version of STAGS (STAGS A) was based on the finite difference discretization referred to in Section 6.4 as the STAGS half-station scheme, Figure 6.7a. The primary weakness of this scheme is its inefficiency in nonlinear and stability analyses. It is sufficient for illustration of the problem to consider a beam element. The strain at the neutral axis of the beam is

$$\varepsilon_x = u,_x + 1/2\ (u,_x^2 + w,_x^2) \tag{6.41}$$

For definition of the strain ε_x, the spatial derivatives $u,_x$ and $w,_x$ must be determined at the same integration points. If w is defined at the node points and u at half stations, it is not possible to use the most favorable expression (the stress window) for $u,_x$ as well as for $w,_x$.

In addition to inefficiency for geometrically nonlinear problems, the half-station scheme has the disadvantage that it requires the definition of inplane displacements at fictitious points outside the shell boundaries. Finally, the strain energy due to a rigid body displacement of a shell element of general shape is not exactly zero but it vanishes with the fourth power of the mesh size.

STAGS Whole-Station Scheme

The STAGS whole-station scheme is illustrated in Figure 6.7b. With the membrane and bending energies integrated over different sets of integration points, it is possible to make use of the stress windows for $u,_x$ as well as for $w,_x$. This results in much better convergence for the buckling or collapse loads.

However, the whole station scheme suffers from difficulties connected with too few integration points. The strain free displacement pattern discussed in Section 6.5 occurs for certain boundary conditions. Furthermore, the stress windows for membrane strains do not coincide with those for the changes of curvature. Therefore, the accuracy for a given grid size deteriorates when coupling between membrane and bending stresses is included (shells with eccentric stiffening). Again, the strain energy under a rigid body motion is not exactly zero.

Modified Whole-Station Scheme

In an effort to remove the major shortcomings of the schemes shown in Figure 6.7, a third finite difference scheme was developed. The integration area (the element) was divided into four different subareas, 1 through 4

as shown in Figure 6.14, and the different quantities in the expressions for strain and change of curvature were determined at the locations indicated.

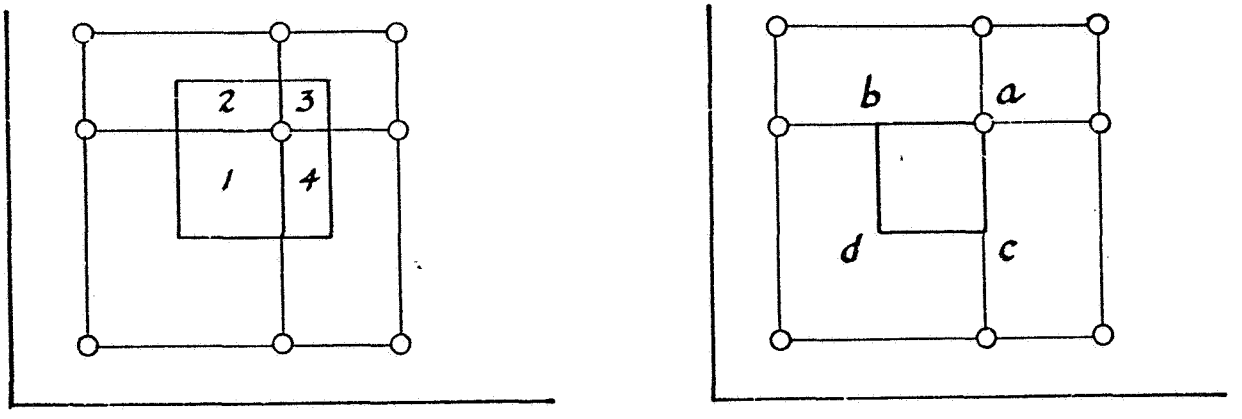

Quantity	Location
ε_x	b
ε_y	c
γ_{xy}	d

Quantity	Location
β_x	b
β_y	c
w_{xx}	a
w_{yy}	a
w_{xy}	d

Figure 6.14. Finite Difference Scheme for STAGSC

This formulation was introduced in a later STAGS version (STAGSC). In many applications it proved to be more efficient than any of the schemes shown in Figures 6.7a and b. However, it requires somewhat longer time for formulation of the first and second variations and the rigid body displacement problem is more acute because the strain energy due to rigid body displacement is proportional to the square of the mesh size.

Curved Element: STAGC

In all the three finite difference schemes discussed above only the three displacement components are used as nodal freedoms (with the

exception of nodes on branch boundaries in STAGSC). Advantage is taken of stress windows so a second order accuracy is obtained with a minimum number of node point values involved in each expression. Therefore, analysis with these STAGS versions has been quite efficient despite the shortcomings discussed above.

The exclusion of rotations as freedoms makes programming quite involved if beams and rotational springs are included in the model or if branch connections along internal gridlines are allowed. Therefore, a scheme was derived for STAGS in which the two inplane rotation components were included as additional degrees of freedom at each node. In that case, the lateral displacement and two rotations at each corner of the element provide twelve nodal freedoms for determination of the lateral displacement field within the element. Since a complete cubic contains no more than ten terms, two fourth order terms were added to the displacement function (compare Eq. 6.3). Twelve corner displacements and rotations are determined from

$$\begin{aligned} w = {} & a_o + a_1 x + a_2 y + b_{11} x^2 + b_{12} x_4 + b_{22} y^2 \\ & + c_{111} x^3 + c_{112} x^2 y + c_{122} x y^2 + c_{22} y^3 \\ & + d_{1112} x^3 y + d_{1222} x y^3 \end{aligned} \tag{6.42}$$

The expressions for the second order derivatives of the lateral displacements so obtained are of third order accuracy at the four integration points. With the displacement field depending on degrees of freedom on the element boundary only, this configuration can be classified as a finite element. The shell wall rotation around a boundary between two elements can only be determined as a first order function from freedoms that are common to two adjacent elements (corner rotations). The displacement field allows cubic variation of this rotation and consequently the element is nonconforming. This reduces the method to one with a first order accuracy. It may be hoped, however, that for grid sizes in the practical range the error due to noncon-

formity is still of approximately the same size as the truncation error in the local expressions for the changes of curvature. If that is the case, it seems reasonable to determine the membrane strain energy to the same order of accuracy as the bending strain energy. This is achieved if the inplane displacement fields are expressed by use of a complete quadratic. The displacement in the x-direction is defined by

$$u = u_1 + u_2$$

where the coefficients in the polynomial

$$u_1 = a_o + b_1 x + b_2 y + c_{12} xy$$

are determined in terms of the displacement components at the element corners. The correction term u_2 representing the so-called bubble modes discussed in Reference 6.4, page 176, completes the quadratic

$$u_2 = c_{11} (\zeta - \zeta^2) + c_{21} (\eta - \eta^2)$$

where ζ and η are dimensionless space coordinates chosen so that they are zero or one on element boundaries (isoparametric mapping).

The two terms of u_2 vanish at corner nodes. The coefficients c_{11} and c_{21} are included as degrees of freedom of the system. The displacement v in the y-direction is treated in the same way.

Use of the bubble modes results in nonconforming inplane displacements. However, it is shown in Ref. 6.4 that a rectangular element with bubble modes will pass the patch test.

Due to the higher order accuracy in the local power series, this element appears in many applications to be more efficient than any of the finite difference formulations discussed above. However, due to the lack of conformity, questions can be raised regarding its reliability, particularly

for elements with nonrectangular plan form. Also, the strain energy due to a rigid body displacement is not exactly zero.

Flat Element: STAGF

A flat element was developed for use in STAGS so that one formulation would be available in which the strain energy due to rigid body displacements is exactly zero. The resulting formulation has much in common with the elements discussed by Kaspar William in Reference 6.10. Some of the equations presented in Ref. 6.10 have been used directly in the derivation of the stiffness matrix.

As a background to this discussion, a node point on a curved shell surface is considered as shown in Figure 6.15. At the node the three displacement components, u,v,w, are obvious degrees of freedom of the system. The two rotation components, β_1 and β_2, along the tangent to the gridlines must also be included as freedoms in a bending element. The practice with respect to the third rotation component varies. This component is not uniquely defined, as in the presence of a shear strain, differently oriented line segments through the node will rotate through different angles. Clearly, the rotation of the boundary line between elements 1 and 2 (see figure) have nothing to do with the rotational compatibility between elements 2 and 3. Hence, there is more than one degree of freedom corresponding to the rotation component β_3. If the shear strain at the node is the same in each of the four elements, there are two freedoms corresponding to normal rotation, each representing the rotation of one of the two gridlines intersecting at the node. Equivalently, an average rotation and a shear strain can be defined as degrees of freedom.

When a curved shell surface is approximated by flat elements, the geometric model has slope discontinuities between adjacent elements. The conditions for displacement compatibility between the elements become quite complicated in this case. For simplicity a cylindrical surface is used here for demonstration of the consequences of slope discontinuities. Two adjacent

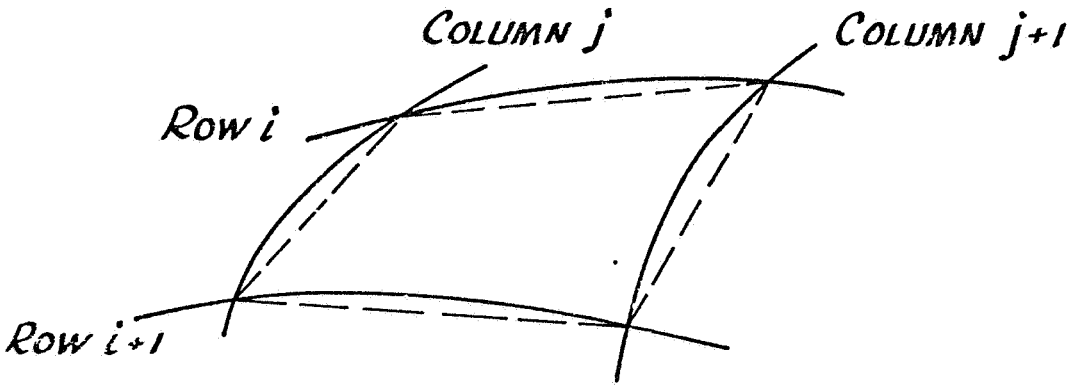

Figure 6.15. Flat Element on Curved Surface

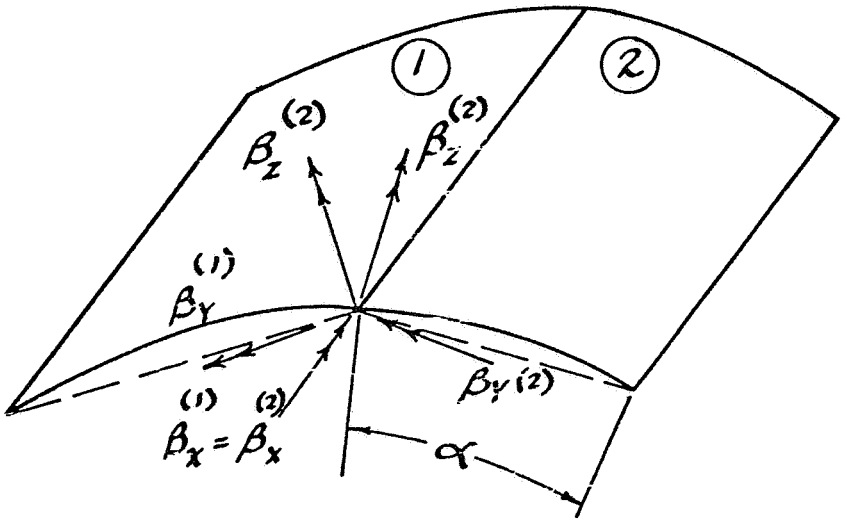

Figure 6.16. Flat Elements on Circular Cylinder

flat elements in a representation of a circular cylindrical surface are shown in Figure 6.16. The superscripts refer to the element number.

The rotation components in the direction of the common boundary must be the same for both elements, i.e., $\beta_1^{(1)} = \beta_1^{(2)}$. However, the other two rotation components are coupled.

$$\left.\begin{aligned} &\left(\beta_2^{(1)} - \beta_2^{(2)}\right) \cos \alpha/2 + \left(\beta_3^{(1)} + \beta_3^{(2)}\right) \sin \alpha/2 = 0 \\ \text{and} \\ &\left(\beta_3^{(1)} - \beta_3^{(2)}\right) \cos \alpha/2 - \left(\beta_2^{(1)} + \beta_2^{(2)}\right) \sin \alpha/2 = 0 \end{aligned}\right\} \qquad (6.45)$$

Therefore, whenever $\alpha \neq 0$, the normal rotation component must be included as a freedom in the system in order to make possible the enforcement of rotational compatibility. Usually the component β_3 is not allowed to affect the inplane displacement fields. Then if the elements are in the same plane ($\alpha = 0$) the normal rotation component does not contribute to the strain energy and the equation system becomes singular. If the angle between the elements is small, the system becomes ill conditioned. Generally for flat elements used in shell analysis the normal rotation component is discarded as a freedom if the angle between the element is less than some predetermined value.

The inplane displacement components (u,v) occur at most in first order derivatives while the changes of curvature are functions of the second order derivatives of the transverse displacement component w. Therefore, w is usually represented by higher order polynomials than those representing u and v. Typically w is represented by bicubic and u and v by biquadratic polynomials.

For two flat elements at an angle with one another complete displacement compatibility (all trial functions in C^0) requires that along the entire boundary

$$\left.\begin{aligned} &\left(v^{(1)} - v^{(2)}\right) \cos \alpha/2 + \left(w^{(1)} + w^{(2)}\right) \sin \alpha/2 = 0 \\ \text{and} \quad &\left(w^{(1)} - w^{(2)}\right) \cos \alpha/2 - \left(v^{(1)} + w^{(2)}\right) \sin \alpha/2 = 0 \end{aligned}\right\} \qquad (6.46)$$

Clearly, these conditions cannot be satisfied if w along the boundary is represented by a third order and v by a second order polynomial. The result is that in the traditional form the flat element is too flexible. The buckling load converges rather slowly from below.

The flat element can be considerably improved if displacement compatibility is enforced. This requires that v be determined from a set of freedoms similar to the set from which w is determined along an element boundary in the axial direction. As w along the boundary is determined from the discrete values of w and $w_{,x}$ at the end points, it is necessary to determine v from end point values of v and $v_{,x}$. Thus, v must be cubic in the x-direction.

Similarly for complete compatibility the displacement component u must be determined from the end point values of u and $u_{,y}$. Discrete values of $v_{,x}$ and $u_{,y}$ can be obtained from the average rotation and the shear strain at the node. Consequently, if these quantities are introduced as degrees of freedom, a third order polynomial can be used for v in the x-direction and for u in the y-direction. An element of this type was developed for use in STAGS. In order to make the inplane displacement at least quadratic, midside nodes were introduced. At these nodes the displacement tangential to the element boundary is used as a degree of freedom. With 7 degrees of freedom at corner nodes and 4 at midside nodes, there are a total of 32 degrees of freedom per element. The details of the derivation of a stiffness matrix for this element are given in Appendix C.

AHMAD-Type Elements

It is not necessary to use a flat element in order to permit rigid body displacements without strain energy. Any shell element geometry can be made free from rigid body strain energy if its reference surface is defined by polynomials that are at most of the same order as those representing the displacements. This so-called isoparametric property is taken advantage of in the Ahmad elements (Figure 6.2e). Such elements are obtained by adaptation of a three-dimensional element for shell analysis and were first introduced by Ahmad (Ref. 6.11) and further developed by Pawsey (Ref. 6.13). Ahmad-type elements can be used for moderately thick shells since transverse shear deformations are included.

A three-dimensional element is shown in Figure 6.17. The degrees of freedom of this element are the three displacement components at each of the 24 node points. However, the number of freedoms may be reduced if the approximations usually made in thin shell theory are introduced, i.e., it is assumed that the stress in the direction of the normal to the middle surface can be neglected and that the normals remain straight during deformation. The assumption of a first order shell theory that the normals remain

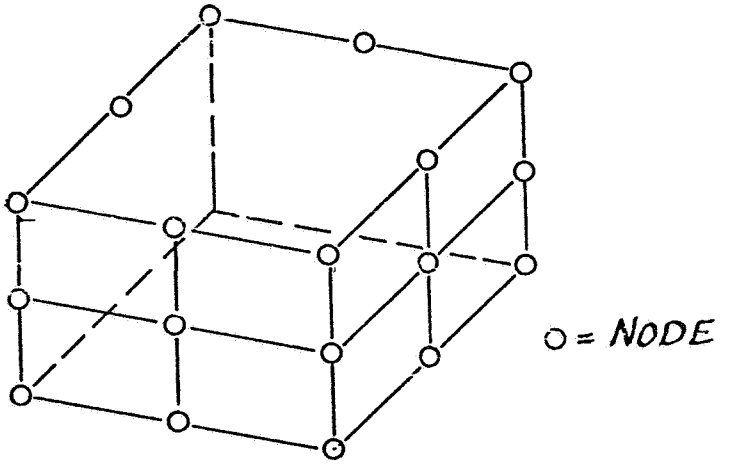

Figure 6.17. Three-Dimensional Element

normal to the middle surface is not made, and therefore the transverse shear deformation is approximately accounted for. With the displacements varying linearly through the thickness, a second order shell theory is obtained. It still overestimates the shear stiffness because it corresponds to constant shear stress through the thickness rather than to a parabolic distribution. This may be compensated for if the modulus for transverse shear is reduced by a factor of 1.2.

The degeneration into a shell element is achieved by introduction of rotations as freedoms at each of the nodes on the middle surface. The displacements at the inner and outer surface are expressed in terms of these freedoms by use of the assumptions of shell theory. There are five degrees of freedom at each of the midsurface nodes. Two Ahmad elements are illustrated in Figure 6.18. There are five degrees of freedom at each of the midsurface nodes, two rotation and three displacement components. Thus, the element AHMAD1 has 40 degrees of freedom and AHMAD2 has 60. In both cases, there is only one midside node on each normal to the shell surface, so this normal must be assumed to remain straight during deformation. The stiffness matrices for the two elements were programmed for nonlinear analysis by Bob Clark in Department 81-12, Lockheed Missiles and Space Company.

The strain energy is computed from the displacements in the equivalent three dimensional element. Bending and membrane actions are not separated. Therefore, it is necessary to use at least two layers of integration points through the shell thickness. For the element AHMAD1, Gaussian integration is used in the three directions with a 2 x 2 x 2 set of integration points. Use of more points results in a system that is too stiff. Pawsey (Ref. 6.12) shows that with a linearly varying bending moment, the transverse shear strain is accurately determined only at the positions $\zeta = \pm 1/\sqrt{3}$, that is at the location of the Gaussian points in a two-point scheme. With the element AHMAD2 a 3 x 3 x 2 set of integration points must be used in order that strain-free displacement modes be prevented.

The AHMAD-type elements have been used extensively in linear stress analysis. They are curved shell elements with zero strain energy under rigid

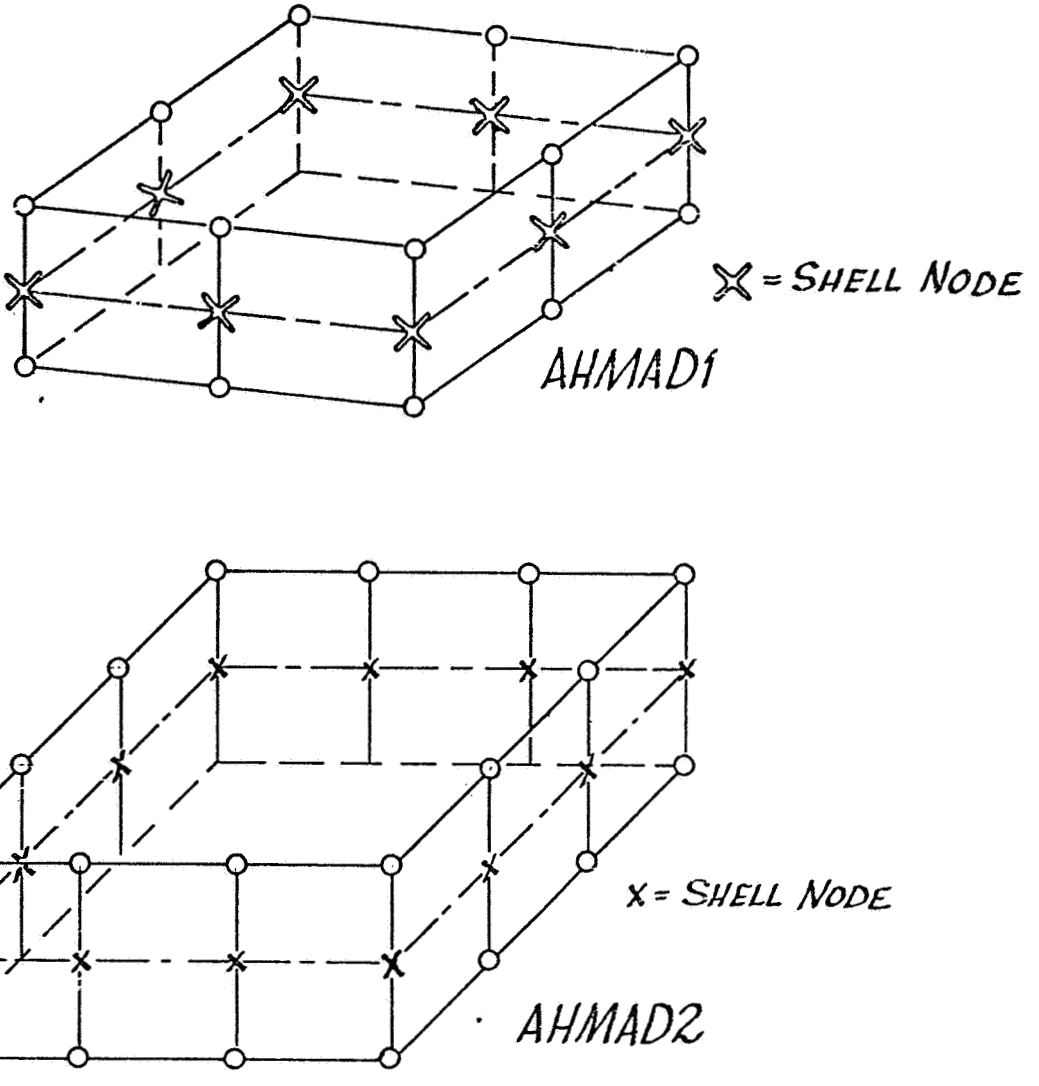

Figure 6.18. Two AHMAD Type Elements

body displacements. The parabolic representation of the curved surface essentially eliminates slope discontinuities at element boundaries (in the unloaded state). Unless the element is used in combination with other types of elements, it will pass the patch test even if nonrectangular. However, the formulation time is relatively long and questions have been raised about their usefulness for very thin shells (Ref. 6.13). A discussion of the implementation of the AHMAD-type elements in STAGS is included in Appendix D.

The Clough-Felippa Elements: CFT, CFQ

A quadrilateral element was constructed by Clough and Felippa (Ref. 6.14) through decomposition of the element into four triangular subelements. The four triangles in one element need not be in the same plane. The element is conforming for flat plate analysis.

The original triangular bending element LCCT-12 includes 12 degrees of freedom to allow a piecewise cubic variation of the lateral displacement, w. It is conforming in plate analysis and yields exact solutions for rigid body displacement and cases with constant strain. The basic triangular element is divided into three triangular subelements. Each of the three subelements are triangles with two of its corner points common with those of the basic triangle. The third corner, common for the three subelements, is an interior point in the basic triangular element. The subdivision is shown in Figure 6.19.

For each of the subelements, the freedoms are w, β_x, β_y at each corner, where β_x and β_y are rotation components in an element-bound Cartesian system. A tenth freedom is provided by the rotation component in the direction of the element boundary at the midpoint of the only boundary line that is external to the basic triangle (see figure). With 10 degrees of freedom, then the 10 coefficients in a complete cubic for the lateral displacement w can be uniquely determined.

The number of degrees of freedom of the system can be reduced on the element level in two different ways. Freedoms at internal nodes do not

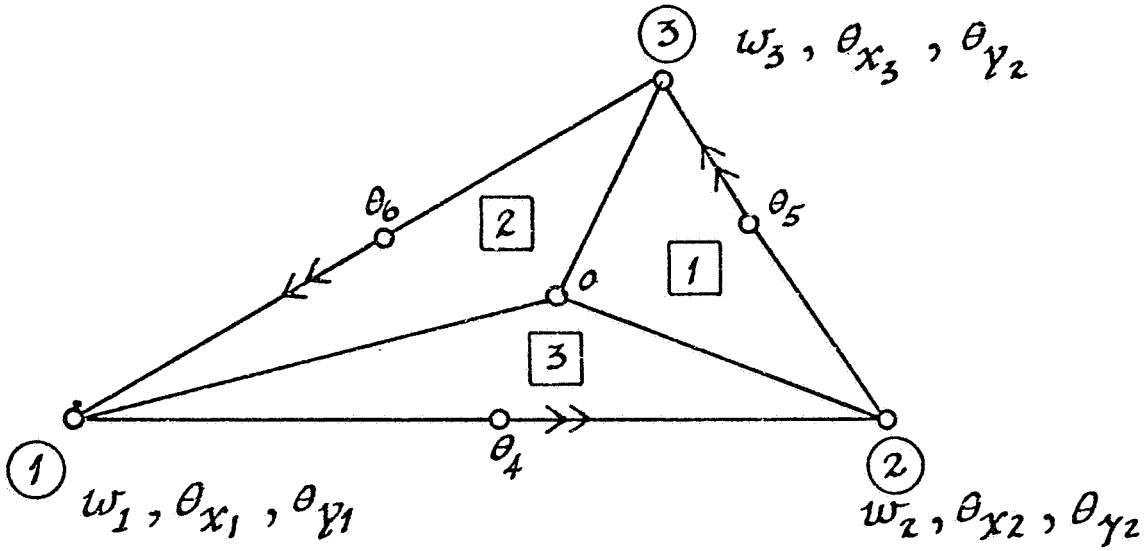

Figure 6.19. Triangular Subelement

couple with those in adjacent elements. Therefore, it is possible through minimization of the strain energy to express these freedoms in terms of the freedoms on the shell boundaries. This procedure is usually referred to as static condensation and does not introduce additional approximation. Freedoms can also be eliminated by the introduction of constraints. For example, the displacement at a midpoint node on an element boundary can be expressed as the average of the values of this displacement component at the end points of the boundary. This introduces constraints on the deformation and consequently makes the element less flexible.

In the basic triangular element, w, β_x, β_y are freedoms at four nodes and in addition there are three rotation comopoients at midlength for a total of 15 degrees of freedom. In the linear analysis the internal freedoms can be eliminated by use of static condensation which means that the basic triangle has 12 degrees of freedom. In nonlinear analysis the usefulness of condensation is doubtful. It is possible in addition to eliminate the rotations β_4, β_5, and β_6 by use of the restriction that the rotation

component in the direction of the element boundary varies linearly from one corner to another. This would result in a triangular element with nine degrees of freedom.

The Clough-Felippa quadrilateral element is composed of two or four basic triangular elements as shown in Figure 6.20. Unless static condensation is used, there are a total of nine corner nodes with three degrees of freedom at each and eight midside nodes with one degree of freedom at each for a total of 35 degrees of freedom in the bending element. By use of static condensation, all the unknowns at internal nodes can be eliminated on the element level and thus only sixteen degrees of freedom would be left. If in addition the midpoint rotation is eliminated by use of the constraint that the rotation varies linearly along the element boundary, a conforming quadrilateral element is obtained with 12 degrees of freedom.

The inplane displacement field for a triangular element can be represented by a full quadratic for each of the two components u and v (each of these containing six terms). The twelve coefficients in the two second order polynomials for u and v are expressed in terms of twelve nodal degrees of freedom. These are u and v at each of the corners of the triangle and the displacements parallel and normal to the element boundary at midside nodes (see Figure 6.21). In the quadrilateral element, there are 26 external and 10 internal degrees of freedom. If internal freedoms are eliminated through static condensation and freedoms at midside nodes by artificial constraints, the membrane element would have only eight degrees of freedom. For a complete quadrilateral, accounting for membrane as well as bending action, there are 61 degrees of freedom (35 + 26). By use of condensation the number of unknowns can be reduced to 32 (16 + 16). By constraining the element so that midside nodal values are eliminated as unknowns, a quadrilateral membrane bending element can be derived with as few as 20 degrees of freedom (12 $\pm$ 8).

The triangular and quadrilateral versions of the Clough-Felippa elements are referred to here as CFT and CFQ, respectively. The availability of a triangular element in a shell program is important for the case of modeling.

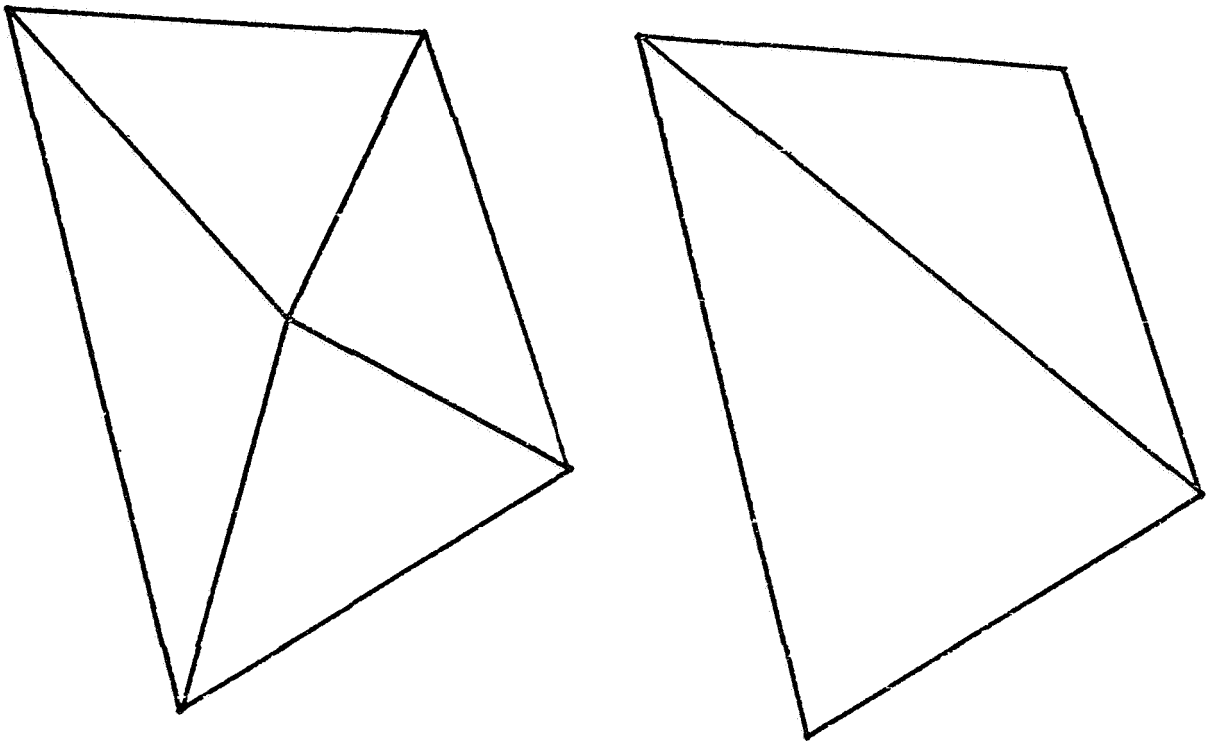

Figure 6.20. Decomposition of Quadrilateral Element

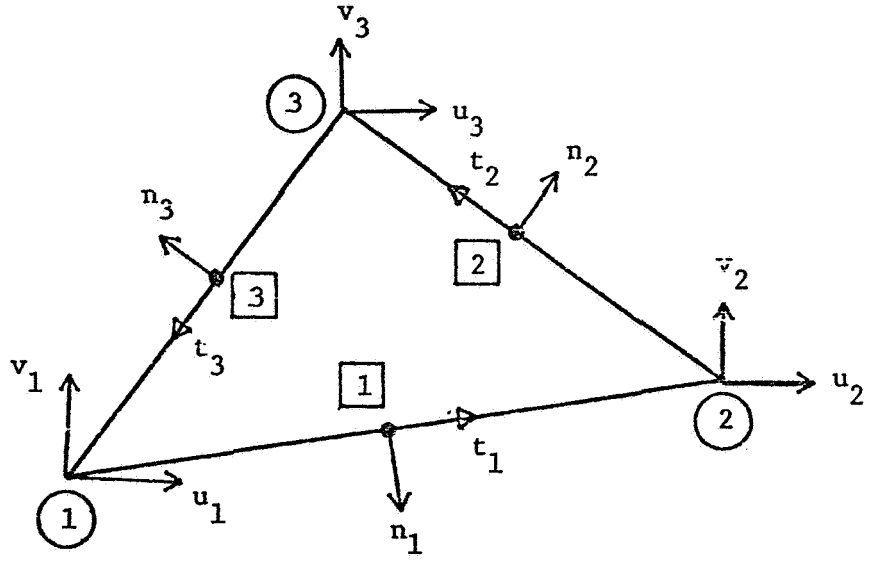

Figure 6.21. Freedoms in Membrane Element

In STAGS triangular elements are used automatically at the apex of closed shells of revolution and at the end points of "discontinued gridlines." The CFQ element is conforming in plate analysis. However, if adjacent triangles are not in the same plane, displacement incompatibility will occur (compare discussion of the STAGF element above) unless the element is constrained. The triangular element is expected to have only limited use in STAGS. Consequently, the efficiency is less important and no other formulation for triangular element is presently contemplated.

The quadrilateral element CFQ may be useful primarily for linear analysis in which case full advantage can be taken of static condensation. The unconstrained element requires considerable computer time and becomes nonconforming for curved shell analysis. If constraints are introduced, the convergence with gridsize may be too slow for efficient operation.

6.7 Discretization in STAGS

An early version of the program, STAGSA, is still being used although it is restricted in scope. This version is based on the half-station scheme discussed in Section 6.6. Other finite difference schemes have been used in intermediate "unofficial" versions of the program.

The STAGC version will initially include the following elements discussed above:

The flat quadrilateral STAGF element
The AHMAD1 and AHMAD2 elements
The Clough-Felippa triangle (CFT)
The Clough-Felippa quadrilateral (CFQ)

The Clough-Felippa elements are used without condensation. A contract with AFFDL, Wright-Patterson, provides funding for evaluation of the relative efficiency of the different formulations. After conclusion of this task, it should be possible to provide the STAGS user with advice regarding the choice between the different formulations. One or more of the formulations may be eliminated as less efficient.

If it is required that rotations be included as nodal freedoms, the bending energy can be expressed with a third order accuracy without use of nodal displacements outside of the closed domain of the element. A lower order accuracy with very rapid formulation is excluded in that case. Consequently, an element formulation is chosen rather than one based on finite differences.

The computer time for formulation of the stiffness matrix with any of the elements discussed above is several times in excess of the formulation time with STAGSA. This may be compensated by the possibility to use a coarser grid with the higher order elements. However, with the simplest finite difference formulation, a second order accuracy can still be maintained in many cases. In particular, this formulation may be useful whenever a relatively fine grid already is required for adequate description of the structure. Therefore, a finite difference formulation is also included in the evaluation under the AFFDL contract. Some form of the finite difference scheme will be reintroduced if the work under the contract indicates that such action would be appropriate.

REFERENCES

6.1 Dahlquist, G., and Å. Björk, Numerical Methods, Prentice Hall, Englewood Cliffs, N.J., 1974

6.2 Noor, A. K., "Improved Multilocal Finite-Difference Variant for the Bending Analysis of Arbitrary Cylindrical Shells," University of South Wales Report No. R-63, Australia, March 1971.

6.3 Brush, D. O., and B. O. Almroth, Buckling of Bars, Plates and Shells, McGraw-Hill, New York, 1975.

6.4 Strang, G., and G. J. Fix, An Analysis of the Finite Element Method, Prentice Hall, Englewood Cliffs, N.J., 1973.

6.5 Sokolinkoff, I. S., Mathematical Theory of Elasticity, McGraw-Hill, N.Y., 1956.

6.6 Forsythe, G. E., and W. R. Wasow, Finite Difference Methods for Partial Differential Equations, Wiley, N.Y., 1960

6.7 Bazeley, G. P., Y. K. Cheung, B. M. Irons, and O. C. Zienkiewics, "Triangular Elements in Plate Bending - Conforming and Nonconforming Solutions," Proc. of Conf. on Matrix Methods in Struct. Mech., AFFDL TR 66-80, October 1965.

6.8 Strang, G.,"Variational Crimes in the Finite Element Method," in Math. Foundations of the Finite Element Method. Editor A. K. Aziz, Academic Press, p. 689, N.Y., 1972.

6.9 Irons, B. M., and A. Razzaque, "Experience with the Patch Test for Convergence of Finite Elements," in Math. Foundations of the Finite Element Method, Editor A. F. Aziz, Academic Press, p. 557, N.Y., 1972.

6.10 Willam, K. J., "Finite Element Analysis of Cellular Structures," Ph.D. Thesis, Department of Civil Engineering, U.C., Berkeley, Calif., 1969.

6.11 Ahmad, S., B. M. Irons, and O. C. Zienkiewicz, "Analysis of Thick and Thin Shell Structures by Curved Elements," Int. J. Num. Meth. Eng., Vol. 2, pp. 419-451, 1970.

6.12 Pawsey, S. F., "The Analysis of Moderately Thick to Thin Shells by the Finite Element Method," Struct. Eng. Lab. Rept. 70-12, Dept. of Civil Engineering, U.C., Berkeley, Calif. 1970.

6.13 Clough, R. W., and C. A. Felippa, "A Refined Quadrilateral Element for Analysis of Plate Bending," AFFDL-TR-68-150, Wright-Patterson Air Force Base, Dayton, Ohio, 1968.

Section 7
SOLUTION PROCEDURES

7.1 Introduction

In this section capital Latin letters are consistently used to denote a matrix. A general operator is denoted by a capital letter followed by a parenthesis. Vectors are referred to by lower case Latin letters and scalars (with a few obvious exceptions) by Greek letters.

Depending on the chosen mode of analysis, the discretization of the physical model leads to a linear equation system, an eigenvalue problem, a nonlinear algebraic equation system, or in the case of transient analysis, an initial value problem. For any of these problems, a number of different procedures are available and the ideal choice between those is often case dependent. Some control parameters set by the program may have profound effect on the computer time required for solution. Therefore, it is important that the user has some understanding of solution procedures involved.

After the displacement functions and their derivatives in the governing equations have been replaced by finite difference or finite element approximations (see Section 6), the strain energy density at integration point i can be written in the form

$$\Delta u^i = \frac{1}{2}(z^i)^T D^i z^i \tag{7.1}$$

where D^i is a 6 x 6 positive definite matrix and z^i is a column vector of strains and curvature changes at station i. The matrix D^i is dependent on the material properties and the geometric parameters of the shell. The vector z^i is a quadratic function of the displacement unknowns and thus u^i is a fourth-order polynomial. The vector of stress resultants s^i at station i is given by

$$s^i = D^i z^i \tag{7.2}$$

The total strain energy Γ is obtained by integration of the strain energy density over the structure. The procedures of integrating by a Gaussian scheme (including the rectangular integration) over each element and adding over all elements can be written in terms of one scalar product

$$\Gamma = \Delta u \cdot a \tag{7.3}$$

where a is a vector representing the weighting factors for all integration points and Δu is a vector whose elements represent the strain energy density at these points. In shell analysis the sum of all the components of the vector a equals the total area of the shell reference surface.

The total potential energy Π is obtained after the work Ω done by the external forces is subtracted from the strain energy

$$\Pi = \Gamma - \Omega \tag{7.4}$$

The work done by uniformly distributed loads can be integrated in the same way as the strain energy. Let v^i be a vector whose elements are the three displacement components in a Cartesian system at integration point i and let the vector g^i represent the values of the tractions (load per unit area) in these directions. If the vector Δw represents the density of the work done by the external forces at integration point i, its ith component is given by

$$\Delta wi = v^i \cdot g^i \tag{7.5}$$

It follows that

$$\Pi = (\Delta u - \Delta w) \cdot a \tag{7.6}$$

The components of Δu are at least second order in the displacement freedoms x_i and the components of w are of first order. Consequently, the first variation of the work done by the external forces is a vector of constants, that

is, it yields the load vector or the right-hand side in the equation system. Derived in this way the load vector is sometimes referred to as a consistent load vector. In a nonconservative system the tractions g may be displacement dependent. In that case the work done by the external forces will contribute also to the second variation of the total potential energy.

Frequently a distributed load or a line load is represented by point forces (or moments) at the nodes. In that case the work done by the external forces is instead obtained as the scalar product

$$\Omega = x \cdot f \tag{7.7}$$

where the vector x represents the freedoms of the system (displacements and rotations) and the vector f represents corresponding nodal forces and moments.

The equations of motion also include inertial forces and possibly damping. In the discretized system the contributions of the inertia forces are represented by a mass-matrix times the displacement unknowns. The elements of the mass matrix can be determined so that the kinetic energy Λ obtained from the mass matrix equals the integral over the structure of the kinetic energy density. In this integration, displacement velocities are obtained from the rate of change of the degrees of freedom of the system and the functions used for approximation of local displacements (inside the element). Consequently, the elements of the mass matrix M can be obtained from

$$\Lambda = \frac{1}{2} (\dot{x})^T M \dot{x} = \frac{1}{2} q \cdot m \tag{7.8}$$

where m is a vector with one component for each integration point representing the product of the mass density and the weighting factor in the Gaussian integration. The components of the vector q are obtained as the sum of the squares of the displacement velocities at each of the Gaussian points. Since each of these velocities generally depend on a number of the freedoms the mass matrix will have off diagonal entries. Derived in this way it is referred to as a consistent mass matrix.

Frequently, a so-called lumped or diagonal mass matrix is used. The simplest way to derive such a matrix is to concentrate the mass at the node points. In that case the entries in the mass matrix corresponding to the three displacements at each node are readily computed. All off diagonal elements and sometimes those that correspond to rotational freedoms are set equal to zero. For certain operations to be discussed below it is necessary to attach some mass to the rotational freedoms. One possibility is to include the "rotary inertia", that is, the contribution to the rotational inertia that is due to the shell thickness. The rotary inertia is an extremely small contribution and therefore other ways to lump the matrix have been proposed (see Ref. 7.1) For any fixed deformation mode an equivalent diagonal matrix can be defined. However, this matrix will not give accurate results for other deformation modes. One possibility is to use the values of the consistent mass matrix on the diagonal for elements corresponding to the rotational freedoms. Consequently, the diagonalization of the mass matrix introduces an additional approximation. The ideal choice of a mass matrix depends on the basic type of analysis and on the solution procedures involved.

The following discussion will first be concerned with the case of static structural behavior. A necessary condition for static equilibrium is that the total potential energy be stationary. This condition requires the vanishing of the first variation of Π and leads to the equation

$$L(x) = f \tag{7.9}$$

where the operator $L(\ )$ is defined by

$$L(x) = \text{Grad } \Pi \tag{7.10}$$

Consequently, $L(\ )$ is a "stiffness" operator which relates displacement components and external forces and is nonlinear in the general case.

7.2 Linear Equation Systems

When only linear terms are included in the definition of the strains and changes in curvature, L( ) is a linear operator which may be readily represented in matrix form. The elements of this matrix, A, are derived from the quadratic terms in the strain energy, while the work done by the external forces (and thermal effects) contribute a right-hand side to the equation system. The matrix is positive definite and Eq. (7.9) may be solved by one of many direct or iterative methods.

In one-dimensional cases, beams and shells of revolution, the coefficient matrix is narrowly banded, and the computer time involved in solution of a linear system is almost negligible. For two- or three-dimensional cases the maximum bandwidth is much larger, but the matrix is sparse, i.e., most of the elements inside the band are zero. The efficiency of the solution procedure depends largely on effective utilization of the knowledge of the location of zero elements in the matrix.

The skyline method is based on the decomposition of the matrix in two factors, one of which, the upper triangular matrix U has all its nonzero entries above the diagonal and the other, the lower triangular matrix L has all its nonzero entries below the diagonal. Given the linear equation system

$$A\,x = y \tag{7.11}$$

the triangular matrices U and L are determined so that

$$A = L\,U \tag{7.12}$$

Then the original system (Eq. 7.11) can be decomposed in two equation systems to be solved sequentially

$$\begin{aligned} L\,b &= y \\ U\,x &= b \end{aligned} \tag{7.13}$$

If the original matrix A is symmetric and positive definite, then there exists a unique decomposition in triangular matrices with only positive real numbers on the diagonal such that (see Ref. 7.2)

$$U = L^T \tag{7.14}$$

The matrix decomposition is referred to as factoring of the matrix. The determinant of the matrix A is equal to the product of all the elements on the diagonal of the factored matrix U.

Equation systems with a relatively small bandwidth are particularly well suited for solution through decomposition or factoring. The reason for this is that the triangular matrices have the same "skyline" as the original matrix A, that is, in each row the upper matrix U will have no nonzero entries beyond the last nonzero entry in A. Consequently, no computer storage space is required for the "tail" of each row and no operations need to be carried out for corresponding matrix elements during factoring and forward and backward sweep (solution of Eqs. 7.13) Procedures are available for automatic renumbering of the unknowns so that the skyline may be kept as low as possible.

The strain energy in the linear case can be written as a quadratic form

$$\Pi = \sum_{i,j=1}^{n} \sum^{n} C_{ij} x_i x_j \tag{7.15}$$

The appearance of negative values on the diagonal in the factored matrix would indicate that the quadratic form is not positive definite. Since the strain energy must be positive definite the occurrence of such negative roots in the linear analysis can only be due to an error in the model or to some numerical problem. Linear dependence among the equations would result in zero values of diagonal elements in U. Due to round-off errors, however, these values will not be exactly zero and they may come out as small negative numbers. Therefore, if an element on the diagonal, positive or negative is of the same order of size as normal round-off errors, it may be assumed that

the system is singular. This can occur, for example, if linearly dependent boundary conditions have been specified or whenever boundary conditions and other constraints allow rigid body displacements. When a zero (for all practical purposes) occurs on the diagonal during factoring with STAGS, corresponding freedom is eliminated, and a message to that effect is included in the output.

If relatively large negative numbers appear on the diagonal, it is likely that the system is ill-conditioned (barring input errors). That is, the roundoff errors are large enough to make the results meaningless. In that case, computations with STAGS are discontinued, and an error message is printed. Ill-conditioning does not necessarily lead to negative roots. Consequently, it is possible that a conditioning problem remains uncovered until "equilibrium forces" are printed. Lack of equilibrium in the final solution probably indicates ill-conditioning. If the ill-conditioning is severe, a change in modeling seems advisable. In less severe cases acceptable solutions may be obtained by use of a linear refinement of the solution. The STAGS user can obtain such a refinement of the solution by requesting a nonlinear solution with the nonlinear terms suppressed. If the first linear solution is not too far off from the true solution, convergence will rapidly be obtained and the final solution will be accurate.

If constraints are introduced by way of Lagrangian multipliers (see Section 8) the positive definiteness of the quadratic form is lost. The factored matrix will have one negative root for each of the constraints in a linearly dependent set. If the number of negative roots is less than the number of constraints imposed by use of Lagrangian multipliers, the set of constraints is probably not linearly independent.

The alternatives to the skyline method are iterative methods and other direct sparse matrix methods such as matrix partitioning, wave front type methods and the conjugate gradient method. If branches of the structure are connected in an unfavorable way such methods may prove to be superior to the skyline method. An efficient computer program for structural analysis probably should include optional solution methods.

The present version of STAGS includes the skyline method only. A study of other possibilities is presently underway.

7.3 Nonlinear Equation Systems

When geometric nonlinearities are included, L( ) becomes a polynomial operator of third degree and iterative methods must be employed for solution of the equations. Special problems with material nonlinearities will be discussed separately. For a general collapse analysis, it is necessary to solve the operator equations, Eq. (7.4) for a sequence of values of the applied loads. In fact, the only practical method often is to solve the equations at a number of load steps chosen so that the initial solution is nearly linear and subsequent solutions change only moderately from one step to the next. Such a procedure (sometimes referred to as the continuation method) is mandatory for two reasons: first, the feasibility of the iterative methods of solution depends on reasonably good initial approximaations and second, a reliable detection of collapse requires such a stepwise procedure because of possible non-uniqueness of solutions to nonlinear equation systems. For solution of the nonlinear algebraic equation systems that are typical for structural analysis a large number of algorithms are available, ususally designed to determine a sequence of equilibrium configurations under increasing load. It may be helpful to classify the methods as is done in Ref. 7.3 in the four groups:

Newton-like methods
Method of successive substitutions
Initial-value methods
Minimum search procedures

The regular Newton method is illustrated here in the case with only one unknown x. The solution of the problem $F(x) = 0$ is defined by the recursion formula

$$x_{n+1} = x_n - F(x_n) / F'(x_n) \tag{7.16}$$

A geometric interpretation of the regular Newton method is shown in Figure 7.1a. A variation of the regular Newton method, usually referred to as the modified Newton method has been found useful in many cases. The method is defined by the equation

$$x_{n+1} = x_n - F(x_n) / F'(x_o) \tag{7.17}$$

A geometric interpretation of the modified Newton is given in Figure 9.1b. The basic difference between the two methods is that in the regular Newton method the derivative in the denominator is always based on the current solution while in the modified method the derivative at the initial estimate is used in all iterations. With the modified method it is possible to update the derivative after x_o has been shifted to a later estimate ($x_o = x_n$).

Both the regular Newton and the modified Newton are readily generalized to n-dimensional space. In the n-dimensional case the computation of $1/F'(x)$ corresponds to the factoring of a matrix of n-th order. For very large systems the modified Newton method becomes more efficient since refactoring is expensive. In the modified Newton method the "obsolete" factored matrix is often maintained (unchanged) for a series of load steps. One problem with the modified Newton method is illustrated for the case with one unknown in Figure 7.2b. If the estimates at a new load step falls at points where the curve has a lesser slope than it has at the true solution, the iterates oscillate and a very close estimate (small load step) is required for convergence. In such cases the regular Newton (Figure 7.2a) may be preferable even for rather large systems.

In the method of successive substitutions the nonlinear terms are considered as pseudo-loads added to the right-hand side of the equation system. They are determined by use of the values of the unknowns in a previous iteration. It may be noticed that mathematically this method is equivalent to a modified Newton method in which updating and refactoring of the coefficient matrix are not permitted at any load step.

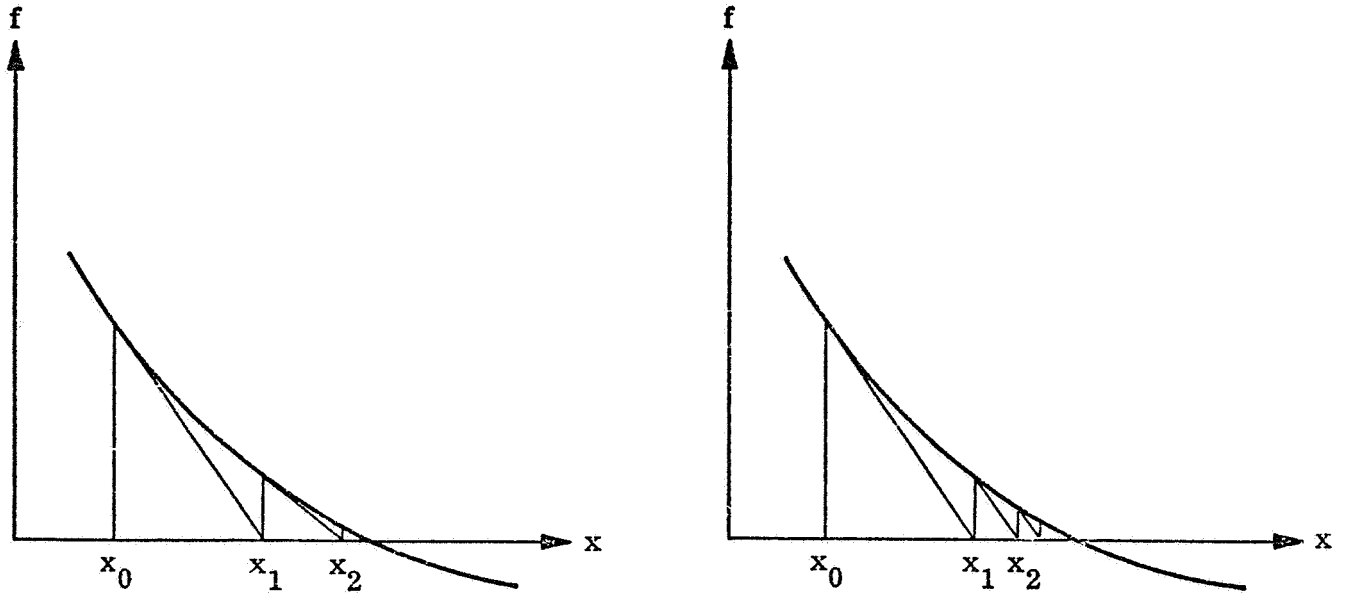

(a) REGULAR NEWTON (b) MODIFIED NEWTON

Fig. 7.1 Two Newton Methods for One Degree of Freedom Systems

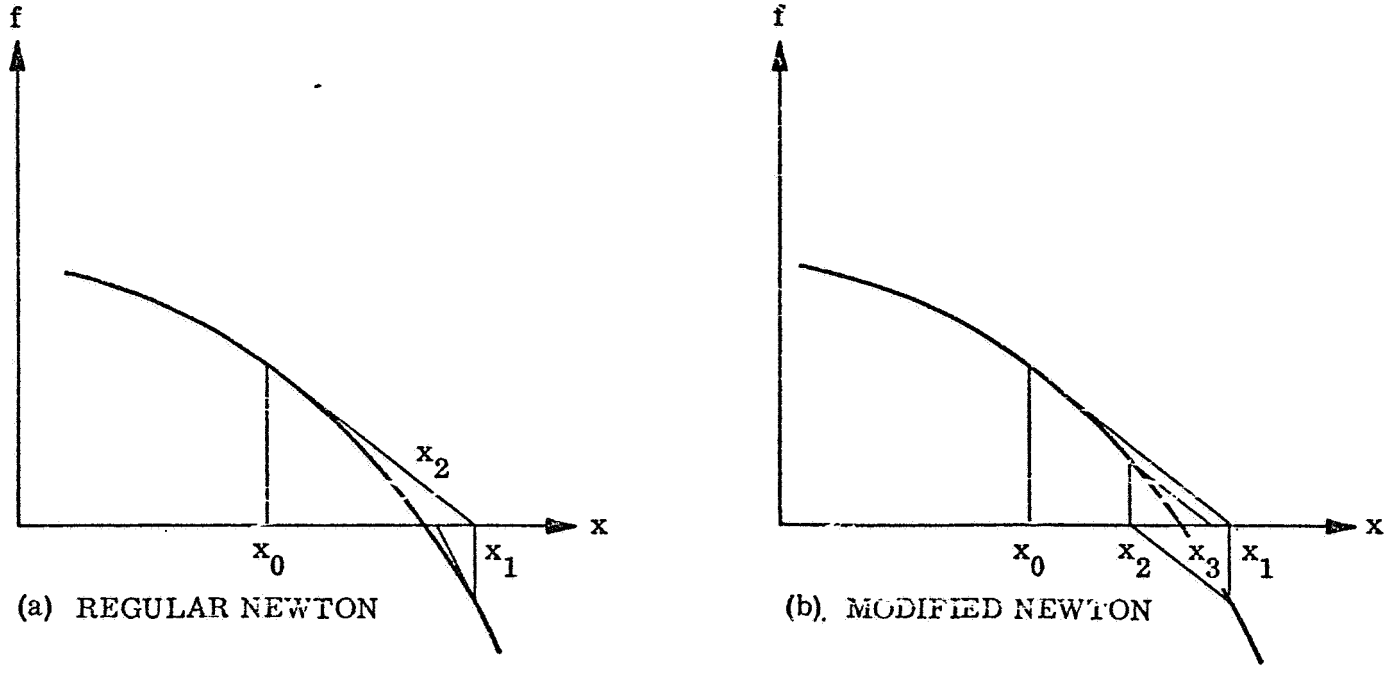

(a) REGULAR NEWTON (b) MODIFIED NEWTON

Fig. 7.2 Oscillating Convergence With the Newton Methods

The initial-value type methods include the incremental method (sometimes referred to as the tangent stiffness method). In this method the tangential stiffness is computed at the beginning of each load step. Within each load step the displacements grow linearly as dictated by this stiffness. The method allows drift from the correct solution. Consequently, the load step must be very small and since refactoring is required on each step the method is not economical.

In a "self-correcting" version of the incremental method, the unbalance in the nonlinear equations is evaluated and added to the load vector corresponding to the following load step. The self-correcting version of the incremental method is identical to a regular Newton method in which only one iteration is made at each load step. Hence, if a relatively coarse convergence criterion is used, the Newton method will work as a self-correcting incremental method, except that an extra iteration may be inserted if the solution tends to drift too much. Use of the self correction method instead of the regular Newton or modified method in a computer program for nonlinear analysis deprives the user of automatic corrective action when the solution is drifting too far. A feasible variation is to compute the norm of the first variation on each step and to insert a zero load step whenever this norm (unbalance) is too large. However, this would essentially be identical to the use of the regular Newton method.

Another initial-value type method is usually referred to as dynamic relaxation. When this method is used, the equations of motion are solved rather than the static equilibrium equations. Damping is introduced so that the static equilibrium configuration is asymptotically approached. The method is certainly not competitive with the modified Newton method for systems with only moderate nonlinearity. For imperfection sensitive structures the dynamic relaxation method may be the most practical way to find equilibrium configurations in the postbuckling range.

Minimum search methods are applied directly to an energy expression rather than to equations of equilibrium or motion. They have seen little use in structural analysis and little can be said about their relative merits.

It appears that based on the present state of the art, it is advisable to include in a computer program for nonlinear analysis the option of using:

The regular Newton method, or
The modified Newton method.

Dynamic relaxation may at times be a competitive method. However, it is not fully developed since good procedures for automatic determination of suitable values for the elements of the fictitious mass and damping matrices are not presently available.

The extension of the Newton methods to multiple degree of freedom systems is facilitated by introduction of the concept of the derivative $L'(\ )$ of $L(\ )$ (Ref. 7.4). After substitution of the current solution vector the derivative $L'(\ )$, sometimes called the Frechet derivative of $L(\ )$, becomes an n by n matrix whose elements are

$$L'_{i,j} = \frac{\partial^2 \Pi}{\partial x_i \ \partial x_j} \tag{7.18}$$

Most of the elementary properties of ordinary derivatives also hold for the Frechet derivatives $L'(\ )$ of an operator $L(\ )$.

The elements of L' are functions of a particular displacement vector x. The Frechet derivative will usually be denoted L'_x to indicate this dependence. With the use of the derivative $L'(\ )$ of the operator $L(\ )$ Newton's method may be readily generalized to obtain a solution of Eq. (7.9). The iteration is defined by (compare Eqs. 7.4 and 7.11).

$$(x_{k+1} - x_k) = (L'_{x_k})^{-1} f - L_{x_k} \tag{7.19}$$

If the initial estimate x_0 is sufficiently close to a solution x and if L'_x is not a singular matrix, the iteration converges to x. Under these assumptions, it also can be shown that the converged solution is unique in some neighborhood of x 7.4).

Similarly, with the aid of the derivative L'_x, the modified Newton method may be applied to the operator Equation (7.9). The general form of the iteration then becomes

$$L'_{x_m} (x_{k+1} - x_k) = (L'_{x_k})^{-1} f - L_{x_k} \tag{7.20}$$

The modified Newton method provides accurate solutions whenever it converges independently on the size of the load step (numerical errors do not accumulate) and at the same time avoids the necessity of frequent recomputation and factorization of the derivative matrix L'. The effective use of the modified Newton method requires intelligent choices of the size of load steps and the criterion that determines when the derivative L' should be recomputed and factored. The STAGS program contains some built-in decison making capability regarding these questions. However, it is still necessary for the user of the program to consider the best overall "strategy" relating to these choices. Methods for automatic choice of step size and strategy have been suggested in the literature (Ref. 7.5, for example) but have yet to be evaluated in practical analysis with respect to their reliability.

The solution procedures commonly used for problems including material nonlinearity are discussed in Section 5. The pseudo force method corresponds to the method of successive substitutions discussed above. In the presence of geometric nonlinearities use of this method may at some load level lead to divergence independently of the size of the load step. It appears that if only material nonlinearities are included the method will not diverge but convergence may be very slow. It is feasible when material as well as geometric nonlinearities are present to treat the material nonlinearities as pseudo forces and still use one of the Newton methods to solve the nonlinear algebraic equations. However, if the geometric nonlinearities make it necessary to update and refactor the matrix, it seems practical to include nonlinear material effects in the update.

The STAGS user is allowed to use either of the two Newton methods for solution of the algebraic equations. The material nonlinearities can either be treated as pseudo-forces or, at the user's choice, the effects of

plasticity can be included in any update of the tangential stiffness matrix ($L'_{i,j}$ in Eq. 7.18). The reason for inclusion of the pseudo force method for plasticity is that numerical problems may be encountered with simultaneous iteration on geometric and material nonlinearities. It is recommended in Ref. 7.5 that the geometric nonlinearities are treated in a separate inner loop. However, for two-dimensional problems this does not appear practical as it would result in a large number of refactorings at each load step.

A dynamic relaxation capability is within the scope of STAGS, but methods for automatic determination of mass and damping matrices are not included. The method is probably unsuitable when material nonlinearities are included because of the path-dependence of plastic strain. For certain cases of post-buckling behavior it may be the only viable way to obtain a solution.

7.4 Eigenvalue Analysis

In bifurcation buckling and vibration analysis the assumption is made that the incremental displacements, corresponding to the buckling or vibration modes, are of infinitesimal amplitude. Thus, higher order terms in the incremental displacements may be discarded and the equilibrium equations or the equations of motion are homogeneous. That is, all the terms in the equations are of the same order in the unknowns. Obviously, such a system has the trivial solution

$$x_i = 0; \quad i = 1,n \tag{7.21}$$

If the coefficient determinant equals zero the system also has nontrivial solutions. Whenever a vector x of unknowns satisfies the equation system, then clearly all vectors αx satisfy the system. The solution of a homogeneous equation system determines the size of the unknowns relative to one another but not their absolute size. Consequently, a buckling or vibration analysis yields a deformation mode only. Due to the original assumption the analysis is valid only for small displacements.

The coefficients of the homogeneous system may be functions of some parameter that can be chosen so that the determinant becomes zero. In

a buckling analysis this eigenvalue parameter is represented by the value of the applied load, a load factor, and in a free vibration analysis by a natural frequency.

The mathematical characterization of bifurcation buckling is discussed in Section 5. The homogeneous equation system is obtained through substitution of a displacement field $x = x_o + x_1$ where x_o represents an equilibrium configuration on the primary path and the infinitesimal x_1 the buckling mode. The formulation is also provided by the generalized Newton method. Let x_o be a solution of Eq. (7.9) under a given vector of external forces. If a neighborhood, no matter how small, of x_o contains another vector y which satisfies the equation

$$L(y) = f \tag{7.22}$$

then bifurcation is said to take place under the load f. It follows that a necessary condition for bifurcation is that L'_{x_o} be a singular matrix, i.e., that

$$\det (L'_{x_o}) = 0 \tag{7.23}$$

Classical bifurcation buckling theory may be obtained easily from Eq. (7.23) It is assumed that x_o may be written

$$x_o = \lambda x_L \tag{7.24}$$

where x_L is the linear solution corresponding to a load vector f_L. Thus, Eq. (7.23) becomes

$$\det (L'_{\lambda x_L}) = 0 \qquad] \tag{7.25}$$

Equation (7.25) is an algebraic eigenvalue problem of the form

$$\det (A - \lambda B - \lambda^2 C) = 0 \tag{7.26}$$

In classical bifurcation buckling analysis, the C matrix, which arises from the prebuckling rotations, is usually omitted and the eigenvalue problem

$$A_x = \lambda B_x \tag{7.27}$$

is obtained.

When bifurcation takes place on a nonlinear primary path the substitution $x_o = \lambda x_L$ is not valid. The most straightforward way to solve the problem in that case would be to compute the determinant (Eq. 7.25) for increasing values of the load factor until a zero crossing is found. It is also possible to apply the eigenvalue approach at some point along the primary path. In that case the primary path is linearized so that it corresponds to the tangential stiffness matrix evaluated at that point. Since the tangential stiffness varies with the applied load, a rigorous estimate of the bifurcation load is only obtained if the eigenvalue is exactly zero. Consequently, a procedure based on eignevalue extraction must include the computation of a series of eigenvalues so arranged that the computed values converge to zero. The use of bifurcation buckling analysis with a nonlinear stress state is further discussed in Section 5. The formation of the A and B matrices of Eq. (7.26) will be considered briefly. The elements of the Frechet derivative matrix $L'_{\lambda x}$ (which define the matrices A and B) are determined according to Eq. (7.18).[L] The rules for computing derivatives of polynomials are easily programmed, and the formation of the A and B matrices therefore is well suited to automatic treatment on the computer. Thus, for example, if x_i and x_j are the ith and jth displacement components, the following is obtained:

$$\frac{\partial^2 \Pi}{\partial x_i \, \partial x_j} = \sum_{k=1}^{m} a^k \frac{\partial^2 \Delta\Pi^k}{\partial x_i \, \partial x_j} \tag{7.28}$$

The kth term of the sum is (compare Eqs. (7.1) and (7.2))

$$\frac{\partial^2 \Delta\Pi^k}{\partial x_i \partial x_j} = \frac{\partial^2 (x^k)^T}{\partial x_i \partial x_j} \lambda s_L^k + \frac{\partial (z^k)^T}{\partial x_I} D^k \frac{\partial z^k}{\partial x_j} \tag{7.29}$$

In the first term on the right-hand side of Eq. (7.29), note that s_L^k is the linear stress resultant vector at integration point k and that only the quadratic terms in the strain vector need be considered in forming the partial derivatives

$$\frac{\partial^2 (z^k)^T}{\partial x_i \partial x_j}$$

Contributions from this term go into the B matrix. Assuming the prebuckling rotations may be neglected for the classical theory, the last term of Eq. (7.29) generates contributions to the A matrix only. The A matrix then is identical to the linear stiffness matrix.

Analysis of natural or free vibrations of a structure is based on the equations of motion. It is assumed that any damping can be omitted and that the force vector is independent of time. A solution is obtained through substitution of

$$x = x_o + \delta x_1 \sin(\omega t) \tag{7.30}$$

into the equation of motion

$$M\ddot{x} + L(x) = f \tag{7.31}$$

where M is the mass matrix, f the force vector and L( ) the generally nonlinear stiffness operator. The displacement field x_o represents a static equilibrium configuration and the vibration amplitude δ is assumed to be infinitesimal. The vibration mode is represented by x_1 generally normalized so that its largest components equal 1.0.

. After substitution of (7.31) in (7.30) the conditions for static equilibrium are subtracted out (eliminating the force vector), terms of

higher than first order in δ can be discarded. An eigenvalue problem is then obtained in the form

$$\omega^2 M\ddot{x} + L'_x x = 0 \tag{7.32}$$

The frequency ω is the eigenvalue parameter. The coefficients in L' are dependent on the vector x_o. Therefore, the frequency depends on the load applied to the structure. However, it makes no difference if the basic stress state has been computed from a linear or a nonlinear analysis and inclusion of the effects of prebuckling rotations does not lead to any complications. Use of the consistent mass matrix gives a more accurate representation. However, use of a lumped matrix results in a weaker system and sometimes if the element stiffness converges from above with grid-size it may be found that convergence to engineering accuracy is better with the lumped matrix. For any element configuration with convergence from below (nonconforming) it is probably best to use the consistent mass matrix.

Bifurcation buckling as well as vibration analysis then leads to a generalized eigenvalue problem of the form

$$Ax = \lambda Bx \tag{7.33}$$

where A represents a stiffness matrix, possibly a tangential stiffness matrix containing nonlinear terms from the basic stress state. The A matrix is symmetric and positive definite (or at least non-negative definite). The B matrix is always symmetric and, in the case of vibration problems, also non-negative definite. However, for bifurcation buckling the B-matrix, the geometric stiffness matrix, may have negative eigenvalues. The properties of A and B ensure that Eq. (7.33) has only real eigenvalues.

It may be noticed here that the substitution indicated by Eq. (7.30) equivalently could have been written

$$x = x_o + \delta x_1 e^{\omega t} \tag{7.34}$$

In that case all the eigenvalues are purely imaginary.

The eigenvalues of the system are the roots of a nonlinear algebraic equation in λ. If A is an n x n matrix, this equation is of the nth order and there are n eigenvalues (provided there is no linear dependence among the equations). The matrix is then referred to as being of rank n. To each eigenvalue λ_i corresponds one eigenvector, x_i (with undetermined amplitude) satisfying the homogeneous equation system.

It is not necessary and generally not practical in analysis of large systems to compute the eigenvalues directly. Whenever an eigenvector x_i of the matrix A is known, the corresponding eigenvalue can be computed as

$$\lambda_i = \frac{(x_i)^T A x_i}{(x_i)^T x_i} \tag{7.35}$$

Whether x_i is an eigenvector or not, the expression on the right-hand side of Eq. (7.35) is referred to as the Rayleigh Quotient.

The Power method is a very simple, and, in case only a few eigenvalues are needed, very efficient method in which the eigenvectors are computed first. Applying this method to the eigenvalue problem

$$(A - \lambda I)\, x = 0 \tag{7.36}$$

where I is the identity matrix, a starting vector x_o is first selected. Subsequently, a sequence of vectors x_j is obtained through solution of the equation system

$$Ax_{i+1} = x_i \qquad i = 0,1,2.... \tag{7.37}$$

This procedure converges toward the eigenvector corresponding to the largest eigenvalue of the system. It is shown in Ref. 7.2 (p. 210), for example, that the error tends to zero at the same rate as $(\lambda_2/\lambda_1)^i$ where λ_1 and λ_2 are the two largest eigenvalues ($\lambda_1 > \lambda_2$) and i the number of iterations. Consequently, when the eigenvalues are well separated the convergence is rapid but when λ_1 and λ_2 are close, the convergence is slow.

Convergence can be expedited by use of a spectral shift. That is, in the original eigenvalue problem $A \rightarrow A - \sigma B$ is substituted. The problem then is formulated so that the eigenvalue parameter becomes the excess in the buckling load or the square of the vibration frequency above a fixed value σ.

In both buckling and vibration analysis the main interest is in the lower eigenvalues. These can be obtained by use of an inverse power iteration. The inverse power iteration with a spectral shift is described in the following.

After introduction of the shift the eigenvalue is of the form

$$(A - \sigma B)\, x = Bx \tag{7.38}$$

Substitution of

$$Q = (A - \sigma B)^{-1} B \tag{7.39}$$

yields

$$x = Qx \quad \text{or (equivalently)} \quad (Q - I)\, x = 0 \tag{7.40}$$

that is, a problem of the form discussed above (Eq. 7.36) is obtained.

The iteration converges to the eigenvectors corresponding to the smallest eigenvalues, i.e., the bifurcation points or frequencies that are closest to the spectral shift σ. The error in the smallest eigenvalue approaches zero at the same rate as $[(\lambda_1 - \sigma)/(\lambda_1 - \sigma)]^n$ where λ_1 and λ_2 are the two smallest eigenvalues of the original system and $\lambda_1 < \lambda_2$.

The iteration by itself has some drawbacks including

- Slow convergence when several eigenvalues are close to the smallest eigenvalue.

- Difficulty in controlling the iteration and shift points in a systematic way so as to find a number of eigenvalues and eigenvectors.

- Rather high computation cost when a number of shift points are used.

- High charges for auxiliary storage; the factored stiffness matrix must be read into core once for each iteration.

The convergence of the power methods can be accelerated to improve the efficiency. Frequently used schemes are the Aitken δ^2 process and Chebyshev polynomial acceleration.

The disadvantages with the need for many shift points for determination of a series of eigenvalues can be overcome if the iteration process is designed to yield a set of vectors y_1, y_2, ... y_k which span the subspace generated by the first k eigenvectors. Let $y = (y_1 \ldots y_k)$ be such a set of vectors. The eigenvectors of the original system of rank n can then be obtained from the solution of a system of rank k. A number of power iterations may be carried out between each time the reduced system is solved.

In STAGSC the simultaneous iteration with Chebyshev polynomials is used to reduce the problem. The reduced problem is solved by Householder transformations followed by application of the LR algorithm (Ref. 7.2). The details of the Chebyshev acceleration and the simultaneous iteration procedure are given in Appendix D.

7.5 Transient Analysis

Static structural analysis leads to a pure boundary value problem, that is, boundary conditions specify local constraints on the solution functions and possibly on their spatial derivatives. Natural boundary conditions (on forces and moments) supply constraints that are automatically satisfied if variational methods are used. Constraints on displacements and rotations must be enforced by use of side conditions in the variational problem

With the addition of time as an independent parameter, initial conditions must also be specified. The analysis of transient behavior of a structure then leads to a mixed initial value and boundary value problem.

From a purely mathematical point of view time as an independent parameter is in no way different from the space variable. The special character of the initial value problem is caused by the fact that only at time zero are all the degrees of freedom (displacements and velocities) specified. In a mixed problem a solution is sought to a set of differential equations that satisfy:

- The boundary conditions, i.e., local constraints at all values of time.

- The initial conditions, i.e., the values of all displacements and their first order time derivatives (velocities) at the initial time.

From a computational point of view an important difference between boundary value and initial value (or mixed) problems, is that in the latter it is not possible to avoid some propagation of error. In a quasistatic analysis (a boundary value problem) the nonlinear static equations are defined at each load step. By use of one of the Newton-type procedures, for example, an accurate solution can be obtained at any loadstep independently of the quality of the previous solutions. In the ingegration of the equations corresponding to the initial value problem, this is not the case. An error early in the analysis results in inaccurate initial conditions for the subsequent deformation history. The error cannot be recovered. As will be seen in the sequel, the initial value problem is also encumbered with certain difficulties related to numerical stability of the solution procedure.

A transient analysis of a deformable body entails the solution of the equation

$$M\ddot{x} + Dx + L(\dot{x}) = f \tag{7.41}$$

where x is the vector of discrete values of the displacement components, M and D are mass and damping matrices and L( ), in the general case, is a nonlinear stiffness operator. If the system is linear, L( ) becomes the stiffness matrix L.

If damping is neglected the homogeneous part of the system of differential equations

$$M\ddot{x} + Lx = 0 \tag{7.42}$$

is linear with constant coefficients. The solution of these equations, as discussed above is represented by the free vibration modes q_n with corresponding frequencies ω_n. The solution of the equations of motion can be written as a linear superposition of vibration modes

$$x = Q\,a \tag{7.43}$$

where Q is a matrix in which each of the n columns consists of an eigenvector of the system (vibration mode). Substitution of this solution into the equation of motion yields (without damping)

$$M\,Q\,\ddot{a} + K\,Q\,a = f \tag{7.44}$$

or after premultiplication with the transpose of Q

$$Q^T M\,Q\,\ddot{a} + Q^T K\,Q\,a = Q^T f$$

Due to the orthogonality between the eigenvectors the matrices Q^TMQ and Q^TKQ are diagonal. If they are normalized so that all elements in Q^TKQ are equal to unity, the equation system is uncoupled and of the form

$$\ddot{a}_i + \omega_i^2\,a = Q^T f, \quad i = 1, n \tag{7.45}$$

where ω_i is the vibration frequency corresponding to the ith node. The diagonal elements of Q^TMQ are then referred to as the generalized masses of

corresponding vibration modes and the elements of the vector $Q^T f$ are the generalized forces.

In the linear case then a solution can be obtained in terms of a superposition of vibration modes. Frequently some of the vibration modes have little influence on the deformation pattern. They are then removed from the system and a becomes a vector with m components where $m < n$ and Q is a rectangular (m x n) matrix. STAGS does not include an option for modal superposition. However, vibration modes and frequencies and corresponding generalized masses can be computed and stored on file for use subsequently in a modal superposition.

If nonlinear terms are included the modal approach as defined above becomes impossible since the nonlinearities introduce couplings between the different modes. Also in many linear cases the method is impractical because too many modes are needed for an accurate description of the deformation pattern. In such cases the discretized equations may be integrated directly. The modal decomposition remains important in such cases as a tool in the study of accuracy and stability of different integration procedures.

For the purpose of integration (in time) of the equations of motion for the discrete system, a discretization in time is introduced. That is, the components of the solution vector x are represented by their values at a number of discrete "points in time". The displacement components are expressed as functions of time by use of polynomials chosen so that they match the solution vector at appropriate values of the time parameter. The basic principles in the numerical solution procedure is demonstrated here by use of an ordinary differential equation of the form

$$\begin{aligned} \dot{y} &= f(y, t) \\ y(t_o) &= y_o \end{aligned} \tag{7.46}$$

It is assumed that the solution y(t) in some way has been obtained at a sequence of timesteps, say up to and including the mth step. The known

values of the function and its first order time derivatives are referred to as the historical data. The solution at the (m + 1)th time step is obtained by the passing of a polynomial through a number of the historical data. The order of the method is given by the order of the truncation error (see Section 6). A higher order method requires a correspondingly higher number of historical data. For simplicity it is assumed that the equation is linear and that the timestep Δt is constant. Substitution of a power series then leads to the form

$$\sum_{i=1}^{m+1} \alpha_i y_i = t \sum_{i=1}^{m+1} \beta_i \dot{y}_i \tag{7.47}$$

If the term $\beta_{m+1} \dot{y}_{m+1}$ is excluded, y_{m+1} can be solved directly from historical data. In that case the procedure is referred to as an explicit integration method. If the term containing $\dot{y}_{m+1}$ is included in the series, then current relation between $\dot{y}$ and y given by the differential equation (Eq. 7.46) is included in the set of equations from which y_{m+1} (and $\dot{y}_{m+1}$) is computed. Such methods are referred to as implicit integration procedures. There are some very basic differences in the behavior between explicit and implicit methods. Since the differential equation must be satisfied for current solutions in the implicit method a typical structural analysis requires the solution of a large algebraic equation system at each timestep. On the other hand, the fact that the elastic force balance is not enforced at the current step in the explicit method leads to special problems with numeric instability. In view of these differences the methods are discussed separately.

Among the explicit schemes it appears that no other method in any case would offer substantial advantages in comparison to the central difference scheme (see Ref. 7.6). Therefore this is the only explicit method considered in the following. It can be shown (see Ref. 7.7, for example) that if the timestep in integration of a one-degree-of-freedom system with the central difference scheme is chosen to be more than Δt_{cr} where

$$\Delta t_{cr} = 2/\omega \tag{7.48}$$

and ω is the frequency of the system (in cps), then any error introduced in the system will grow exponentially. In practical analysis this mathematical instability becomes quite evident, the solution vector grows very rapidly. The solution is accurate if the timestep equals the critical. The solution does not become more accurate if Δt is somewhat less than Δt_{cr}.

For a linear system with mnay degrees of freedom it is necessary for stability that the timestep be chosen so that

$$\Delta t \leq 2/\omega_{max} \tag{7.49}$$

where ω_{max} is the highest eigenfrequency of the system. For nonlinear equations it has been suggested (Ref. 7.8) that the same equation for the critical step can be used if ω_{max} represents the maximum eigenvalue of the system under current stresses.

The equations of motion for a discretized structural system consist of a set of coupled second order differential equations. Each of these equations can be decomposed into two first order differential equations. The decomposition is not unique. It was shown in Ref. 7.9 that a procedure proposed by Jensen (Ref. 7.10) is favorable both with respect to the numerical work involved and the rate of error propagation. Accordingly, the equations of motion are written

$$\begin{aligned} y &= M\dot{x} + D\,x \\ \dot{y} &= f - L\,x \end{aligned} \tag{7.50}$$

In implementation of this scheme it is favorable, for reduction of propagation of roundoff errors to define the auxiliary parameter y at half stations in time (see Ref. 7.11) The solution algorithm is given by the recurrence formulas

$$\begin{aligned} x_i &= x_{i-1} + \Delta t\, M^{-1} (y_{i-\frac{1}{2}} - D\, x_{i-1}) \\ y_{i+\frac{1}{2}} &= y_{i-\frac{1}{2}} + \Delta t\, (f - L\, x_i) \end{aligned} \tag{7.51}$$

The method is self-starting. With initial velocity loading, the initial value of $y_{-\frac{1}{2}}$ is obtained as $M\dot{x}$ where $\dot{x}$ is the vector of initial displacement velocities. With $x_{i-1} = 0$ the values of x can be obtained from the first of the equations, for subsequent substitution in the second equation, etc. If a load is applied to a system at rest, $x_o = y_{-\frac{1}{2}} = 0$ and the procedure can be started by solution for $y_{+\frac{1}{2}}$ in the second equation.

It is necessary therefore in integration with explicit methods that some mass is attached to each degree of freedom. If Lagrangian multipliers are included for enforcement of side conditions, it is not possible to use explicit integration unless special arrangements are made. Also, a mass must be attached to each of the rotational degrees of freedom. If only the rotary inertia (proportional to the cube of shell thickness) is included the critical timestep is very small. On the other hand, a consistent mass matrix is nondiagonal and in that case execution of the first step indicated by the Eq. (7.51) entails the solution of a large equation system. Therefore, the use of a consistent mass matrix with the explicit method is generally not recommended. The best choice is probably a carefully chosen lumped matrix with relatively large masses to go with the rotational freedoms. Since these masses vanish with the grid size convergence to the correct solution is not jeopardized; only the rate of convergence with grid size depends on the choice of mass matrix elements corresponding to the rotational freedoms. The choice of time step for explicit integration is further discussed in Volume 2, Section 6.

Characteristic for discretized structural systems is that the eigenvalues (vibration frequencies) vary over a wide range. Such systems are usually referred to as stiff, and their integration presents special problems. The critical timestep in explicit integration corresponds to Π timesteps on each period of the highest frequency in the system. In an analysis of stress wave propagation the deformation corresponding to the low-frequency modes is of little interest and the central difference scheme discussed above presents a suitable method. However, for an accurate representation of the wave propagation a rather fine grid (see Ref. 7.12) and consequently a small timestep is needed.

In most cases of dynamic analysis of structural shells (dynamic stability problems), the deformation modes corresponding to the lowest frequencies are of primary importance. The period of these deformation modes is usually very large in comparison to the critical timestep and explicit methods with a time step based on the highest frequency become hopelessly uneconomical for large systems. For such problems an integration method is needed that remains stable for large time steps.

Much can be learned about the accuracy and stability of implicit integration methods through application to the free vibrations of a one-degree-of-freedom system (Ref. 7.13). The performance of a method is judged on the basis of frequency distortion and artificial damping for a freely vibrating system. The energy in a vibrating system is usually preserved for one specific value of the product of timestep and frequency. As the timestep is increased beyond the ideal value for the method the artificial damping becomes increasingly larger; the energy is gradually decreasing. For smaller values of the timestep energy is gradually added to the system. Consequently, if the integration is carried over a sufficiently long time the function (displacement) will grow beyond any bound. This is referred to as instability, although of a somewhat different character than that encountered in explicit integration. For a system with more than one degree of freedom, the solution of the homogeneous part of the equations of motion can be written in the form

$$x = \sum a_i e^{\lambda_i t} \tag{7.52}$$

In the linear case without damping all the λ_i (eigenvalues) are imaginary and $e^{\lambda_i t}$ becomes $\sin(\omega t)$ (compare Eq. (7.30)). The modes are uncoupled and the discussion of stability of the solution of single degree of systems applies to each of the vibration modes. The instability manifests itself in a multi-degree-of-freedom system as a gradual growth of a vibration in the mode (or modes) for which $\omega\Delta t$ is below the critical value.

Some implicit methods of second order or lower are called unconditionally stable. This means that the error is on the side of decreasing energy for all values of Δt. It has been shown that no method of higher than the second order can be unconditionally stable.

In a stiff system the higher modes will be poorly represented in a solution based on an implicit method. Frequently these are of no interest and the most prominent feature of the implicit methods may be that they allow the analyst to sacrifice some accuracy in order to make the analysis economically feasible.

For a system with complex eigenvalues ($\lambda_i = \alpha_i \pm i\,\beta_i$ in Eq. (7.52)) the stability criterion must be defined in the complex plane. With any given integration method there exists a curve in this plane symmetric about the real axis, so that the energy remains constant during integration if the complex pair $\lambda_i \Delta t$ for a one-degree-of-freedom system fall on this line. If a smaller timestep is chosen, instability will occur and if $\lambda\Delta t$ falls outside the curve, artificial damping is introduced. For a linear undamped system all eigenvalues are on the imaginary axis. If structural damping is added the eigenvalues will be complex pairs with a negative real part. That is, all eigenvalues are in the left half-plane. An integration method for which the unstable range is confined to the part of the complex plane where the real part is positive is called A-stable. Consequently, an A-stable method is unconditionally stable for all <u>linear</u> structural systems.

The stability boundaries are shown in Figure 7.3 for a few frequently used implicit integration methods. With the exception of Gear's third order method these are A-stable.

The trapezoidal method is a simple and efficient implicit method. Applied to the equation

$$\begin{aligned} \dot{x} &= \bar{F}(x, t) \\ x(o) &= c \end{aligned} \qquad . \qquad (7.53)$$

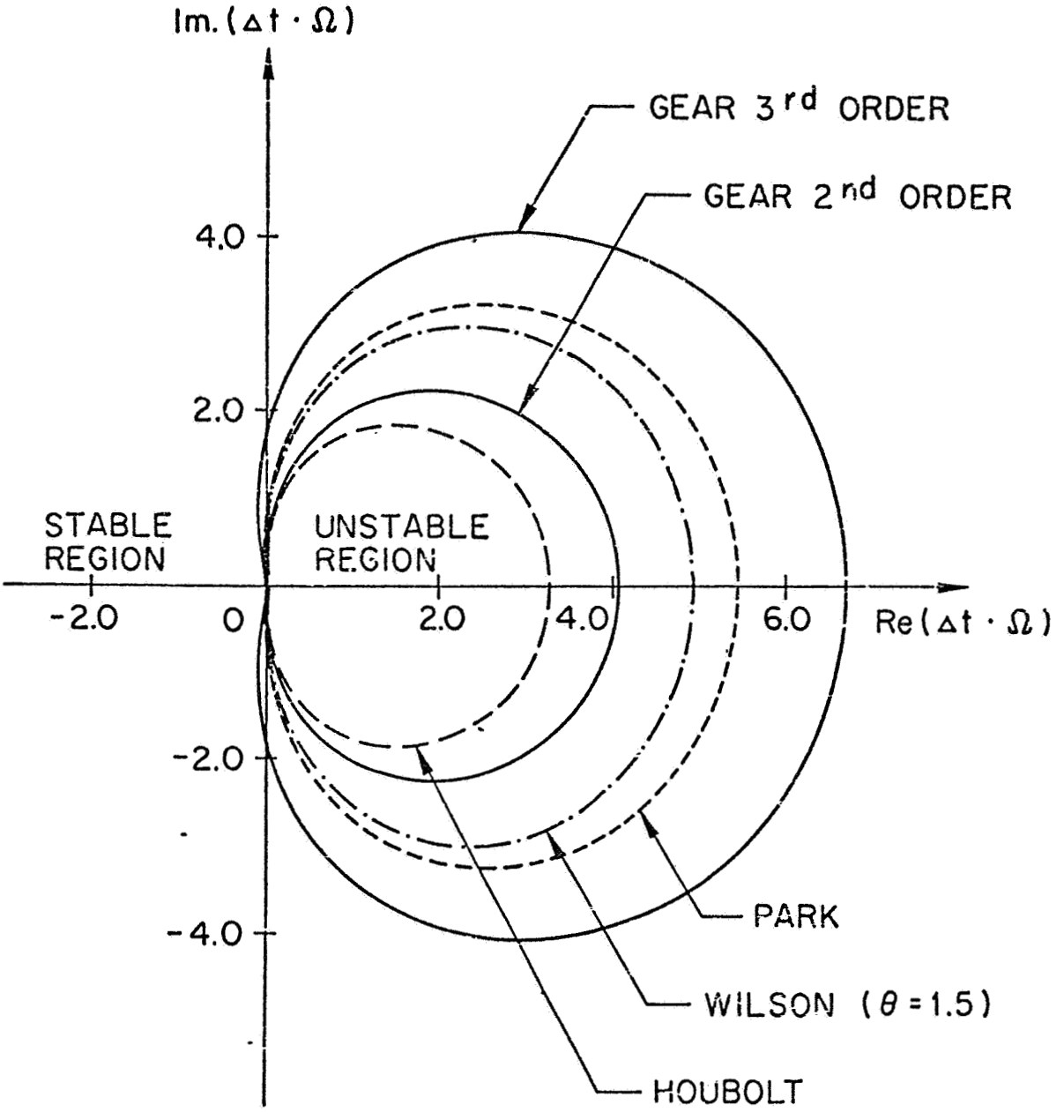

TRAPEZOIDAL RULE : ENTIRE LEFT - HAND PLANE INCLUDING IMAGINARY AXIS

CENTRAL DIFFERENCE : $-2j \leq \Omega \cdot \Delta t \leq 2j$

Figure 7.3. Stability Region of Some Multistep Methods

the trapezoidal method leads to the integration formula

$$x_{n+1} - x_n = \frac{1}{2}\Delta t \, [F(x_n, t) + F(x_{n+1}, t_{n+1})] \tag{7.54}$$

The method is implicit since x_{n+1} appears on the right-hand side. The equations of motion are reduced to a set of the first order form (Eqs. 7.50). In the discretized analysis of a multiple-degree-of-freedom system, the term $F(x_{n+1}, t_{n+1})$ introduces couplings between the unknowns (x_{n+1}). Hence, an equation system must be solved for each time step. For the trapezoidal method, the vertical axis separates the stability zones so that the entire left half-plane corresponds to stability. Consequently, the method is unconditionally stable and for linear undamped system the energy corresponding to all the different free vibration modes is maintained constant during integration in time.

The stiffly stable methods by Gear were designed specifically for stiff systems. Characteristic for Gear's and other stiffly stable methods is that they do not include historical values of the displacement derivatives (velocities) as a basis for the approximating polynomials. Gear's second order method is A-stable but all higher order methods have some region of instability in the left half-plane. The higher order methods can remain stable at all time-steps in the presence of some structural damping. The coefficients in the multi-step method are given in Appendix D for Gear's second and third order methods and for K. C. Park's method. The stability boundaries for these methods are shown in Figure 7.3.

The stability criteria are not exactly valid if nonlinear terms are included, i.e., if the stiffness oeprator L( ) (Eq. 7.41) is nonlinear. Rigorous criteria for this case have not been developed. The eigenvalues of the stiffness operator (the Frechet derivative) vary with the applied load. It seems reasonable to apply the same criteria in the nonlinear case with the only difference that current values of the eigenvalues are used. However, the stability depends not only on the eigenvalues themselves, but also on their rate of change. Stability limits determined on the basis of current eigenvalues give an approximation and can be used to initiate a trial and error procedure. Since the stiffly stable methods do not use historical values of the velocities it seems less likely that their stability boundary would be sensitive to the presence of nonlinear terms (see Ref. 7.6).

A nonlinear system can have eigenvalues with a positive real value. Such a situation will occur if the current displacement configuration in the static case would correspond to unstable equilibrium, for example, if the axial stress in a column temporarily exceeds that corresponding to the Euler load, the structural stiffness is negative. In the nonlinear case no integration method exists that can be considered unconditionally stable. Therefore, it may at times be difficult to decide whether a rapid growth in displacement is caused by actual physical instability or by spurious mathematical instability. Presumably, the former would result in uniform rapid growth of one displacement pattern and the latter in an oscillation with increasing amplitude. Still, it seems advisable to include a check on the energy balance in a computer program for transient analysis of nonlinear systems. That is, at each timestep the sum of the increments in the kinetic and strain energies is compared to the work done by external forces during the timestep.

Regarding the choice of mass matrix for use in implicit integration it appears that the consistent mass matrix generally should give more accurate results. It is possible though that if the structural stiffness is overestimated (conforming elements) the error in the diagonalized matrix will tend to compensate for this stiffness and may improve the results in the range of engineering accuracy.

Little is known about the structural damping. In practical analysis it has been customary for convenience to chose a damping matrix that is proportional either to the mass matrix or to the stiffness matrix. In the former case the eigenvalues (of a linear system) will be located on a circle in the left half-plane. With damping proportional to the mass matrix they are located on a line in the left half-plane parallel to the imaginary axis.

The STAGSC code includes as options: The explicit central difference scheme and the following implicit schemes:

- The trapezoidal method
- Gear's second order method
- Gear's third order method
- Park's method

In the User's Instructions (Volume II), advice is given regarding the choice between optional procedures.

Presently only a diagonal mass matrix is available. In the case of implicit integration the masses corresponding to the rotational freedoms include only the rotary inertia. In cases of explicit integration these mass matrix elements are chosen so that the vibration modes corresponding to pure membrane action will determine the timestep. Addition of an option to use a consistent mass matrix is desirable.

The user can define structural damping that is proportional to the mass matrix or to the stiffness matrix (linearized). In addition the user is allowed to define an "intensity of damping" as a function of the shell coordinate. Such damping may be useful in some cases to represent damping caused by a surrounding medium.

None of the STAGS versions includes a check on energy balance. However, such a check would definitely be a valuable addition to the program.

REFERENCES

7.1 Key, S. W., and Z. E. Beisinger, "The Transient Dynamic Analysis of Thin Shells by the Finite Element Method," Proc. of the Third Conf. on Matrix Methods in Struct. Mech., Air Force Flight Dynamics Laboratory, AFFDL-TR-71-160, Dec. 1973.

7.2 Dahlquist, G., and Å. Björk, Numerical Methods, Prentice-Hall, Englewood Cliffs, New Jersey, 1975.

7.3 Almroth, B. O., and C. A. Felippa, "Structural Stability," Proc. Int. Symp. Structural Mech. Software, U. of Maryland, College Park, Md., June 1974.

7.4 Collatz, L., Functional Analysis and Numerical Mathematics, Academic Press, 1966.

7.5 Schmidt, W. F., "Extending the Convergence Domain of the Newton-Raphson Method in Structural Analysis," Proc. Sixth Canadian Congress of Appl. Mech., U. of British Columbia, Vancouver, B.C., 1977.

7.6 Park, K. C., "Practical Aspects of Numerical Time Integration," Computers & Structures, Vol., 7, pp. 343-353, 1977.

7.7 Leech, J. W., P. T. Hsu, and E. W. Mack, "Stability of a Finite Difference Method for Solving Matrix Equations," AIAA J., Vol. 3, pp. 2172-2173, 1965.

7.8 McNamara, J. F., "Solution Schemes for Problems of Nonlinear Structural Dynamics," J. of Pressure Vessel Tech., ASME, Vol. 96, Series, J, pp. 96-102, 1974.

7.9 Park, K. C., and C. A. Felippa, "Computational Aspects of Time Integration Procedures in Structural Dynamics," J. Appl. Mech., to be published, 1978.

7.10 Jensen, P. S., "Transient Analysis of Structures by Stiffly Stable Methods," J. Comp. Struct., Vol. 4, pp. 615-626, 1974.

7.11 Underwood, P., "Transient Response of Inelastic Shells of Revolution," J. Comp. Struct., Vol. 2, pp. 975-989, 1972.

7.12 Belytschko, T., N. Holmes, and R. Mullen, "Explicit Integration-Stability, Solution Properties, Cost," in Finite Analysis of Transient Nonlinear Structural Behavior, ASME, Vol. AMD-14, 1975.

7.13 Park, K. C., "Evaluating Time Integration Methods for Nonlinear Dynamics Analysis," in Finite Element Analysis of Transient Nonlinear Structural Behavior, ASME, Vol. AMD-14, 1975.